Negative microfilm
received from university

66-5104

PATEL, Prafullchandra Raojibhai, 1937-
STUDIES ON ACID DEMINERALIZATION KINETICS OF ENAMEL.

The University of Michigan, Ph.D., 1965
Chemistry, pharmaceutical

University Microfilms, Inc., Ann Arbor, Michigan

STUDIES ON ACID DEMINERALIZATION KINETICS OF ENAMEL

by
Prafullchandra Raojibhai Patel

A dissertation submitted in partial fulfillment
of the requirements for the degree of
Doctor of Philosophy in the
University of Michigan
1965

Doctoral Committee:

Associate Professor William I. Higuchi, Chairman
Associate Professor Robert G. Craig
Professor Albert M. Mattocks
Associate Professor Joseph E. Sinsheimer
Assistant Professor George Zografi

ACKNOWLEDGEMENTS

The author wishes to express his sincere appreciation:

To Associate Professor William I. Higuchi for his suggestion of the problem, and his advice and inspiring interest during the course of this investigation.

To Dr. John J. Hefferren for supplying the powdered enamel.

To Professor Albert M. Mattocks for his advice during the work in the radioactive laboratory.

To Mr. Nasim A. Mir and to Miss Erika A. Wilinski for their technical assistance.

To Upjohn Company and to the National Institute of Dental Research, U. S. Public Health Service, for financial assistance which enabled the author to continue his studies and pursue this research.

Prafullchandra R. Patel

TABLE OF CONTENTS

	Page
ACKNOWLEDGEMENTS	ii
LIST OF TABLES	v
LIST OF FIGURES	vi
INTRODUCTION	1
LITERATUTE REVIEW	3
STATEMENT OF THE PROBLEM	7
THEORETICAL STUDY	9
Hydroxyapatite Model	9
Computation of Gh	12
Considerations in the Selection of Constants.	20
Variables used in the Computation of Gh	23
Results of the Theoretical Study	25
Theoretical Study in the Absence of Common Ions	25
Theoretical Common Ion Study	34
Study in the Presence of Common Ions	70
Study in the Presence of Phosphate Ions	71
EXPERIMENTAL	74
Synthetic Hydroxyapatite Samples	74
Preparation of Samples C, P, and R	75
Powdered Tooth Enamel	78
Preparation of Buffers	79
Assay for Phosphate	80
Assay for Calcium	81
Chemical Analysis	81
Radioactivity Determination	83
Procedure for Determination of Solubility	84
Procedure for Synthetic Hydroxyapatite Dissolution Rate Experiments	84
Procedure for the Enamel Dissolution Rate Experiments	86
Results of the Experimental Study	86
Solubility Study	86
Dissolution Rate Study in the Absence of Common Ions	89
Procedure for the Estimation of the Initial Dissolution Rates	90

Page

Comparison of the Experimental Initial Dissolution Rates with the Theory..... 97
Dissolution Rate Study in the Presence of Common Ions..... 98
Comparison of the Experimental Initial Dissolution Rates with the Theory..... 100

DISCUSSION..... 106

Equilibrium Constants..... 106
The Meaning of the h value in the Comparison of the Theoretical and Experimental Dissolution Rates..... 106
Granulated Synthetic Hydroxyapatite Samples versus Powdered Tooth Enamel..... 108
Stoichiometry of Hydroxyapatite Samples..... 110
Solubility Product of Hydroxyapatite..... 110
Biological Significance..... 113

SUMMARY..... 115

APPENDICES..... 118

I. Experimental Data for Dissolution Rates of Synthetic Hydroxyapatite Samples and Powdered Tooth Enamel in Acetate and Lactate Buffers and in Hydrochloric Acid Solutions.. 118
II. Experimental Dissociation Constants of Acetic and Lactic acids..... 145
III. The Values of h' employed to obtain fits of Theoretical Gh Values to the Experimental Data (Figures 47-53)..... 146

LIST OF REFERENCES..... 148

LIST OF TABLES

Table		Page
1.	Thermodynamic Constants for Theoretical Calculations.....	21
2.	Concentration Equilibrium Constants Estimated for Ionic Strengths = 0.1-0.2..	22
3.	Key for the Curves in Figures 11-44.....	35
4.	Composition of Samples.....	77
5.	Calculated Values of K_{HAP} from Solubility Experiments, Figure 45.....	111

LIST OF FIGURES

Figure		Page
1.	Hydroxyapatite Model.....	10
2.	Computer Program in MAD Language.....	15
3.	Flow Chart for the Computer Program.....	17
4.	Theoretical Dissolution Rates of Enamel in Chloracetic Acid Buffers as a function of $[TB]_h$; pH; and K_{HAP}.....	26
5.	Theoretical Dissolution Rates of Enamel in Lactic Acid Buffers as a function of $[TB]_h$; pH; and K_{HAP}.....	27
6.	Theoretical Dissolution Rates of Enamel in Acetic Acid Buffers as a function of $[TB]_h$; pH; and K_{HAP}.....	28
7.	Theoretical Dissolution Rates of Enamel in 'X' Acid Buffers as a function of $[TB]_h$; pH; and K_{HAP}.....	29
8.	Theoretical Dissolution Rates of Enamel in Hydrochloric Acid Solutions as a function of $[TB]_h$; pH; and K_{HAP}.....	31
9.	Effects of Varying Diffusion Coefficient Values of various Species on the Theoretical Dissolution Rates of Enamel in Acetate Buffers.....	32
10.	Effects of Varying Diffusion Coefficient Values of various Species on the Theoretical Dissolution Rates of Enamel in Hydrochloric Acid Solutions.....	33
11.	Effects of Calcium Ions on Theoretical Dissolution Rates in 'X' Acid Buffers, $K_{HAP} = 1 \times 10^{-120}$.....	36
12.	Effects of Calcium Ions on Theoretical Dissolution Rates in 'X' Acid Buffers, $K_{HAP} = 1 \times 10^{-116}$.....	37
13.	Effects of Calcium Ions on Theoretical Dissolution Rates in 'X' Acid Buffers, $K_{HAP} = 1 \times 10^{-113}$.....	38

Figure		Page
14.	Effects of Calcium Ions on Theoretical Dissolution Rates in 'X' Acid Buffers, $K_{HAP} = 1x10^{-108}$.....	39
15.	Effects of Calcium Ions on Theoretical Dissolution Rates in Acetic Acid Buffers, $K_{HAP} = 1x10^{-120}$.....	40
16.	Effects of Calcium Ions on Theoretical Dissolution Rates in Acetic Acid Buffers, $K_{HAP} = 1x10^{-116}$.....	41
17.	Effects of Calcium Ions on Theoretical Dissolution Rates in Acetic Acid Buffers, $K_{HAP} = 1x10^{-113}$.....	42
18.	Effects of Calcium Ions on Theoretical Dissolution Rates in Acetic Acid Buffers, $K_{HAP} = 1x10^{-108}$.....	43
19.	Effects of Calcium Ions on Theoretical Dissolution Rates in Lactic Acid Buffers, $K_{HAP} = 1x10^{-120}$.....	44
20.	Effects of Calcium Ions on Theoretical Dissolution Rates in Lactic Acid Buffers, $K_{HAP} = 1x10^{-116}$.....	45
21.	Effects of Calcium Ions on Theoretical Dissolution Rates in Lactic Acid Buffers, $K_{HAP} = 1x10^{-113}$.....	46
22.	Effects of Calcium Ions on Theoretical Dissolution Rates in Lactic Acid Buffers, $K_{HAP} = 1x10^{-108}$.....	47
23.	Effects of Calcium Ions on Theoretical Dissolution Rates in Chloracetic Acid Buffers, $K_{HAP} = 1x10^{-120}$.....	48
24.	Effects of Calcium Ions on Theoretical Dissolution Rates in Chloracetic Acid Buffers, $K_{HAP} = 1x10^{-116}$.....	49
25.	Effects of Calcium Ions on Theoretical Dissolution Rates in Chloracetic Acid Buffers, $K_{HAP} = 1x10^{-113}$.....	50
26.	Effects of Calcium Ions on Theoretical Dissolution Rates in Chloracetic Acid Buffers, $K_{HAP} = 1x10^{-108}$.....	51

Figure | Page

27. Effects of Calcium Ions on Theoretical Dissolution Rates in Hydrochloric Acid Solutions..... 52

28. Effects of Phosphate Ions on Theoretical Dissolution Rates in 'X' Acid Buffers, $K_{HAP} = 1x10^{-120}$..... 53

29. Effects of Phosphate Ions on Theoretical Dissolution Rates in 'X' Acid buffers, $K_{HAP} = 1x10^{-116}$..... 54

30. Effects of Phosphate Ions on Theoretical Dissolution Rates in 'X' Acid Buffers, $K_{HAP} = 1x10^{-113}$..... 55

31. Effects of Phosphate Ions on Theoretical Dissolution Rates in 'X' Acid Buffers, $K_{HAP} = 1x10^{-108}$..... 56

32. Effects of Phosphate Ions on Theoretical Dissolution Rates in Acetic Acid Buffers, $K_{HAP} = 1x10^{-120}$..... 57

33. Effects of Phosphate Ions on Theoretical Dissolution Rates in Acetic Acid Buffers, $K_{HAP} = 1x10^{-116}$..... 58

34. Effects of Phosphate Ions on Theoretical Dissolution Rates in Acetic Acid Buffers, $K_{HAP} = 1x10^{-113}$..... 59

35. Effects of Phosphate Ions on Theoretical Dissolution Rates in Acetic Acid Buffers, $K_{HAP} = 1x10^{-108}$..... 60

36. Effect of Phosphate Ions on Theoretical Dissolution Rates in Lactic Acid Buffers, $K_{HAP} = 1x10^{-120}$..... 61

37. Effects of Phosphate Ions on Theoretical Dissolution Rates in Lactic Acid Buffers, $K_{HAP} = 1x10^{-116}$..... 62

38. Effects of Phosphate Ions on Theoretical Dissolution Rates in Lactic Acid Buffers, $K_{HAP} = 1x10^{-113}$..... 63

39. Effects of Phosphate Ions on Theoretical Dissolution Rates in Lactic Acid Buffers, $K_{HAP} = 1x10^{-108}$..... 64

Figure		Page
40.	Effects of Phosphate Ions on Theoretical Dissolution Rates in Chloracetic Acid Buffers, $K_{HAP} = 1x10^{-120}$.....	65
41.	Effects of Phosphate Ions on Theoretical Dissolution Rates in Chloracetic Acid Buffers, $K_{HAP} = 1x10^{-116}$.....	66
42.	Effects of Phosphate Ions on Theoretical Dissolution Rates in Chloracetic Acid Buffers, $K_{HAP} = 1x10^{-113}$.....	67
43.	Effects of Phosphate Ions on Theoretical Dissolution Rates in Chloracetic Acid Buffers, $K_{HAP} = 1x10^{-108}$.....	68
44.	Effects of Phosphate Ions on Theoretical Dissolution Rates in Hydrochloric Acid Solutions.....	69
45.	Solubilities of Synthetic Hydroxyapatite Samples A and P and Enamel as a function of amount of the Solids Exposed to 20 ml. -Aliquots of 0.2M Acetate Buffer pH 6.0 for 114 hours (30°C.).....	87
46.	Solubilities of Synthetic Hydroxyapatite Samples A and P and Enamel as a function of amount of the Solids Exposed to 20 ml. -Aliquots of 0.2M Acetate Buffer pH 5.7 Containing 0.5M NaCl for 114 hours (30°C.)	88
47.	Initial Dissolution Rates of Sample A in Acetic Acid Buffers with and without the Presence of 0.5M NaCl as a function of $[TB]_h$ and pH.....	91
48.	Initial Dissolution Rates of Sample P in Acetic Acid Buffers with the Presence of 0.5M NaCl as a function of $[TB]_h$ and pH..	92
49.	Initial Dissolution Rates of Powdered Tooth Enamel in Acetic Acid Buffers with and without the Presence of 0.5M NaCl as a function of $[TB]_h$ and pH.....	93
50.	Initial Dissolution Rates of Sample A in Lactic Acid Buffers with the Presence of 0.5M NaCl as a function of $[TB]_h$ and pH..	94

Figure		Page
51.	Initial Dissolution Rates of Sample P in Lactic Acid Buffers with and without the Presence of 0.5M NaCl as a function of $[TB]_h$ and pH.....	95
52.	Initial Dissolution Rates of Powdered Tooth Enamel in Lactic Acid Buffers with and without the Presence of 0.5M NaCl as a function of $[Tb]_h$ and pH.....	96
53.	Initial Dissolution Rates of Synthetic Hydroxyapatite Samples and Enamel as a function of Hydrochloric Acid Concentration (containing 0.5M NaCl).....	99
54.	Effects of Calcium Ions on the Initial Dissolution Rates of Synthetic Hydroxyapatite Samples and Enamel in a 0.05M Acetate Buffer pH 4.5 with and without the Presence of 0.5M NaCl.....	101
55.	Effects of Phosphate Ions on the Initial Dissolution Rates of Synthetic Hydroxyapatite Samples and Enamel in a 0.05M Acetate Buffer pH 4.5 with and without the Presence of 0.5M NaCl.....	102
56.	Effects of Calcium Ions on the Initial Dissolution Rates of Synthetic Hydroxyapatite Samples and Enamel in a 0.05M Lactate Buffer pH 4.5 with and without the Presence of 0.5M NaCl.....	103
57.	Effects of Phosphate Ions on the Initial Dissolution Rates of Synthetic Hydroxyapatite Samples and Enamel in a 0.05M Lactate Buffer pH 4.5 with and without the Presence of 0.5M NaCl.....	104

INTRODUCTION

Dental caries is primarily a lesion initiated on the enamel. The most significant clues to the cause and prevention of dental caries are believed to be found in the study of the chemical events which lead to the demineralization of the enamel.

The main constituent of tooth enamel is inorganic mineral which accounts for approximately 97% by weight of enamel. This inorganic mineral phase which is presumed to be largely hydroxyapatite [$Ca_{10}(PO_4)_6(OH)_2$] is embedded in an organic matrix (keratin and other proteins) comprising 1% by weight of enamel. Water accounts for the remaining 2%.

In view of such a high proportion of the inorganic phase, and due to the fact that organic acids develop in the mouth, the most important mechanism of carious process is the selective acidic dissolution of inorganic mineral of enamel. It appears, therefore, that a quantitative understanding of the mechanism of human dental enamel dissolution in acidic media is important. Such knowledge could assist the clear description of the causative factors in caries formation. Moreover, such information can be profitably employed in the design of meaningful screening methods for potential anticaries agents.

Therefore, the present work is an attempt to describe mathematically the acid demineralization of enamel. The mathematical model is compared with experimental demineralization results in various acidic buffers obtained from enamel as well as from synthetic hydroxyapatite.

LITERATURE REVIEW

That acid demineralization is the first step in dental caries was postulated years ago (1), and it was explained on the basis of constant acid generation from bacterial-enzymatic breakdown of food left in the mouth. Several acids are known to be produced along with lactic acid from carbohydrate and glucose degradation by oral microorganisms (2,3). However, many investigators considered the role of lactic acid in dental caries to be the most significant (4,5). Consequently, many investigators have used lactic acid to study enamel changes associated with dental caries (6,7).

Several other researchers (8,9) have used acetate buffers to determine enamel solubility and to study the effect of solubility retarding agents such as fluoride. Much interest has been shown in past in studying dissolution rate of powdered enamel and synthetic hydroxyapatite in acid buffers with added low concentrations of foreign ions (10-14). These studies were conducted often for the purpose of devising tests for anticaries agents that were expected to act through their anti-solubility properties or by repressing the demineralization rate. Synthetic hydroxyapatite was used for studies designed to seek out basic enamel reactions under different conditions.

Stralfors (15) postulated that dissolution of enamel is controlled by diffusion. However, because of the lack

of enough data he was unable to prove the mechanism. Gray (16), in 1962, reported some carefully conducted experiments with block enamel exposed to a number of acids, and he demonstrated that a solution diffusion controlled mechanism was, indeed, operating. Generally, when dissolution rate of a solid is controlled by diffusion, through a film of liquid at the surface of the dissolving solid, the rate increases with stirring over a wide range of speed (17). This effect was observed by Gray on enamel. He was also able to show that his data fitted a general empirical relationship involving the hydrogen ion concentration, the total buffer concentration, the buffer acid dissociation constant, and other terms for common ions and foreign ions affecting the rate. He observed that temperature had a relatively small effect on rate, i.e., 20% rate increase for the 10 degree rise going from 27°C to 37°C. Generally, activation energies for dissolution rates controlled by diffusion range from about 4 to 8 kcal. per mole (18). Calculating this energy from Gray's data, one gets a value of 3.4 kcal. per mole, which also suggests that dissolution rate for enamel is diffusion controlled. Gray attributed the retarding effect of foreign cations to the formation of surface insoluble phosphate phase. Similarly, he concluded that anions e.g., phosphate, fluoride, etc., formed insoluble calcium salts.

The success of Gray's empirical relationship suggested that detailed mathematical models could be formulated and

tested employing simultaneous diffusion and chemical reaction as has been done in the dissolution behavior of benzoic acid (19) in basic and buffered media. This approach was recently, applied to the demineralization problem of enamel by Higuchi, Gray, Hefferren and Patel (20). They have analyzed several realistic mathematical models. They found remarkably good quantitative agreement between Gray's data on initial rates of enamel dissolution in acid buffers and the model in which hydroxyapatite was assumed to be the thermodynamically governing phase in enamel. These significant findings stimulated a research program to simultaneously correlate the theory with experiments on enamel and on synthetic apatite minerals.

Higuchi, Patel and Hefferren (21) have reported preliminary findings of this research program and found that the three way correlation was good, supporting the previous findings that the hydroxyapatite model appeared to describe the data adequately. The demineralization rates were studied in acetate buffers over various acidic pH values for powdered enamel and five different synthetic hydroxyapatite samples, two of which were commercially obtained, while the other three were prepared in the laboratory under varied conditions of precipitation. The two commercially obtained samples of hydroxyapatite and the sample which was prepared in the laboratory under rapid precipitation conditions gave essentially identical initial rates. The first of the other two laboratory made

samples was prepared under slow precipitation conditions and gave results about twice those of the previous three samples, while the second, which differed from the slow precipitated sample in that it was sintered at 900°C for 72 hours, gave rates one half of the unsintered sample. Comparison of the results of synthetic hydroxyapatite with those obtained with powdered enamel showed that enamel dissolved much more slowly than any of the synthetic samples. However, when reasonable parameters were employed in the theory, the comparison was favorable. In the case of synthetic mineral results, the relative pH and buffer concentration behaviors of various samples were similar, even though some of them differed in absolute rates. The use of $K_{sp}=1x10^{-113}$ instead of $K_{sp}=1x10^{-120}$ for hydroxyapatite appeared to give somewhat better agreement of the data for synthetic mineral with theory but the reverse was true in the case of enamel powder. The data for enamel agreed remarkably with the theory employing the constants that gave good fit between theory and Gray's data.

STATEMENT OF THE PROBLEM

Upon reviewing the literature it was seen that the mathematical model developed by Higuchi *et al.* (20) was remarkably successful in establishing that hydroxyapatite is the thermodynamically governing phase in demineralization of tooth enamel.

Aim of this study was to obtain more theoretical information about the effects of the following variables on demineralization rates of enamel, using the "hydroxyapatite model":

1. Diffusion coefficients of various species involved,
2. Buffer acid dissociation constant through the use of different buffer acids,
3. Presence of common ions at varying total buffer concentrations,
4. Solubility product of hydroxyapatite (since reported values in literature vary from 1×10^{-120} to 1×10^{-110}),
5. Hydrogen ion concentration,

and 6. Total buffer concentration.

In order to further investigate some of the theoretical results thus obtained, it was planned to study experimentally dissolution rates of powdered enamel and various synthetic hydroxyapatite samples in acetate and lactate buffers, with and without the presence of electrolyte *e.g.*, sodium chloride, at varying hydrogen ion

concentrations. Also, it was decided to study the dissolution rates of some of the samples in hydrochloric acid at several concentrations.

It is anticipated that the findings may provide further support to the idea that simultaneous theoretical and experimental studies with enamel and synthetic minerals will lead to a better understanding of many enamel reaction mechanisms.

THEORETICAL STUDY

Hydroxyapatite Model

Since the mineral portion of tooth enamel is mostly hydroxyapatite, the assumption that the surface of the enamel is hydroxyapatite during dissolution is a plausible one. The hydroxyapatite model described by Higuchi *et al.* (20), which will be used throughout this study, is illustrated in Figure 1.

When the enamel is exposed to an acid buffer solution, the following processes take place. Acid buffer molecules and hydrogen ions diffuse toward the surface across a liquid diffusion layer of constant thickness *h*. These acidic molecules and ions meet the PO_4^{3-} and/or HPO_4^{2-} that are diffusing outward from the enamel surface through the liquid diffusion layer. Reaction occurs in the diffusion layer to the extent determined by the dissociation constants for the HPO_4^{2-}, $H_2PO_4^-$ and the buffer acid as well as by the concentrations of all the species involved. The reaction products then diffuse out of the diffusion layer into the bulk solution along with the Ca^{2+} and the remaining unreacted phosphate species. In this model it is assumed that enamel surface exposed to the solution is $Ca_{10}(PO_4)_6(OH)_2$ and that the solution immediately adjacent to the interface is in equilibrium with this phase.

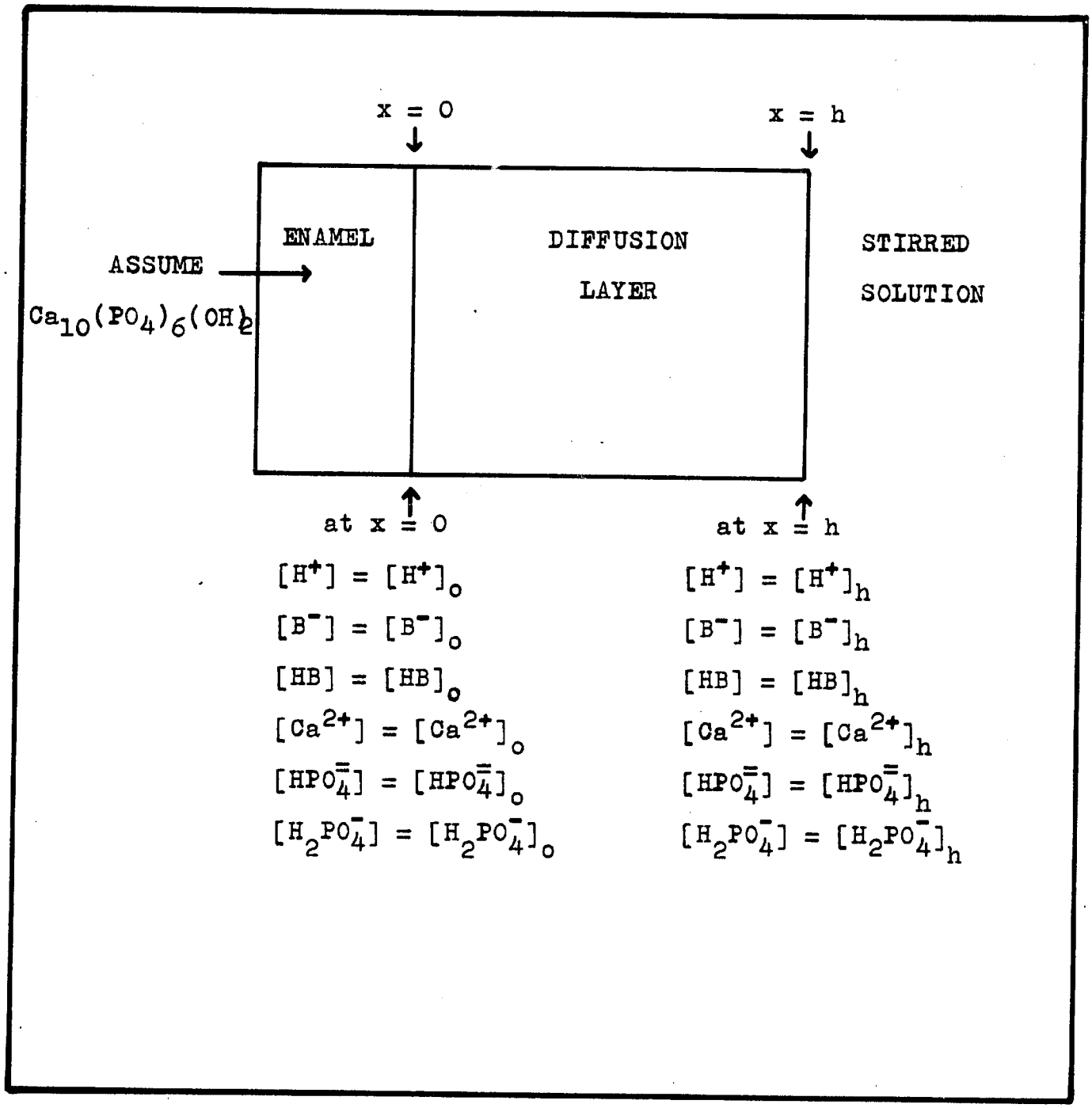

Figure 1.-Hydroxyapatite Model. Dissolution of enamel in acid buffer solutions. $[H^+]$, $[B^-]$, etc., are the concentrations of the respective species. Solution adjacent to surface is in equilibrium with hydroxyapatite phase.

This model is mathematically described by Higuchi et al. (20), in terms of Fick's law expressions for all diffusing species involved, taking into account the mass balances in the simultaneous diffusion and rapid chemical reaction. When these equations were integrated two times using several boundary conditions and eliminating several unknowns, the following two equations were obtained. For complete derivation of these equations, the reader is referred to the original paper (20).

$$\frac{0.6Gh + D_{HP}[HPO_4^{=}]_h + D_{H_2P}[H_2PO_4^{-}]_h}{D_{H_2P} + (D_{HP}K_{2P})/([H^+]_o)} =$$

$$[H_2PO_4^{-}]_h + \frac{D_H}{D_{H_2P}}[H^+]_h - \frac{D_H}{D_{H_2P}}[H^+]_o + \frac{D_{HB}}{D_{H_2P}}[HB]_h$$

$$- \frac{D_{HB}}{D_{H_2P}}\left(\frac{D_{HB}[HB]_h + D_B[B^-]_h}{D_{HB} + (D_BK_A)/([H^+]_o)}\right) - \frac{0.8Gh}{D_{H_2P}} \qquad \text{(Eq.1)}$$

$$[H^+]_o^{14} = \frac{K_{3P}^6 K_W^2}{K_{HAP}}\left\{[Ca^{2+}]_h + \frac{Gh}{D_{Ca}}\right\}^{10}$$

$$x\left\{\frac{0.6Gh + D_{HP}[HPO_4^{=}]_h + D_{H_2P}[H_2PO_4^{-}]_h}{(D_{H_2P})/(K_{2P}) + (D_{HP})/([H^+]_o)}\right\}^6 \qquad \text{(Eq.2)}$$

Here, G is the stoichiometric dissolution rate, h is a hydrodynamic factor for constant agitation conditions,

the D's are the diffusion coefficients for the species indicated by the subscripts, and the quantities in the parentheses are the concentrations of the indicated species at x=0 or x=h, the boundaries of the diffusion layer. K_{2P}, K_{3P}, K_W, K_{HAP}, and K_A are, respectively, the second and third dissociation constants for phosphoric acid, the ionic product of water, the solubility product for hydroxyapatite, and the dissociation constant for the buffer acid. The symbols, HB, B, HP, and H_2P represent undissociated acid molecule, the dissociated buffer ion, the monohydrogen phosphate ion, and the dihydrogen phosphate ion, respect-

Taking Gh as a single unknown, it should be possible, in principle, to eliminate $[H^+]_o$ from equations 1 and 2. However, in this case, because the situation is algebraically complicated, a single explicit equation for Gh is difficult to obtain.

Computation of Gh

It seemed tedious to solve for Gh for a set of known variables, manually, due to the tremendous time involved in the method of successive approximations and then graphical extrapolation or interpolation of the value. Therefore, it was decided to use the Digital Computer* to do the planned theoretical work.

---

* IBM 7090 Computer, Computing Center, University of Michigan.

This necessitated the rewriting of the above two working equations into a more tractable form. Throughout this study, except where mentioned otherwise, the value of 1×10^{-5} $cm.^2$ per second was used for all diffusion coefficients. With perhaps the exception of the diffusion involving hydrogen ions $\underline{H^+}$, this should be a reasonably good approximation for the molecules and ions involved here, and it will be shown later that the diffusion of $\underline{H^+}$ is not important in most of the situations involving weak acid buffers. Substituting the following into equation 1:

a). All diffusion coefficients = 1×10^{-5} $cm.^2$ per second,

b). $K_{2P} = 2.0 \times 10^{-10}$ moles per $cm.^3$,

c). $[HPO_4^{=}]_h + [H_2PO_4^{-}]_h = [TP]_h$,

d). $[HB]_h + [B^-]_h = [TB]_h$,

e). $$[H_2PO_4^-]_h = \frac{[TP]_h[H^+]_h}{K_{2P} + [H^+]_h},$$

f). $$[HB]_h = \frac{[TB]_h[H^+]_h}{K_A + [H^+]_h},$$

g). $[H_2PO_4^-]_h + [H^+]_h + [HB]_h = [PHB]_h$,

h). $$[PHB]_h - [H^+]_o - \frac{[TB]_h[H^+]_o}{K_A + [H^+]_o} = Z,$$

and i). $K_{3P}^6 K_w^2 / K_{HAP} = K$,

and rearranging one gets,

$$Gh = \frac{(1x10^{-5}[H^+]_o + 2x10^{-15})(Z) - ([TP]_h[H^+]_o x10^{-5})}{(1.4[H^+]_o + 16x10^{-11})} \qquad \text{(Eq. 3)}$$

and substituting the same as well as equation 3 into equation 2 yields:

$$[H^+]_o = (K)^{0.07143}{}_x$$

$$\left\{[Ca^{2+}]_h + \frac{([H^+]_o + 2x10^{-10})(Z) - ([TP]_h[H^+]_o)}{(1.4[H^+]_o + 16x10^{-11})}\right\}^{0.7143} x$$

$$\left\{\frac{(6x10^{-6}[H^+]_o^2 + 1.2x10^{-15}[H^+]_o)(Z) + [TP]_h(8x10^{-6}[H^+]_o^2 + 16x10^{-16}[H^+]_o)}{(7x10^4[H^+]_o^2 + 2.2x10^{-5}[H^+]_o + 16x10^{-16})}\right\}^{0.4286} \qquad \text{(Eq. 4)}$$

Thus, knowing $[H^+]_h$, $[TB]_h$, K_A, K, $[TP]_h$, and $[Ca^{2+}]_h$, it was possible to calculate $[H^+]_o$ from equation 4 by process of successive approximations, and once a fairly close value of $[H^+]_o$ is obtained, it can be inserted into equation 3 with the same set of variables to get the Gh.

Computer program was written in MAD (Michigan Algorithm Decoder) language to calculate Gh from equations 3 and 4 and this is given in Figure 2. The flow chart depicting the various stages of the program is illustrated in Figure 3.

COMPUTER PROGRAM

Instruction No.		Instruction
1.	P0	SETEOF.(PN)
2.		READ FORMAT IN, H, TB, KA, K, TP, CAL
3.		EXP=-10.01
4.		INC=.1
5.		LT=400
6.	LOOP1	THROUGH P3, FOR I=1,1,I.G.5
7.		INC=INC*.1
8.	LOOP2	THROUGH P1, FOR J=1,1,J.G.LT
9.		EXP=EXP+INC
10.		SHR=10.P.EXP
11.		PHB=((TP*H)/(2E-10+H))+H+((TB*H)/(KA+H))
12.		INT1=PHB-SHR-(TB*SHR)/(SHL+KA)
13.		INT2=(((SHR+2E-10)*INT1-TP*SHR)/(1.4*SHR+ 1 16E-11)+CAL)
14.		WHENEVER INT2.L.0, TRANSFER TO P2
15.		INT3=INT2.P..7143
16.		INT4=INT1*(6E-6*SHR*SHR+1.2E-15*SHR)
17.		INT5=INT4+TP*(8E-6*SHR*SHR+16E-16*SHR)
18.		WHENEVER INT5.L.0, TRANSFER TO P2
19.		INT6=INT3*K.P..07143
20.		SHL=INT6*(INT5/(SHR*(7E4*SHR+2.2E-5)+ 1 16E-16)).P..4286
21.		WHENEVER SHR-SHL.GE.0
22.		EXP=EXP-INC
23.		LT=10

Computer Program (continued)

Instruction No.		Instruction
24.	P1	PRINT COMMENT $0SYSTEM IS BLOWN.$
25.		TRANSFER TO P0
26.	P2	PRINT COMMENT $0MAKE INCREMENTS SMALLER.$
27.		TRANSFER TO P0
28.	P3	CONTINUE
29.		INT7=PHB-SHL-(TB*SHL)/(SHL+KA)
30.		INT8=INT7*(1E-5*SHL+2E-15)-TP*SHL*1E-5
31.		GH=INT8/(1.4*SHL+16E-11)
32.		PRINT FORMAT OUT, H, TB, KA, K, TP, CAL
33.		PRINT FORMAT OUTB, SHR, SHL, GH
34.		TRANSFER TO P0
35.	PN	PRINT COMMENT $4END OF THE DATA FILE.$
36.		SYSTEM.
37.		VECTOR VALUES IN=$6E10.4*$
38.		VECTOR VALUES OUT=$4H8H =E15.8,3HTB=E15.8, 1 4HKA =E15.8,3HK =E15.8,3HTP=E15.8, 1 4HCAL=E15.8*$
39.		VECTOR VALUES OUTB=$9HO SHR =E19.12, 1 12H SHL =E19.12,9H GH =E19.12*$
40.		INTEGER LT,I,J
41.		END OF PROGRAM

Figure 2.-Computer Program for Computing Demineralization Rates from the "Hydroxyapatite Model" Equations, Written in MAD Language.

FLOW CHART

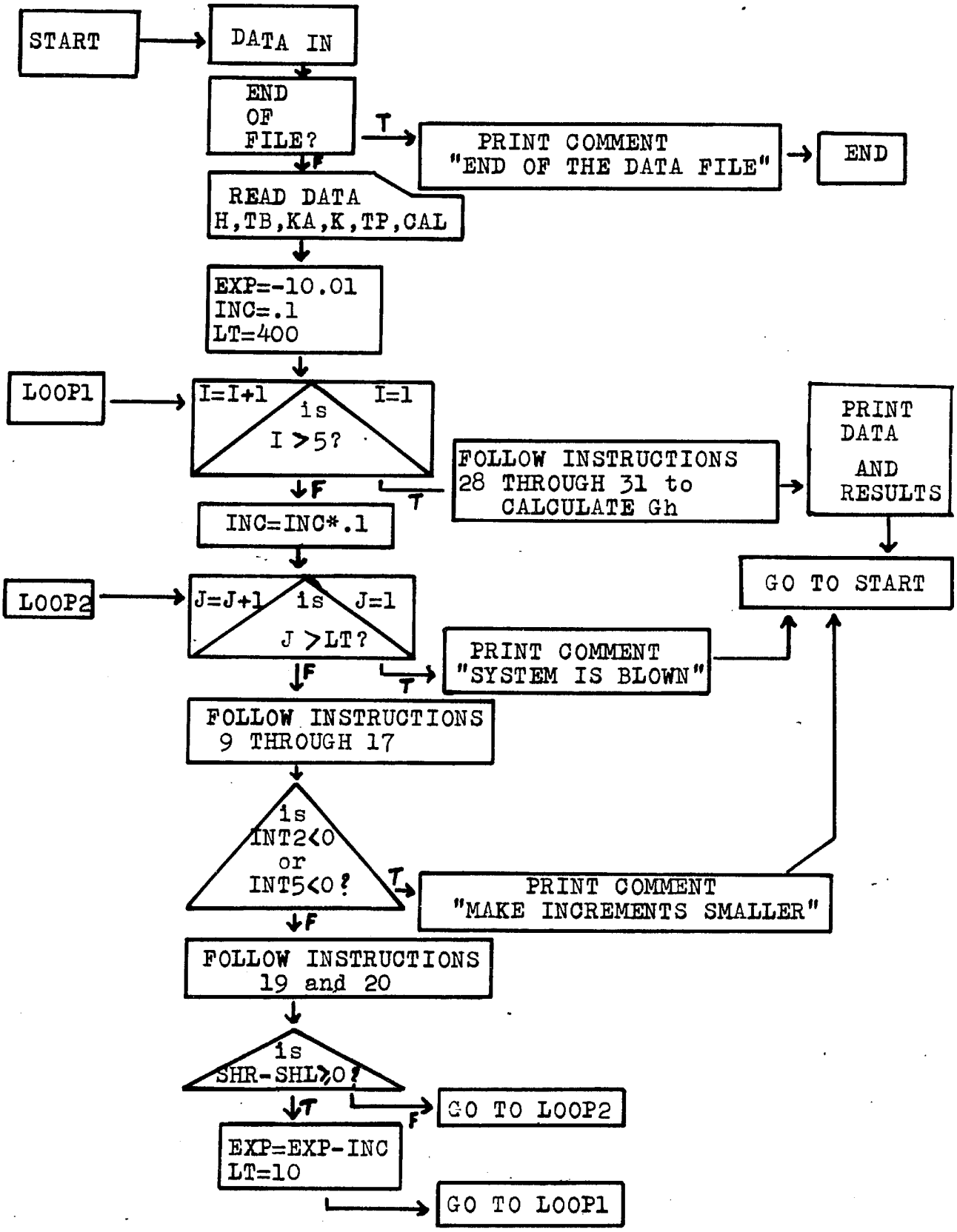

Figure 3.-Flow Chart for the Computer Program.
T-true; F-false.

According to the program, a punched data card containing a set of variables, for which Gh is to be computed, is read in by instructions 1 and 2. Arbitrarily, as a first guess, surface hydrogen ion concentration on the right hand side of equation 4 (SHR) is set to be equal to $1x10^{-10}$ moles per cm^3, i.e., pH = 7, by instructions 3, 4, 7, 9, and 10. Then, following the subsequent instructions 11 through 20, the surface hydrogen ion concentration on the left hand side of equation 4 (SHL) is computed through several intermediate computations. In a preliminary programming study, by substituting increasing increments of 0.01 in the exponent values of SHR starting from $1x10^{-10}$ moles per cm^3 the corresponding values of SHL were calculated. The plot of SHL versus SHR was non-linear, and the difference (SHR-SHL) was shifting from positive to negative side. This change is used as a key to pick up the value of SHR, which when substituted in equation 4, will give the closest possible SHL to true answer for this initial increment range of 0.01 in the exponent. So, the instruction 21 is the key instruction which judges whether the difference (SHR-SHL) is greater than zero (positive) or less than zero (negative). If the difference is negative, instructions 5 and 8 are followed, and computation of SHL is repeated with a further increment of 0.01 in the exponent of SHR. This is continued until the difference (SHR-SHL) becomes positive, and then only instructions 22 and 23 are followed. The process is repeated, but now with increments of 0.001 in

the exponent of SHR beginning with that value of the exponent to which if 0.01 is added, the difference (SHR-SHL) just becomes positive. This two-loop cycling is repeated until condition of instruction 6 is met, that is, a value of SHR generates a value of SHL accurate upto ± 0.000001 in the exponent. Instructions 28 through 34 are now followed to compute Gh from the equation 3, employing the final value of SHL. Then, the final values of SHR, SHL, and Gh, together with the set of variables used for this computation, are printed out.

Instructions 5, 8, 24, and 25 provide a rapid exit system for a case in which 400 increments of 0.01 in the exponent of SHR are made (when SHR will be 1×10^{-6} moles per cm^3 or pH=3), but the difference (SHR-SHL) does not become positive. Then, a comment, "System is Blown", is printed for that particular set of variables, and the next data card is processed. There is another exit system built in the program by instructions 14 and 18, which tests whether intermediate-2 (INT2) and intermediate-5 (INT5) are different than zero, respectively. If one of them is negative, then it can not be exponentiated as the subsequent instructions demand. In that case instructions 26 and 27 are followed, and a comment, "Make Increments Smaller", is printed, and the next data card is processed.

The whole process continues until all the data cards in the file are processed as demanded by instruction 1, and then a comment, "End of the Data File", is printed.

Instructions 36 through 41 provide the format for reading the data in computer, the format for printing out the results, and to declare the integers used in the program.

Considerations in the Selection of Constants

Except the solubility product of hydroxyapatite, K_{HAP}, the values for most of the thermodynamic* equilibrium constants required in this study are known accurately. However, the values for these constants will be different at various ionic strengths. So, it was decided to correct the thermodynamic values for the ionic strength effect in the range of 0.1 to 0.2 with the appropriate activity coefficients.

In Table 1 is given a set of thermodynamic values. Except for K_{HAP}, the thermodynamic constants are based on the values suggested by Brown (22) or taken from the tabulations of Robinson and Stokes (23). Even within a given sample, thermodynamic solubility product values for hydroxyapatite range from $1x10^{-120}$ to $1x10^{-110}$ (24). Therefore, four different values of K_{HAP} were selected as indicated in the Table 1.

The values given in Table 2 are the activity coefficient corrected values for ionic strengths between 0.1 and 0.2. Activity coefficient values for Ca^{2+} (0.36), $HPO_4^{=}$ (0.23), and $H_2PO_4^{-}$ (0.62) were taken from Levinskas and

---

* Infinite dilution values, i.e., activity coefficient = unity.

TABLE 1

THERMODYNAMIC CONSTANTS

FOR THEORETICAL CALCULATIONS

K_{2P} (phosphoric)	6.33×10^{-8} Moles per Liter
K_{3P} (phosphoric)	4.73×10^{-13}
K_A (chloracetic)	1.40×10^{-3}
K_A (lactic)	1.39×10^{-4}
K_A (acetic)	1.75×10^{-5}
K_W	2.57×10^{-14}*
K_{HAP}	1.0×10^{-120}
	1.0×10^{-116}
	1.0×10^{-113}
	1.0×10^{-108}

* value at 37°C.

TABLE 2

CONCENTRATION EQUILIBRIUM CONSTANTS ESTIMATED FOR IONIC STRENGTHS = 0.1-0.2

K_{2P} (phosphoric)	2.0×10^{-7} Moles per Liter
K_w	4.1×10^{-14}*
K_{HAP}	6.3×10^{-110}
	6.3×10^{-106}
	6.3×10^{-103}
	6.3×10^{-98}
$K_{3P}^6 K_w^2 / K_{HAP}$	1.6×10^{11}*
	1.6×10^{7} *
	1.6×10^{4} *
	1.6×10^{-1}*
K_A (chloracetic)	1.9×10^{-3}
K_A (lactic)	2.0×10^{-4}
K_A (acetic)	2.2×10^{-5}
K_A ('X'acid)	1.0×10^{-6}**

* K_w at 37°C. is used.

** Arbitrarily selected acid.

Neuman (25) and Strates, Neuman and Levinskas (26). The activity coefficients for H^+ (0.83) and for OH^- (0.76) were estimated from Kielland's tables (27).

The values given in the Tables 1 and 2 are for 25°C., except where indicated otherwise. For theoretical computations Table 2 values were used throughout this study. Although concentration K_{HAP} values of Table 2 were used in actual computations for discussion purposes only the thermodynamic K_{HAP} values will be mentioned in future.

Variables Used in the Computation of Gh

In computing Gh's in absence of common ions, i.e., $[TP]_h = [Ca^{2+}]_h = 0$, the variables with their values employed were as follows:

1. pH, taking values of 4.0, 4.5, 5.0 and 6.0,
2. Total buffer concentration, $[TB]_h$, taking values of 0.005, 0.01, 0.025, 0.05, 0.075, 0.1, 0.175, 0.25, 0.375, and 0.5 Moles per Liter,
3. Dissociation constant of acid, K_A, as shown in Table 2,

and 4. Solubility product of hydroxyapatite, K_{HAP}, taking values as indicated in Table 2.

Whereas, in computing Gh's in the presence of common ions two more variables, namely,

5. Total phosphate concentration, $[TP]_h$, taking

values of 0.003, 0.0065, 0.01, 0.025, and 0.05 Moles per Liter,

and 6. Calcium ion concentration, $[Ca^{2+}]_h$, assuming values same as variable 5,

were used in addition to the first four variables, except that now the variable 2 assumed values 0.005, 0.05, and 0.5 Moles per Liter. Only one common ion was studied at a time, the ion being either calcium or phosphate. All these computations were made, employing the computer program described earlier, for equations 3 and 4 in which all diffusion coefficient values were set to $1x10^{-5}$ $cm.^2/sec.$.

To study the effect of varying values of diffusion coefficients for different species on the calculated Gh, programs were written for equations similar to equations 3 and 4 but differing in the values of the diffusion coefficient employed. Five different cases were considered:

Case I. All diffusion coefficient values set equal to $1x10^{-5}$ $cm.^2/sec.$,

Case II. $D_H = 3x10^{-5}$ and all other D's = $1x10^{-5}$ $cm.^2/sec.$,

Case III. $D_H = 1x10^{-4}$ and all other D's = $1x10^{-5}$ $cm.^2/sec.$,

Case IV. $D_H = 3x10^{-5}$, $D_{Ca} = 2x10^{-5}$, and all other D's = $1x10^{-5}$ $cm.^2/sec.$,

and Case V. $D_H = 3x10^{-5}$, $D_{HP} = D_{H_2P} = 2x10^{-5}$, and all other D's = $1x10^{-5}$ $cm.^2/sec.$.

Case I is the familiar one, since all earlier studies were done with this set of diffusion coefficients. Moreover, this case was also used to compute Gh's in hydrochloric acid solutions, wherein hydrogen ion concentration varied from $1x10^{-4}$ to $5x10^{-1}$ Moles per Liter, $[TB]_h = 0$, K_A = very large, and with and without the presence of several concentrations of either of the two common ions.

Cases II, III, IV and V were used to study Gh's, in acetic acid buffers, wherein pH = 4.5, 5.0, and 6.0, $[TB]_h$ varied from 0.005 to 0.5 Moles per Liter, $K_A = 2.2x10^{-5}$, $K_{HAP} = 1x10^{-120}$, without the presence of common ions. These last four cases were used to make similar studies in hydrochloric acid at different hydrogen ion concentrations without the presence of common ions at $K_{HAP} = 1x10^{-120}$.

Results of the Theoretical Study

Theoretical Study in the Absence of Common Ions

Results of the study without common ions are plotted as the product Gh versus total buffer concentration for the four acids at various pH values and various K_{HAP} values for hydroxyapatite in Figures 4, 5, 6, and 7. It is seen that Gh-total buffer concentration relationship becomes more and more linear as one goes from the acid with smaller dissociation constant e.g., acid 'X' ($K_A=1x10^{-6}$, Figure 7), to the acid with larger dissociation constant

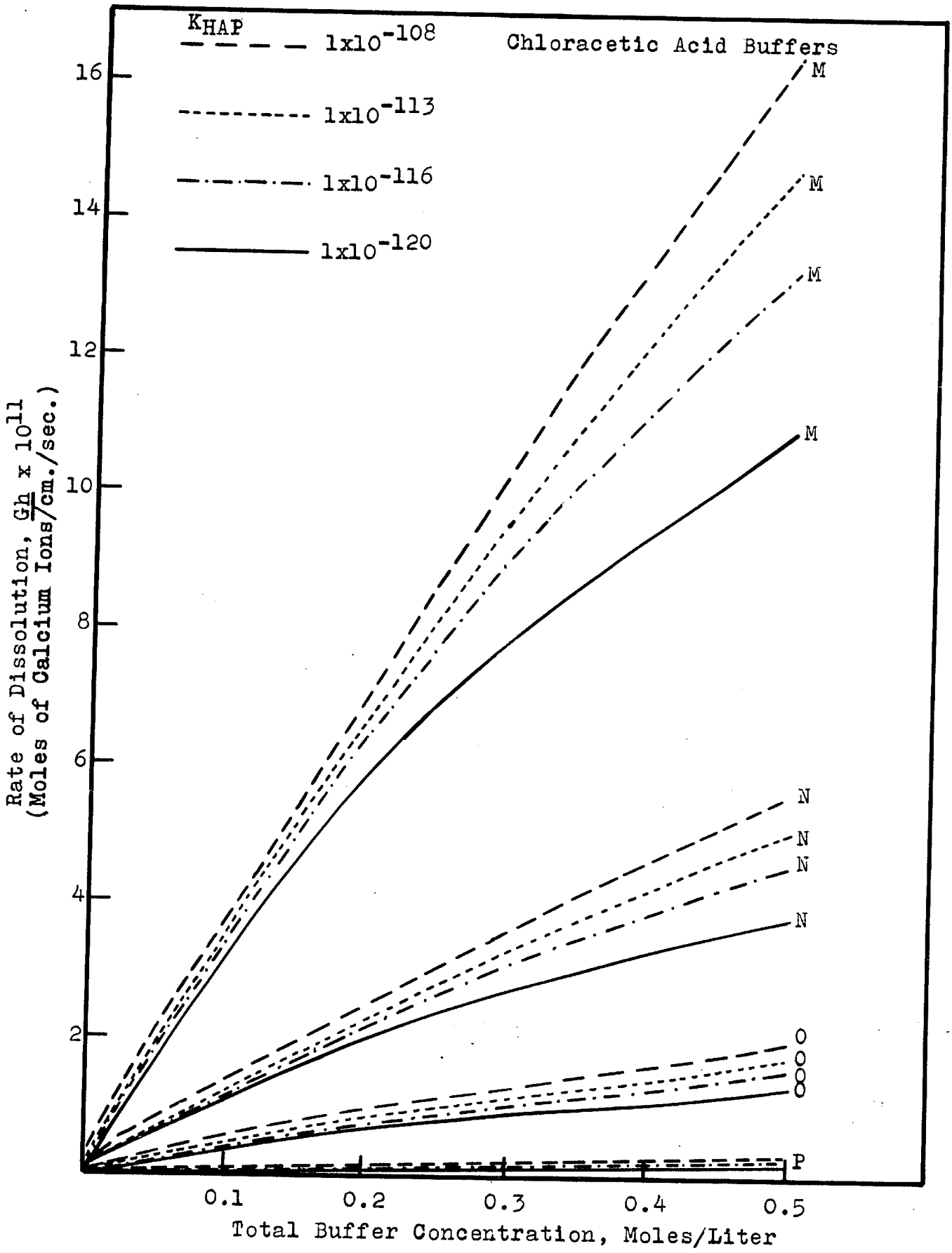

Figure 4.- Theoretical Dissolution Rates of Enamel in Chloracetic Acid Buffers as a Function of $[TB]_h$; pH; and K_{HAP}. M = pH 4.0; N = pH 4.5; O = pH 5.0; and P = pH 6.0.

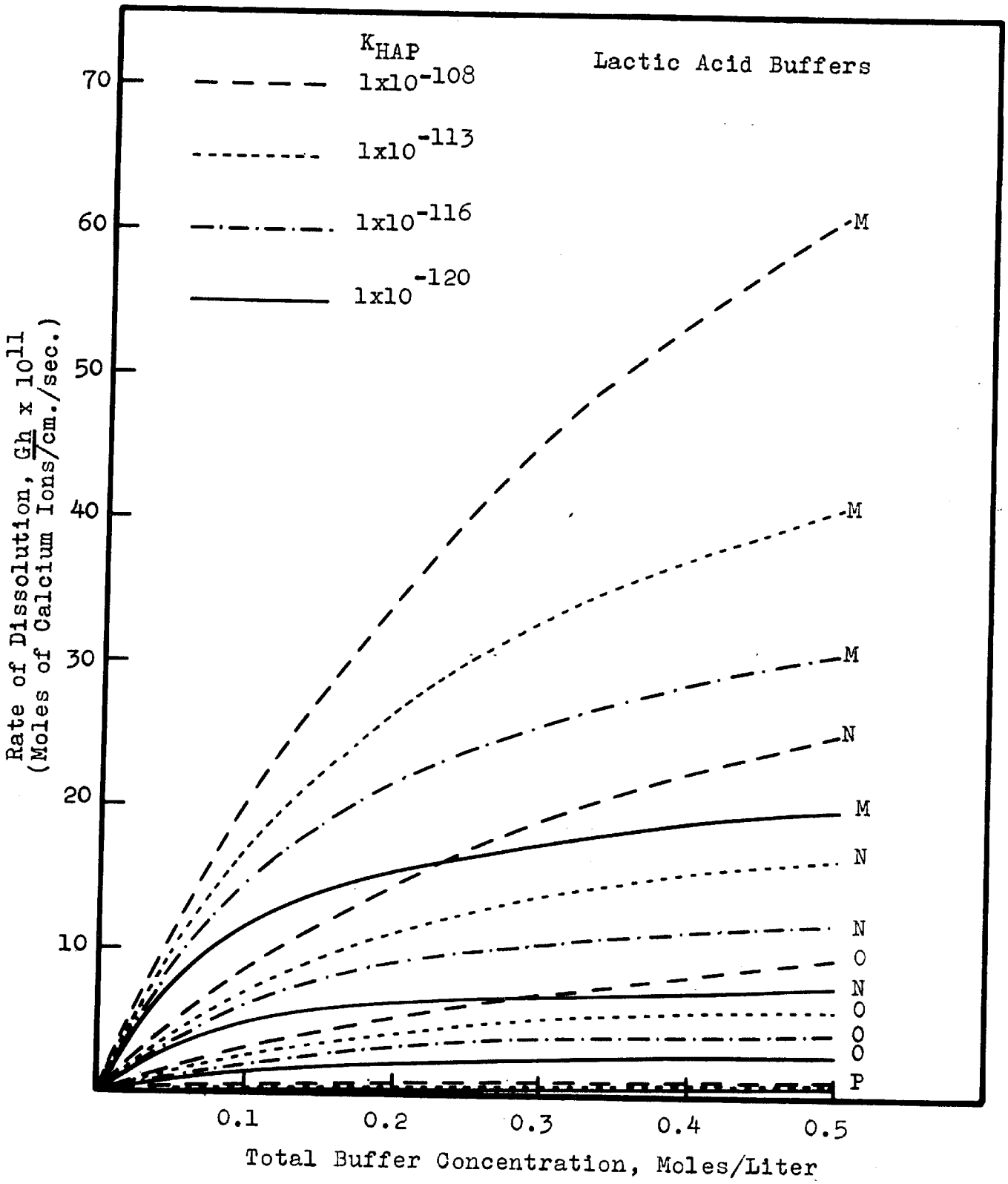

Figure 5.- Theoretical Dissolution Rates of Enamel in Lactic Acid Buffers as a Function of $[TB]_h$; pH; and K_{HAP}. M = pH 4.0; N = pH 4.5; O = pH 5.0; and P = pH 6.0.

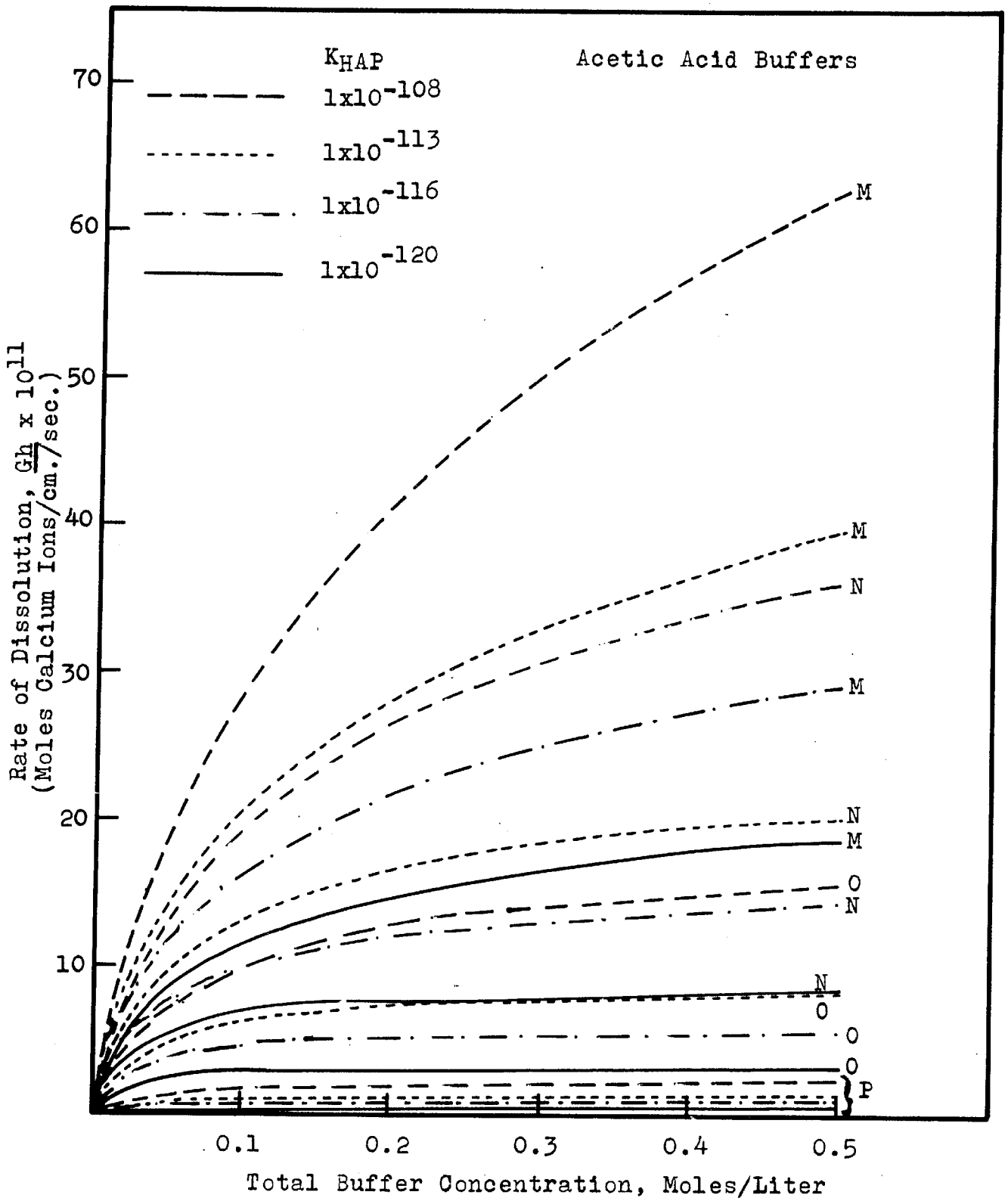

Figure 6.- Theoretical Dissolution Rates of Enamel in Acetic Acid Buffers as a Function of $[TB]_h$; pH; and K_{HAP}. M = pH 4.0; N = pH 4.5; O = pH 5.0; and P = pH 6.0.

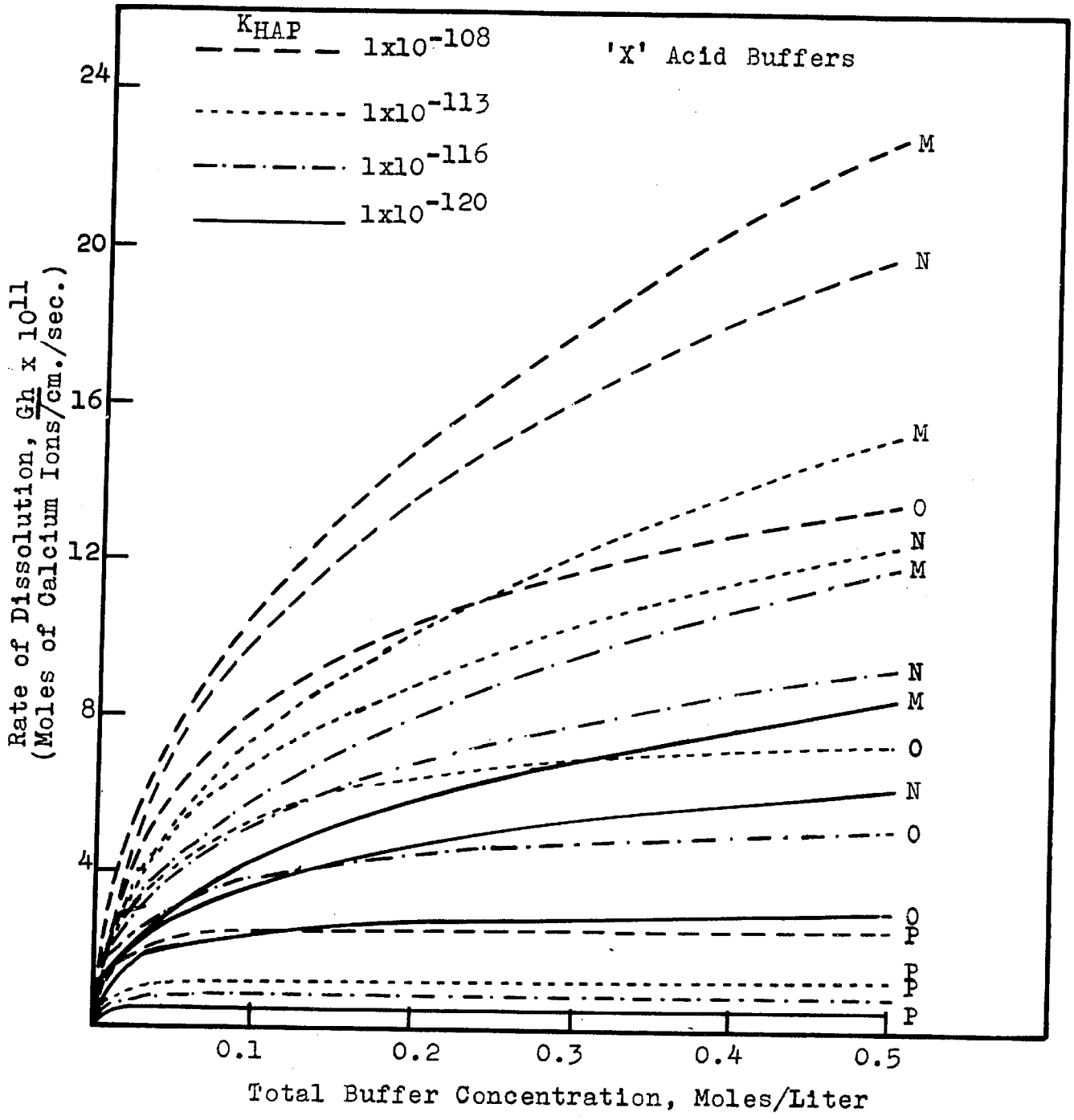

Figure 7.- Theoretical Dissolution Rates of Enamel in 'X' Acid Buffers as a Function of $[TB]_h$; pH; and K_{HAP}. M = pH 4.0; N = pH 4.5; O = pH 5.0; and P = pH 6.0.

e.g., chloracetic acid (K_A=1.9x10^{-3}, Figure 4). In all the acids studied at all pH values, the effect of increasing the value of K_{HAP} from 1x10^{-120} to 1x10^{-108}, is that of increasing the Gh value.

In Figure 8, values of Gh at different concentrations of hydrochloric acid are plotted at various K_{HAP} values. It is seen that there is negligible effect of increasing the K_{HAP} value on the Gh-hydrochloric acid concentration relationship, which is linear (K_A = very large).

Effects of varying diffusion coefficient values on Gh in acetic acid and hydrochloric acid are shown in Figures 9 and 10, respectively. In the case of acetic acid, the effect of increasing D_H from 1x10^{-5} (case I) to 3x10^{-5} (case II) and to 1x10^{-4} (case III) has no effect on Gh values. However, increasing D_{Ca} by a factor of two (case IV versus case III) and increasing D_{HP} and D_{H_2P} both by a factor of two (case V versus case III) show some increase in the Gh values. But if in cases IV and V the Gh values were normalized to case III values, in view of the uncertainty of h (hydrodynamic factor) to be discussed later, then it can be shown that these increased Gh values do not affect the general shape of the Gh-total buffer concentration relationship to any appreciable extent. On the other hand, Figure 10 shows that in hydrochloric acid diffusion of hydrogen ions is important as indicated by a proportionate increase in Gh as D_H is increased. Changing the values of D_{Ca}, D_{HP}, and D_{H_2P} have no importance in

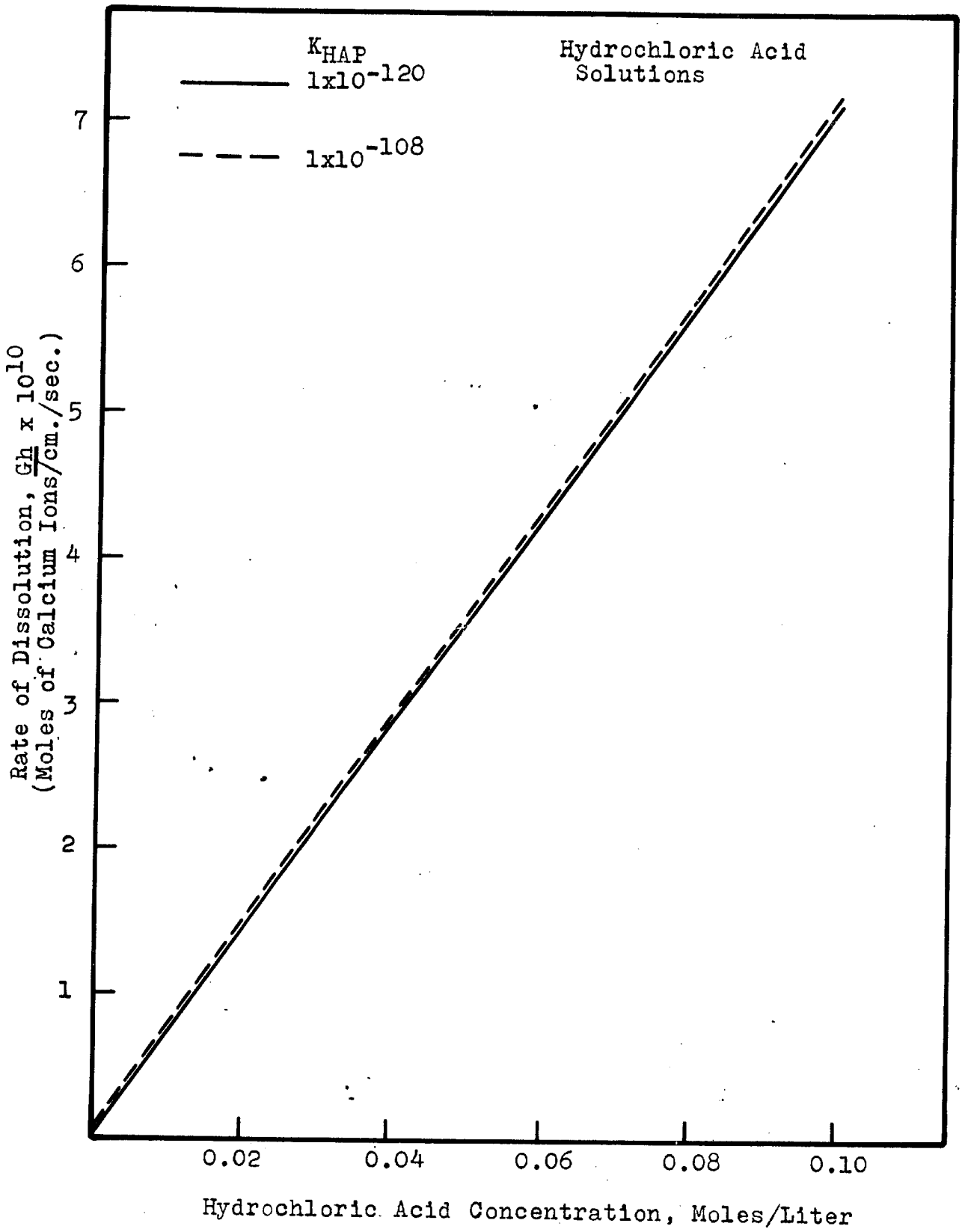

Figure 8.- Theoretical Dissolution Rates of Enamel in Hydrochloric Acid Solutions as a function of HCl concentration and K_{HAP}.

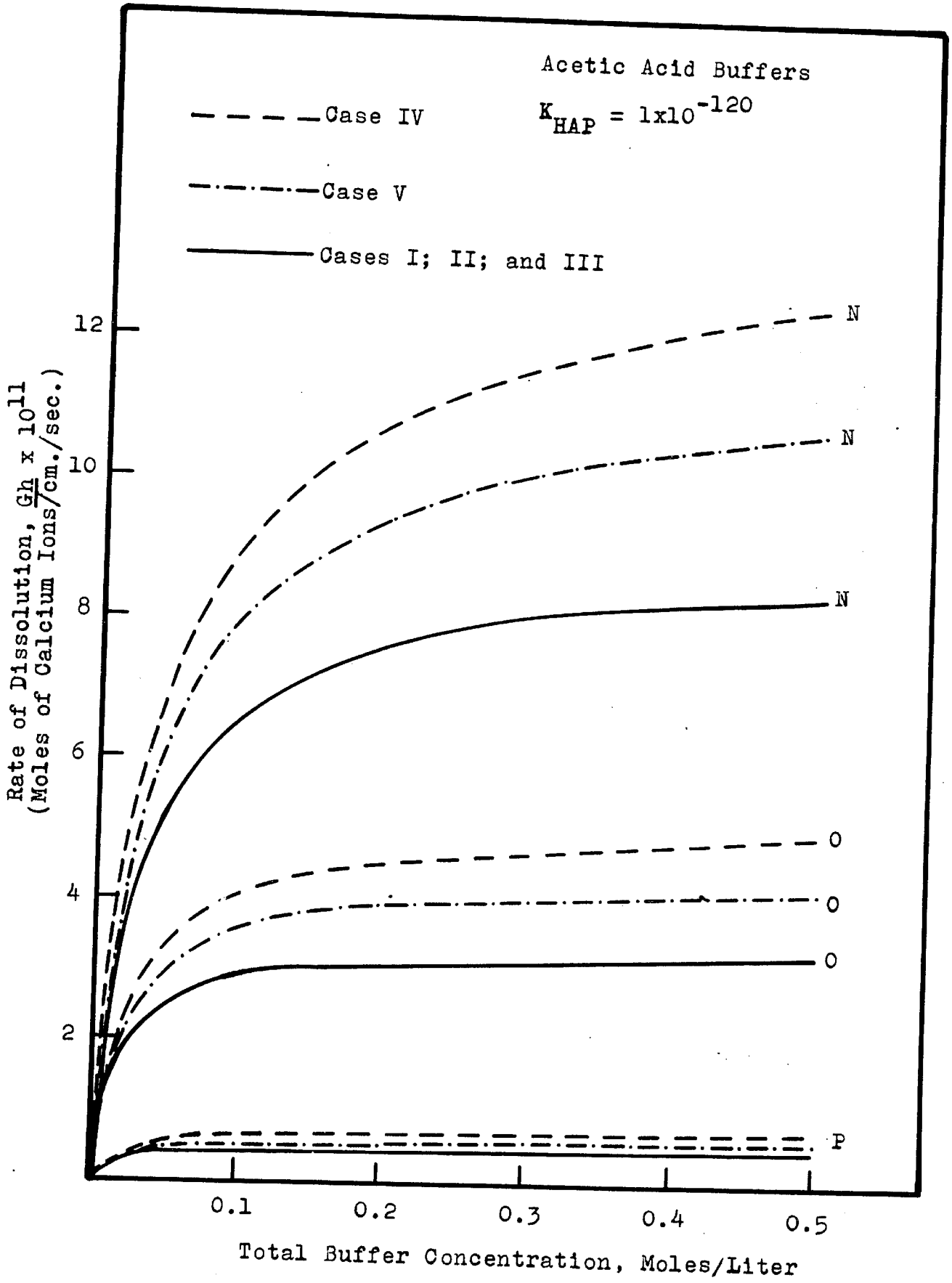

Figure 9.- Effects of varying Diffusion Coefficient Values of various Species on the Theoretical Dissolution Rates of Enamel in Acetate Buffers. Cases I-V. $K_{HAP} = 1x10^{-120}$. N=pH 4.5; O=pH 5.0; and P=pH 6.0.

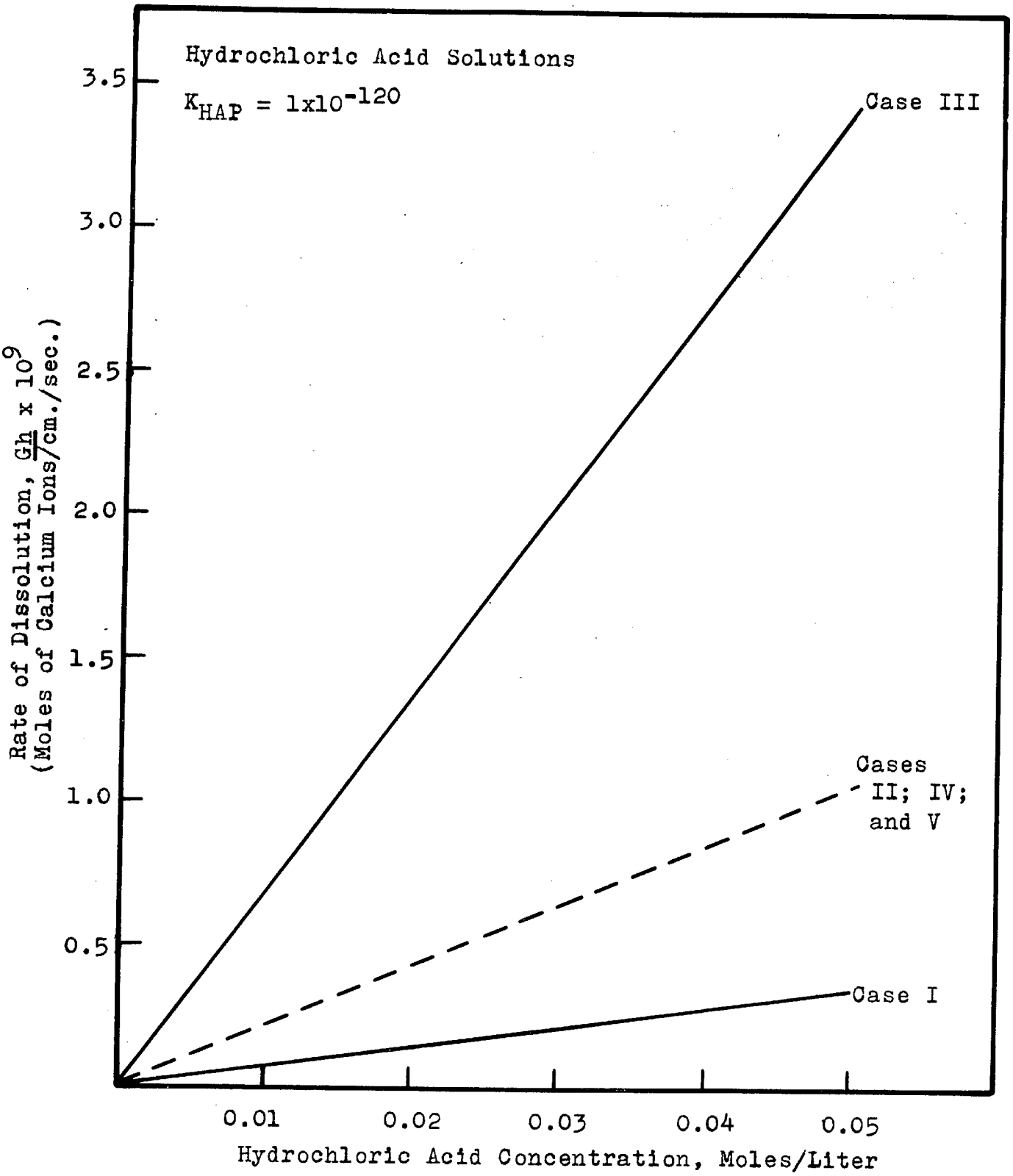

Figure 10.- Effects of varying Diffusion Coefficient values of various Species on the Theoretical Dissolution Rates of Enamel in Hydrochloric Acid Solutions. Cases I-V. K_{HAP} = 1x10^{-120}.

determining the Gh in the case of hydrochloric acid.

Theoretical Common Ion Study

Considering the realistic situation in oral cavity, saliva, containing 4-12 mg% calcium and 12-17 mg.% inorganic phosphorous (28), continuously bathes the teeth. That the presence of the common ions reduces the demineralization rate of enamel has been shown by several investigators (16, 29). In view of this it was decided to compute theoretical dissolution rates, Gh, in several acid buffers at various pH values and buffer concentrations in the presence of calcium and phosphate ions. The effect of calcium and phosphate ions was studied taking either one of them at a time in order to understand the effect of each common ion individually. Common ion concentrations in the range of 5×10^{-2} to 3×10^{-3} Moles per Liter were used, which includes the range in saliva as well as between the tooth surface and plaque (30).

Effects of calcium and phosphate ions on values of Gh are plotted as % of Gh for no common ion versus calcium ion concentration and total phosphate ion concentration as shown in Figures 11 to 27 and Figures 28 to 44, respectively. In these Figures, curves A, B, and C represent buffer at pH = 4.0 and buffer concentrations, $[TB]_h$ = 0.5, 0.05, 0.005 Moles per Liter, respectively; curves D, E, and F designate buffer at pH = 4.5 and $[TB]_h$ = 0.5, 0.05, and 0.005 Moles per Liter, respectively. Similarly, curves

G, H, and I as well as curves J, K, and L represent pH = 5.0 and 6.0, respectively, with $[TB]_h$ = 0.5, 0.05, and 0.005 Moles per Liter, respectively in each pH group. These designations are tabulated in Table 3.

TABLE 3

KEY FOR THE CURVES IN FIGURES 11-44

Curve	pH	$[TB]_h$
A	4.0	0.500 Moles/Liter
B	4.0	0.050
C	4.0	0.005
D	4.5	0.500
E	4.5	0.050
F	4.5	0.005
G	5.0	0.500
H	5.0	0.050
I	5.0	0.005
J	6.0	0.500
K	6.0	0.050
L	6.0	0.005

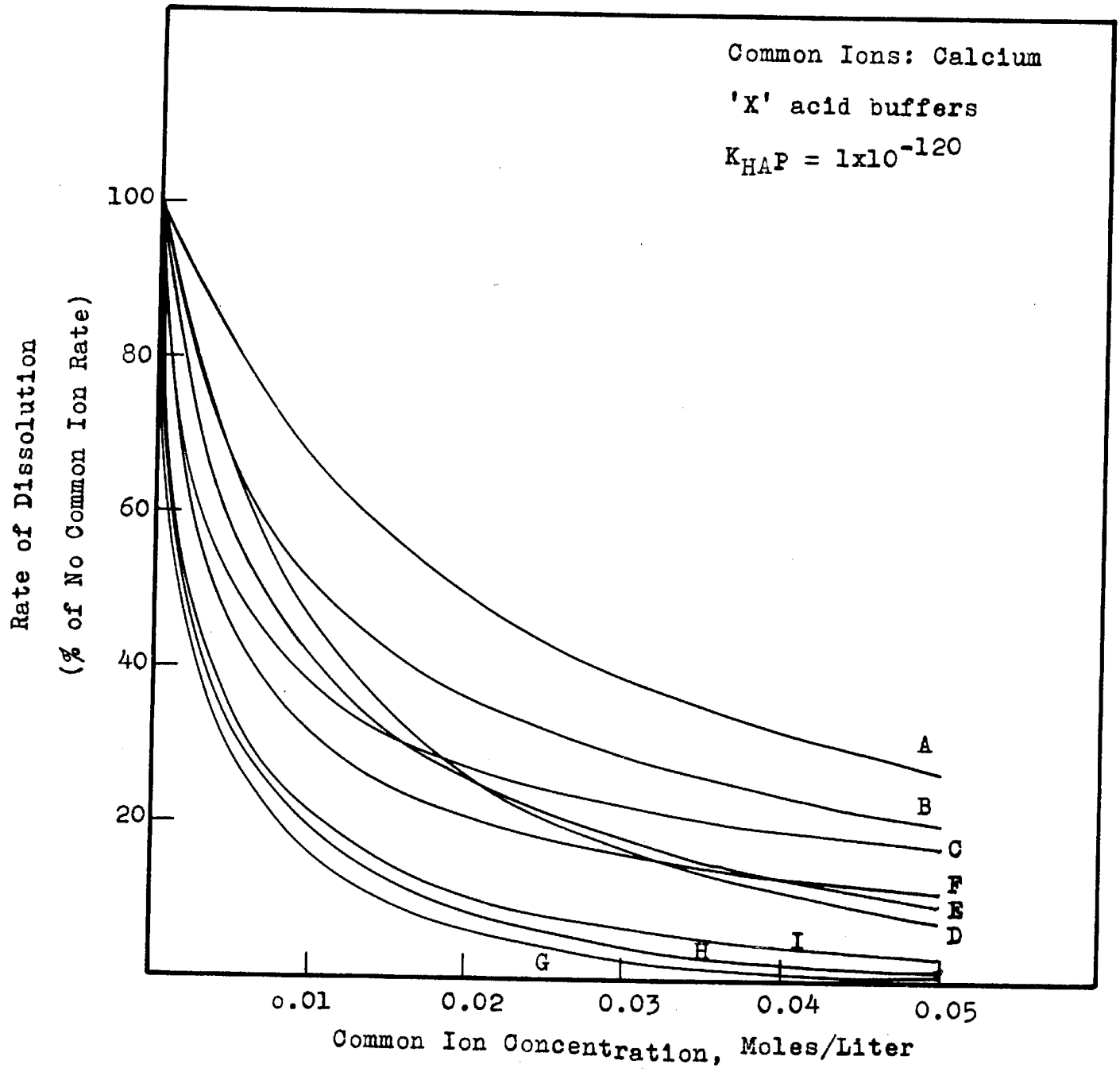

Figure 11.-- Effects of Calcium Ions on Theoretical Dissolution Rates in 'X' Acid Buffers. $K_{HAP} = 1x10^{-120}$.

See Table 3 for decoding the curves.

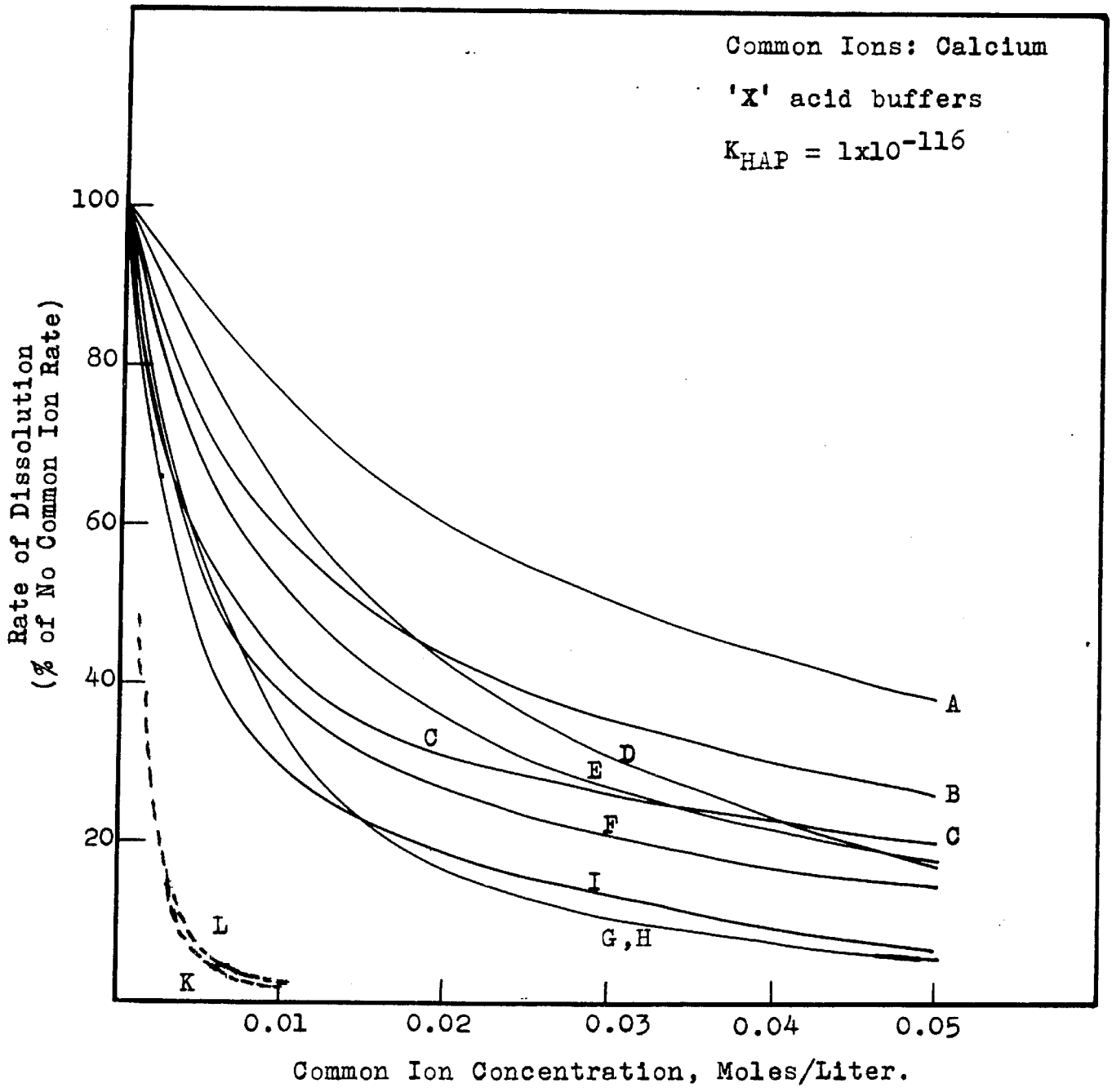

Figure 12.- Effects of Calcium Ions on Theoretical Dissolution Rates in 'X' Acid Buffers. $K_{HAP} = 1x10^{-116}$.

See Table 3 for decoding the curves.

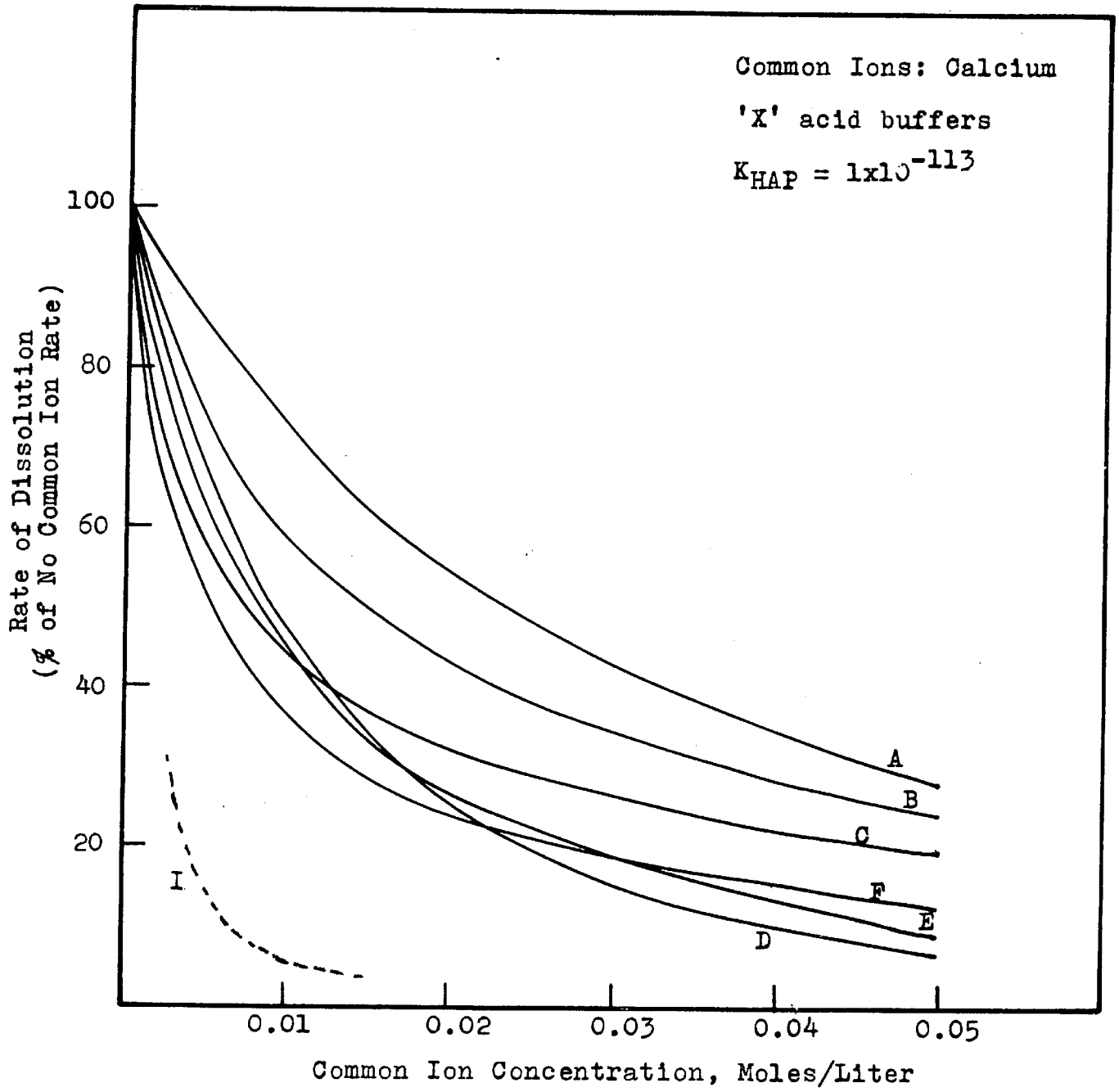

Figure 13.- Effects of Calcium Ions on Theoretical Dissolution Rates in 'X' Acid Buffers. $K_{HAP} = 1x10^{-113}$.

See Table 3 for decoding the curves.

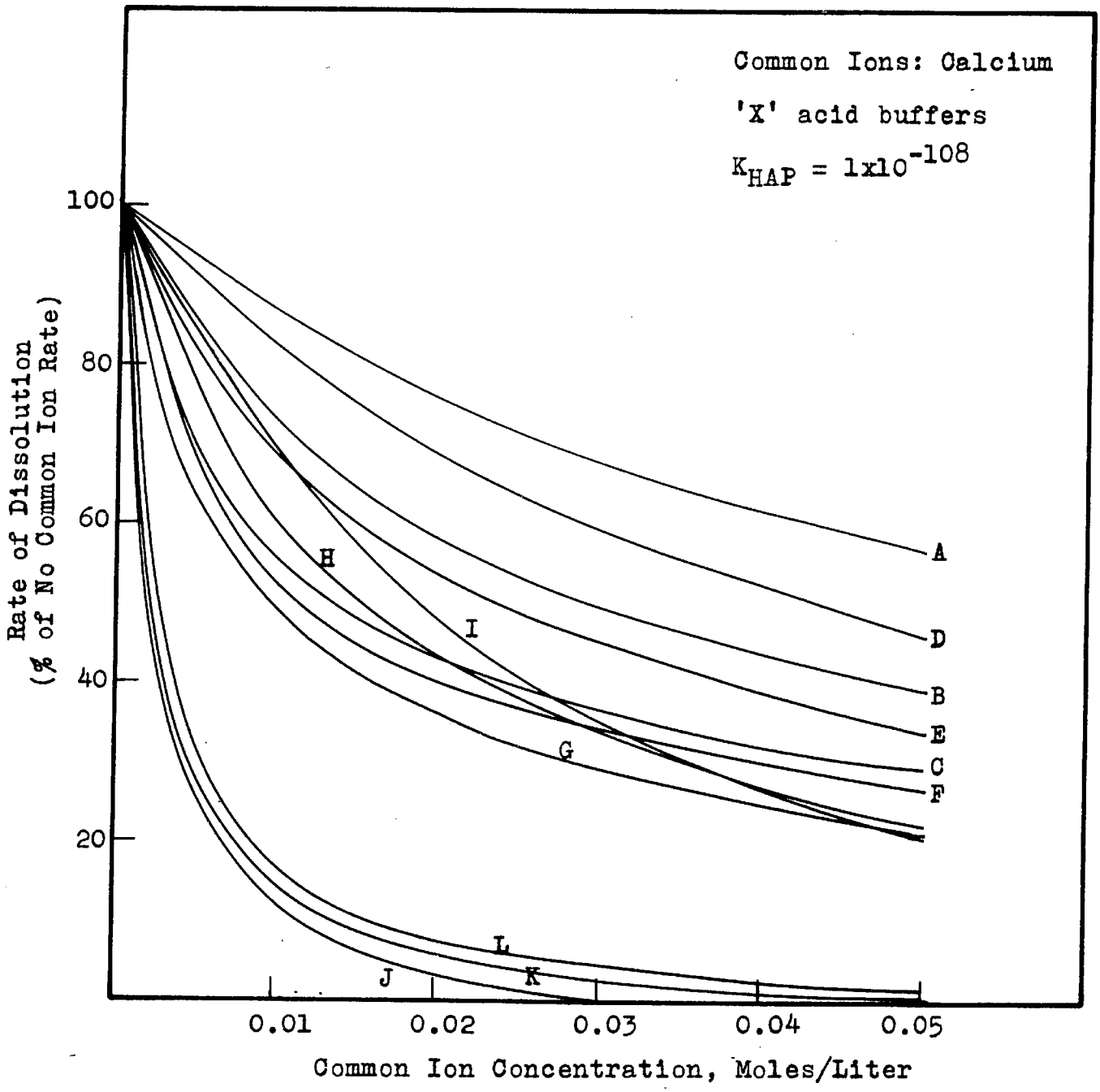

Figure 14.- Effects of Calcium Ions on Theoretical Dissolution Rates in 'X' Acid Buffers. $K_{HAP} = 1x10^{-108}$.

See Table 3 for decoding the curves.

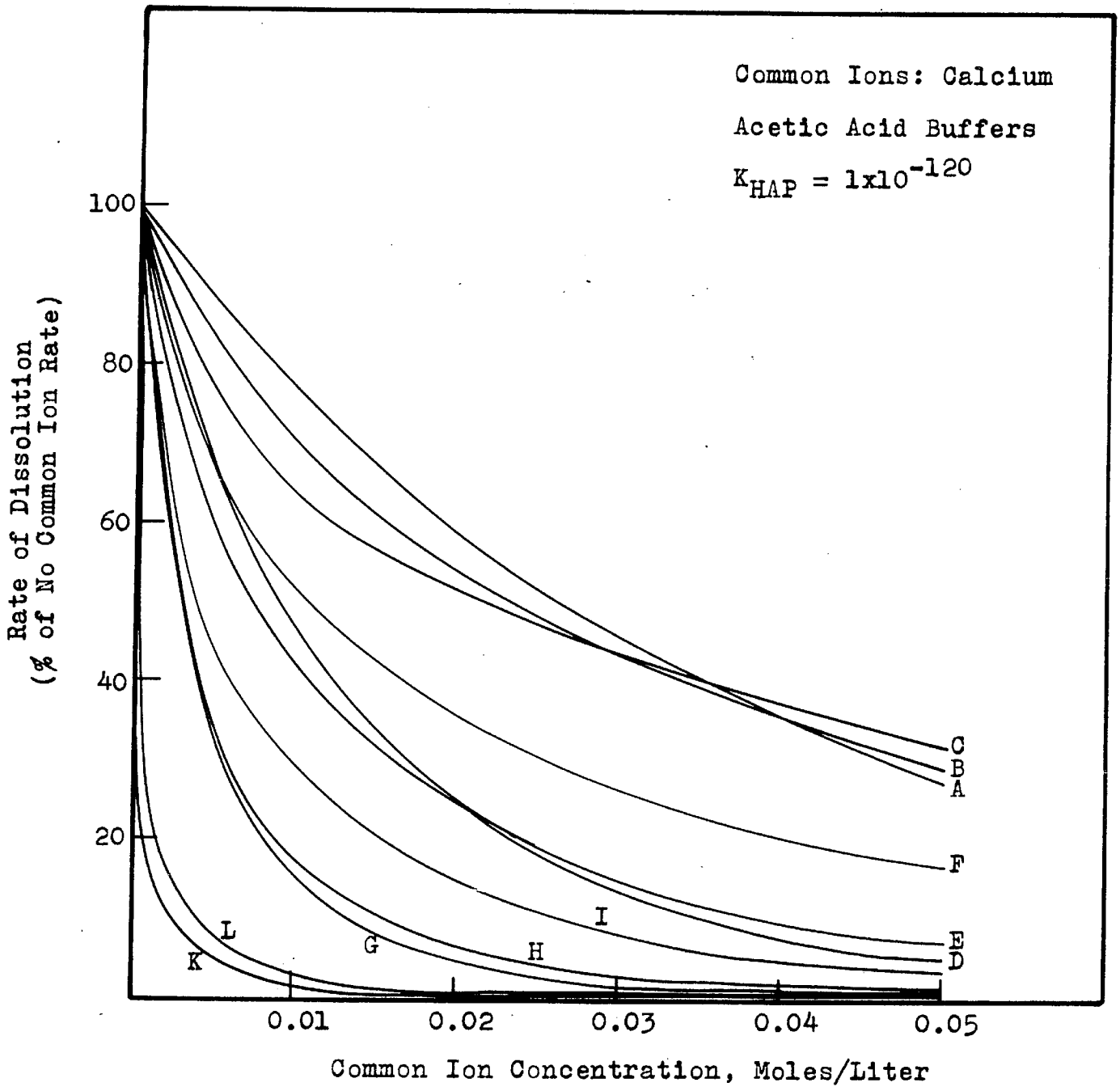

Figure 15.- Effects of Calcium Ions on Theoretical Dissolution Rates in Acetic Acid Buffers. $K_{HAP} = 1x10^{-120}$.

See Table 3 for decoding the curves.

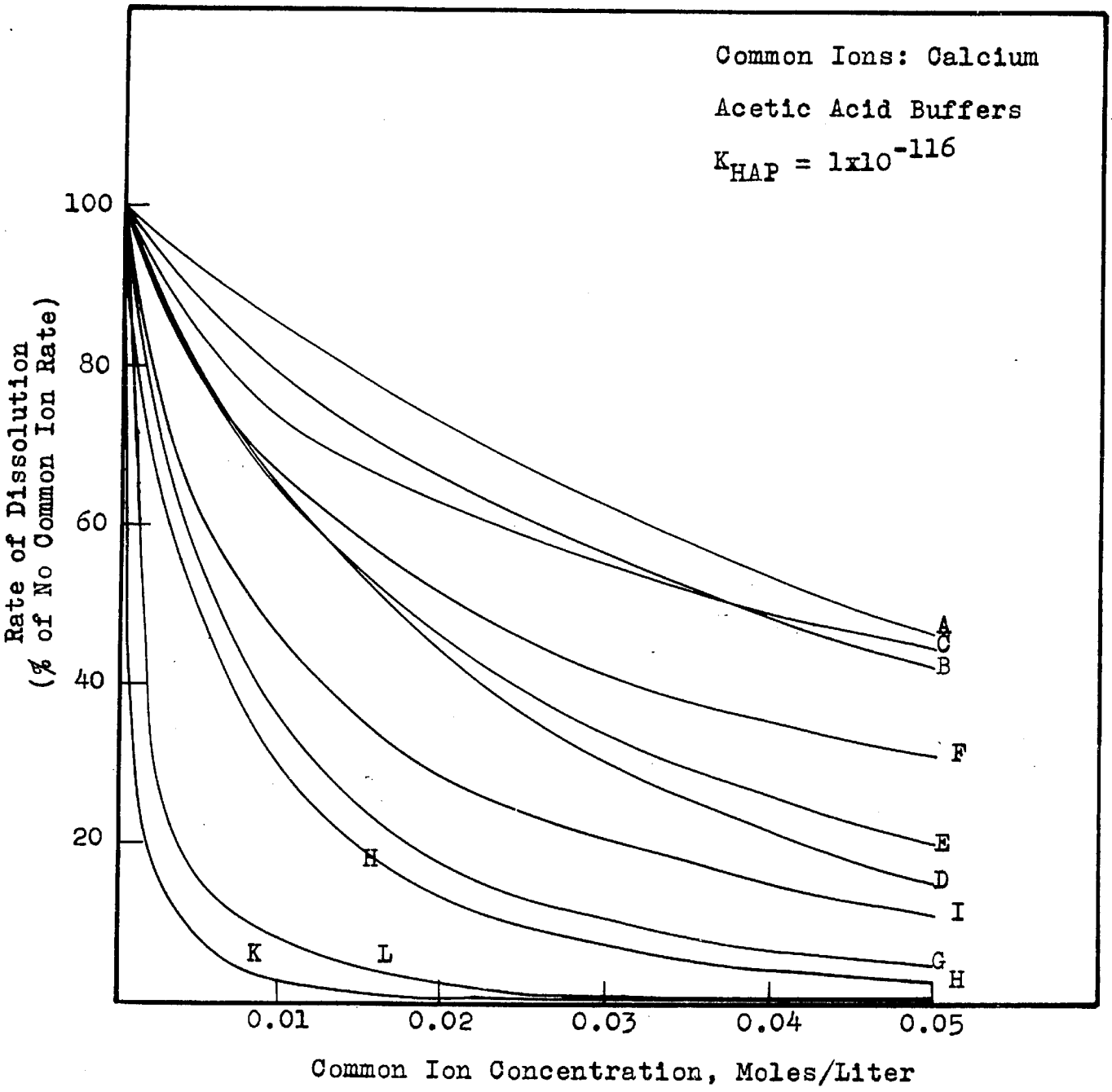

Figure 16.- Effects of Calcium Ions on Theoretical Dissolution Rates in Acetic Acid Buffers. $K_{HAP} = 1x10^{-116}$.

See Table 3 for decoding the curves.

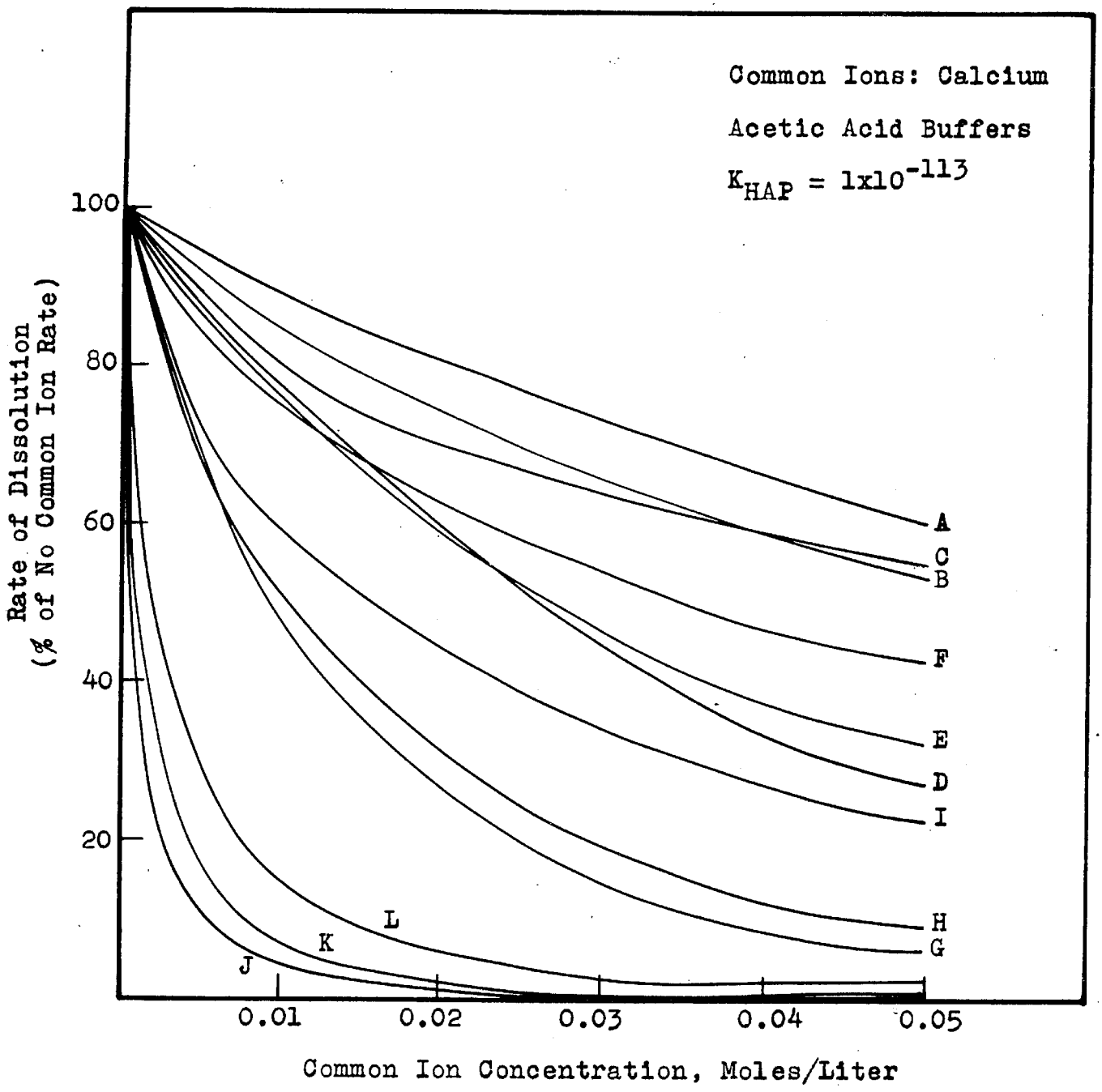

Figure 17.- Effects of Calcium Ions on Theoretical Dissolution Rates in Acetic Acid Buffers. $K_{HAP} = 1x10^{-113}$.

See Table 3 for decoding the curves.

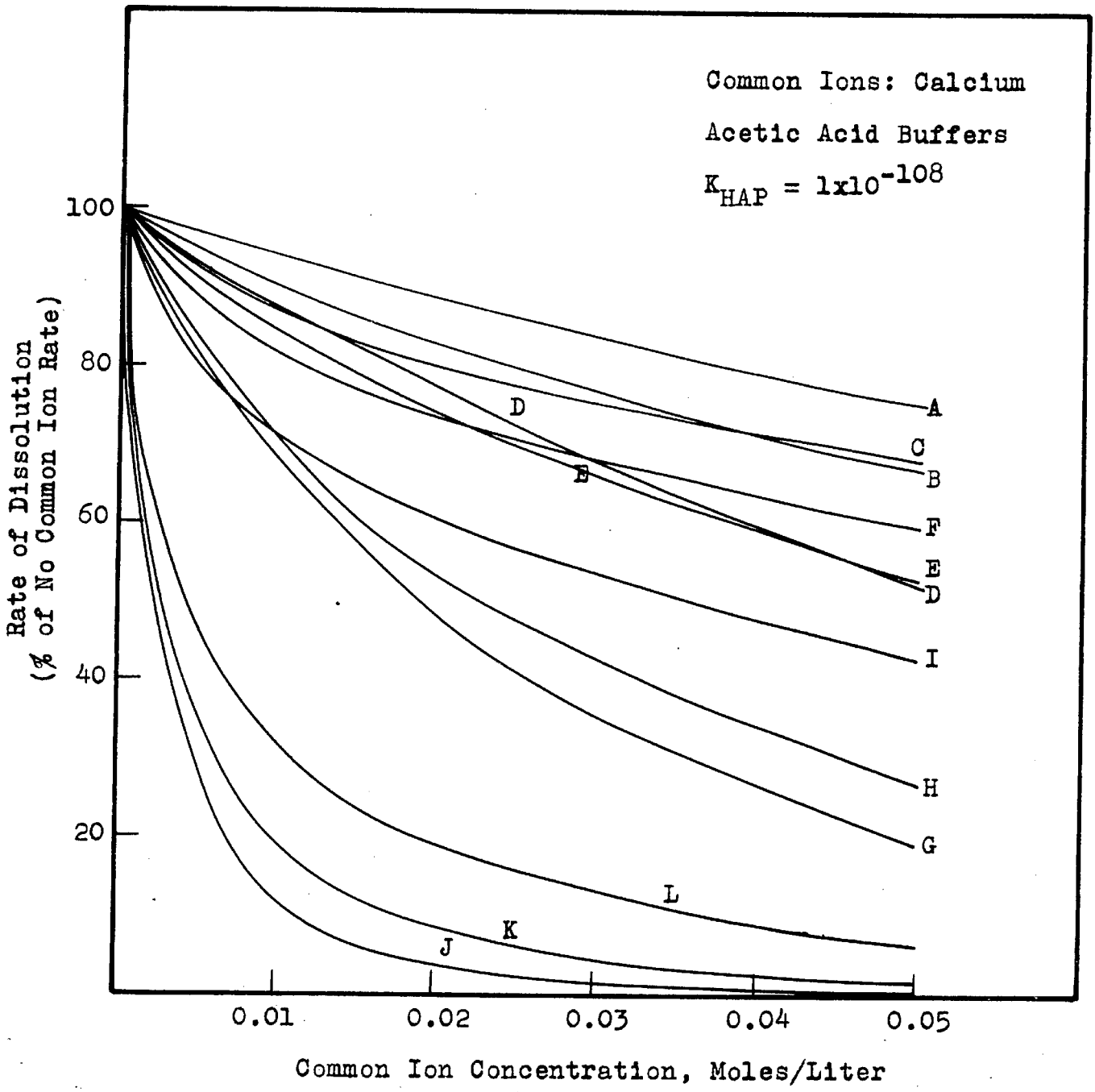

Figure 18.- Effects of Calcium Ions on Theoretical Dissolution Rates in Acetic Acid Buffers. $K_{HAP} = 1x10^{-108}$.

See Table 3 for decoding the curves.

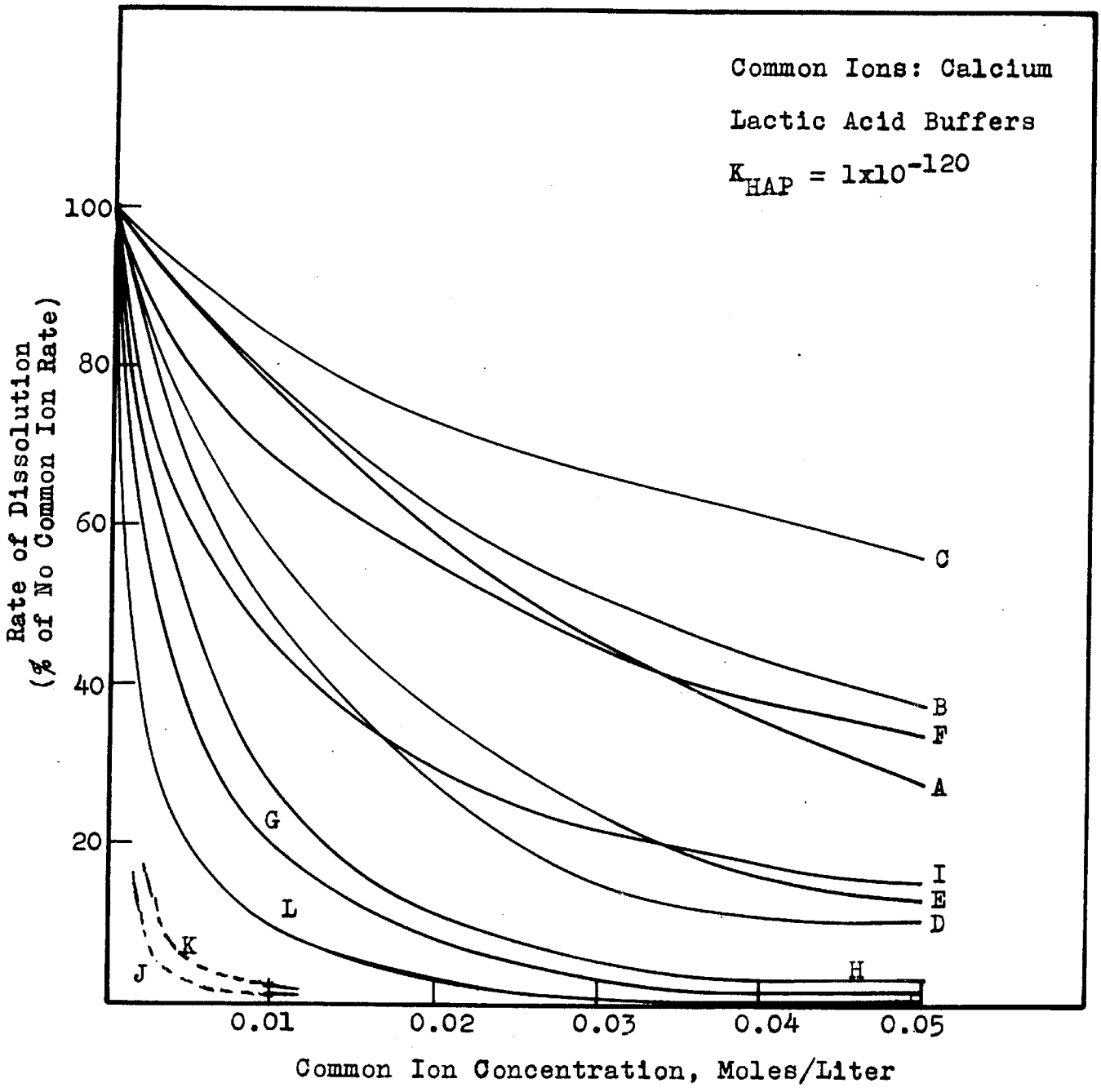

Figure 19.- Effects of Calcium Ions on Theoretical Dissolution Rates in Lactic Acid Buffers. $K_{HAP} = 1x10^{-120}$. See Table 3 for decoding the curves.

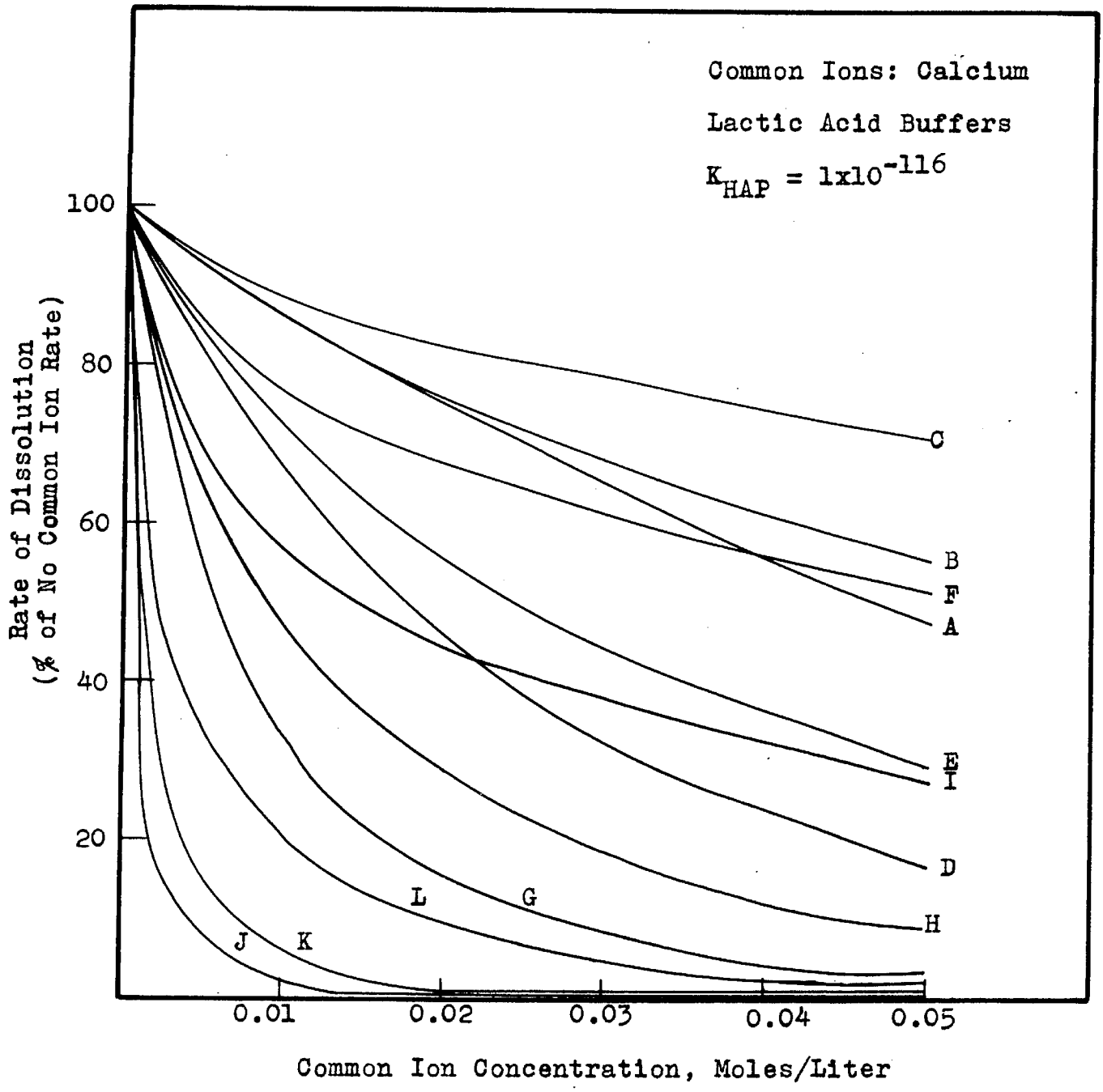

Figure 20.- Effects of Calcium Ions on Theoretical Dissolution Rates in Lactic Acid Buffers. $K_{HAP} = 1x10^{-116}$. See Table 3 for decoding the curves.

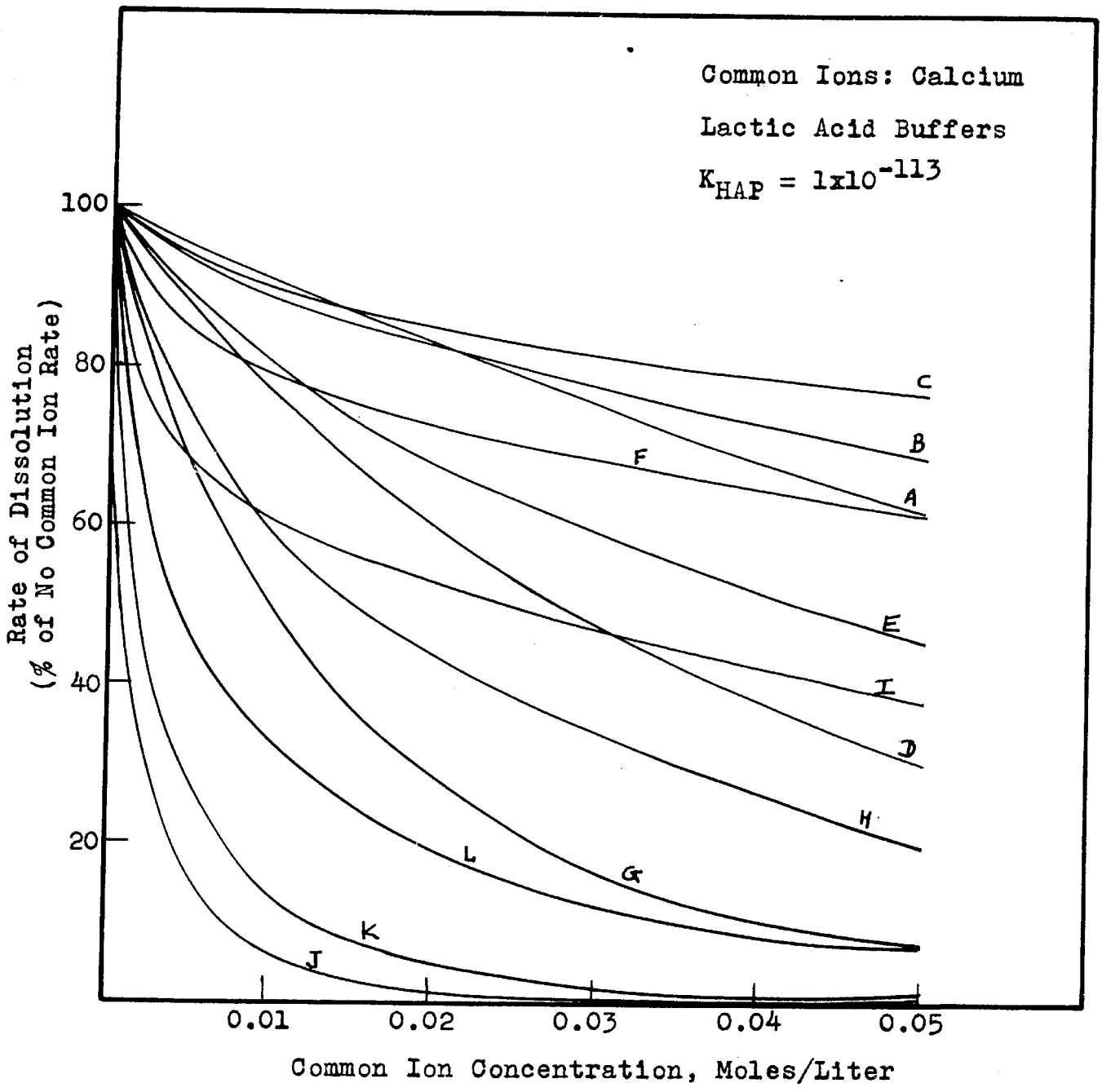

Figure 21.- Effects of Calcium Ions on Theoretical Dissolution Rates in Lactic Acid Buffers. $K_{HAP} = 1x10^{-113}$. See Table 3 for decoding the curves.

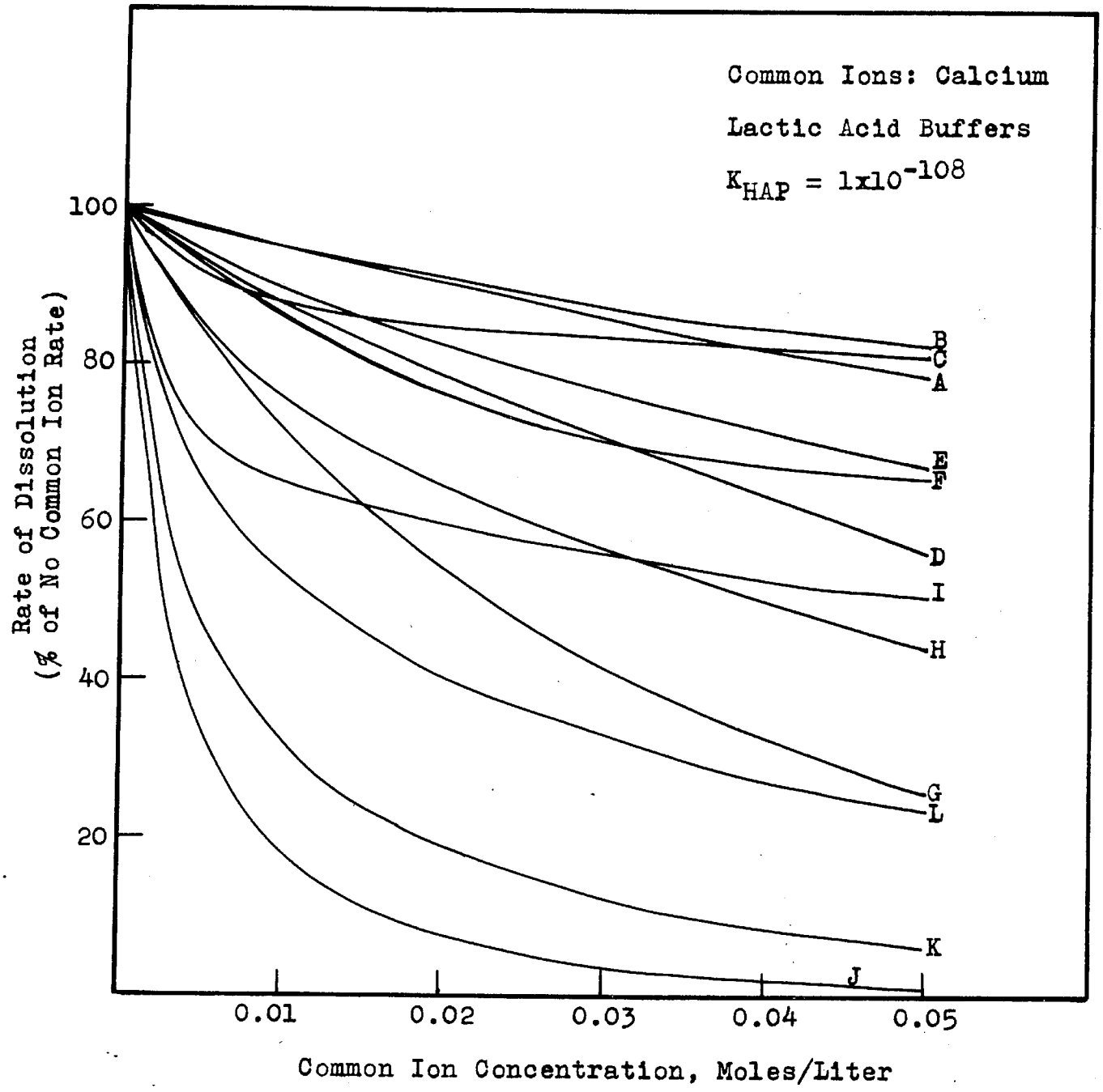

Figure 22.- Effects of Calcium Ions on Theoretical Dissolution Rates in Lactic Acid Buffers. $K_{HAP} = 1x10^{-108}$. See Table 3 for decoding the curves.

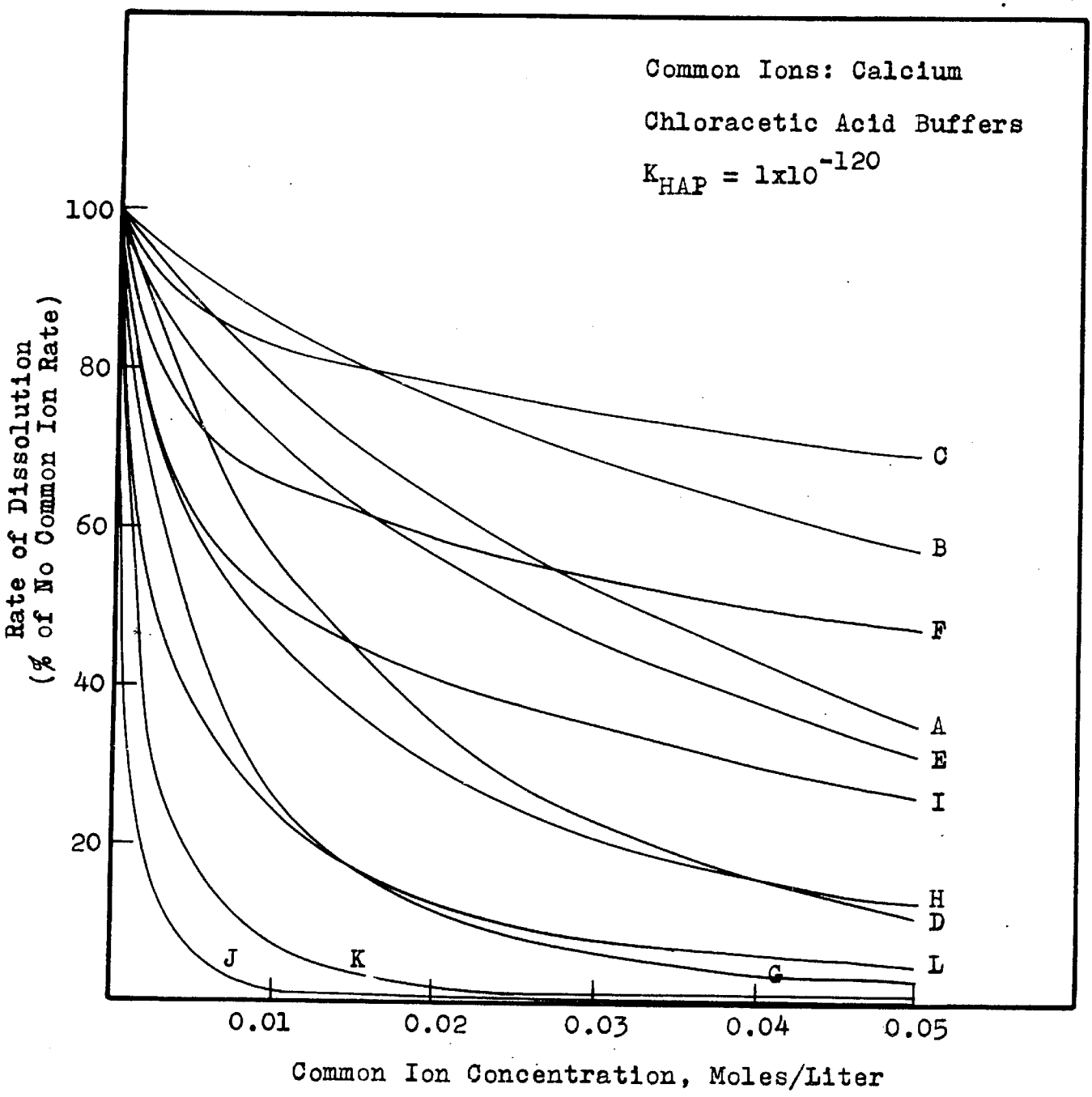

Figure 23.- Effects of Calcium Ions on Theoretical Dissolution Rates in Chloracetic Acid Buffers. $K_{HAP} = 1x10^{-120}$. See Table 3 for decoding the curves.

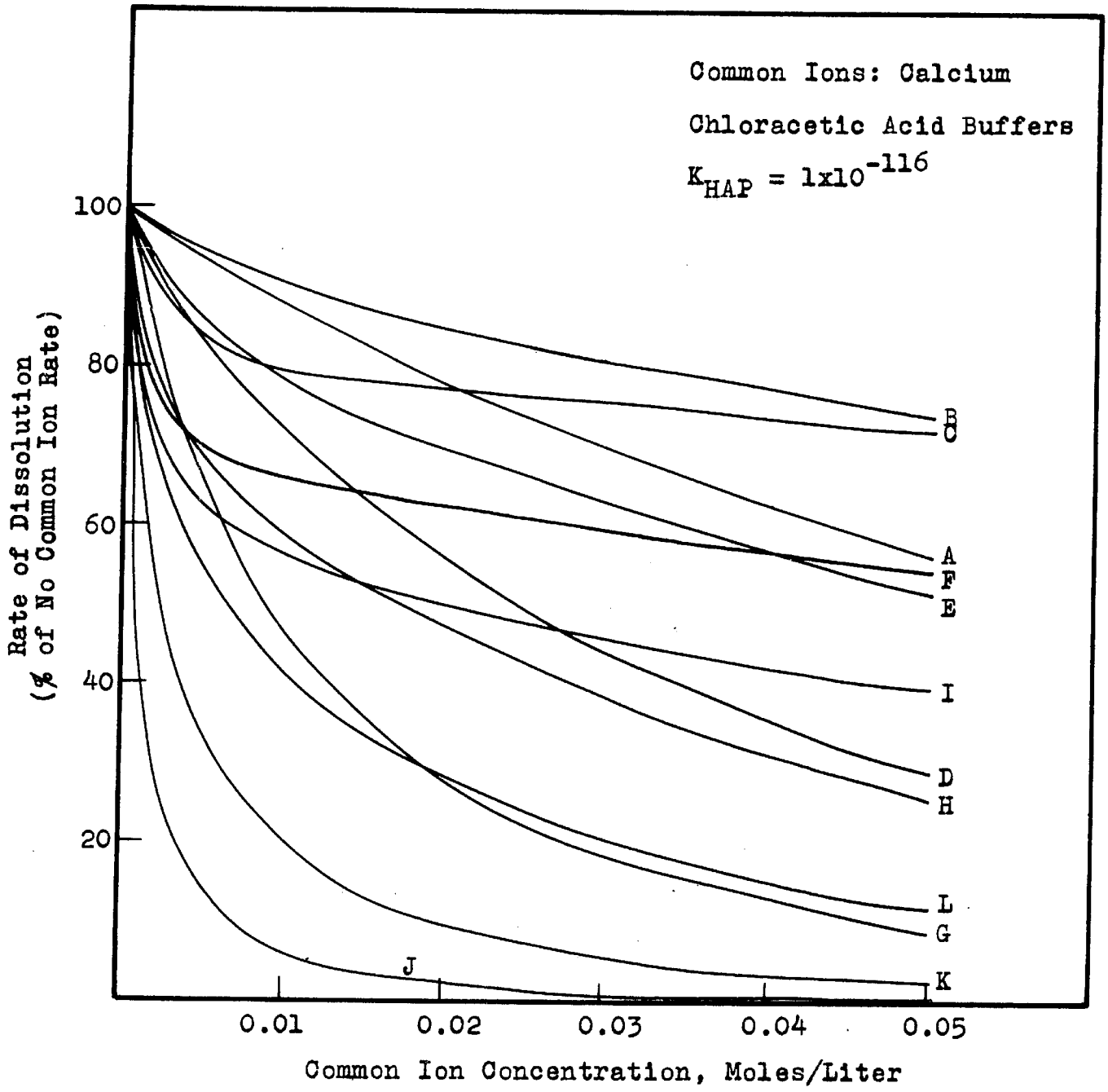

Figure 24.- Effects of Calcium Ions on Theoretical Dissolution Rates in Chloracetic Acid Buffers. $K_{HAP} = 1x10^{-116}$. See Table 3 for decoding the curves.

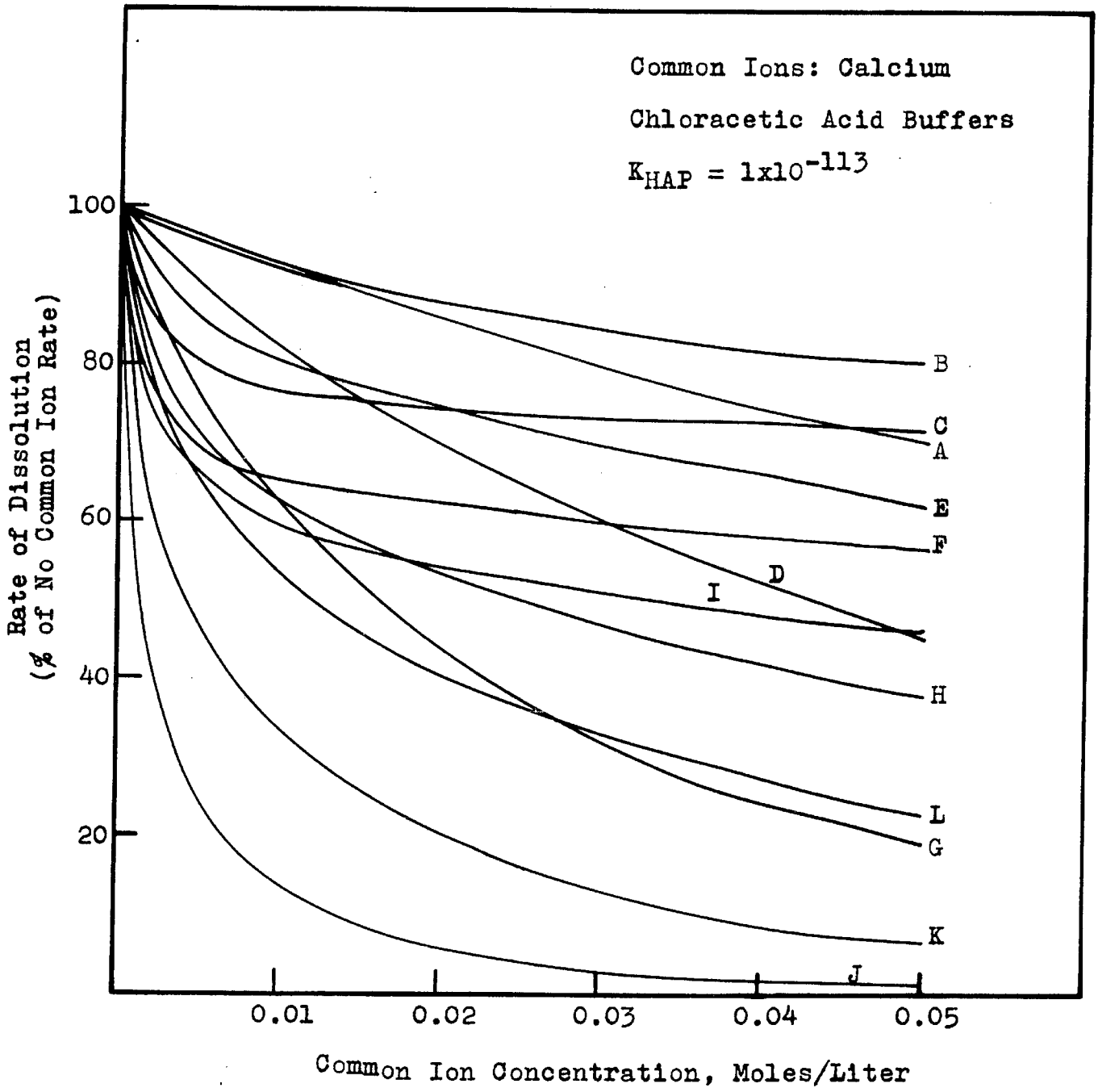

Figure 25.- Effects of Calcium Ions on Theoretical Dissolution Rates in Chloracetic Acid Buffers. K_{HAP} = 1x10^{-113}. See Table 3 for decoding the curves.

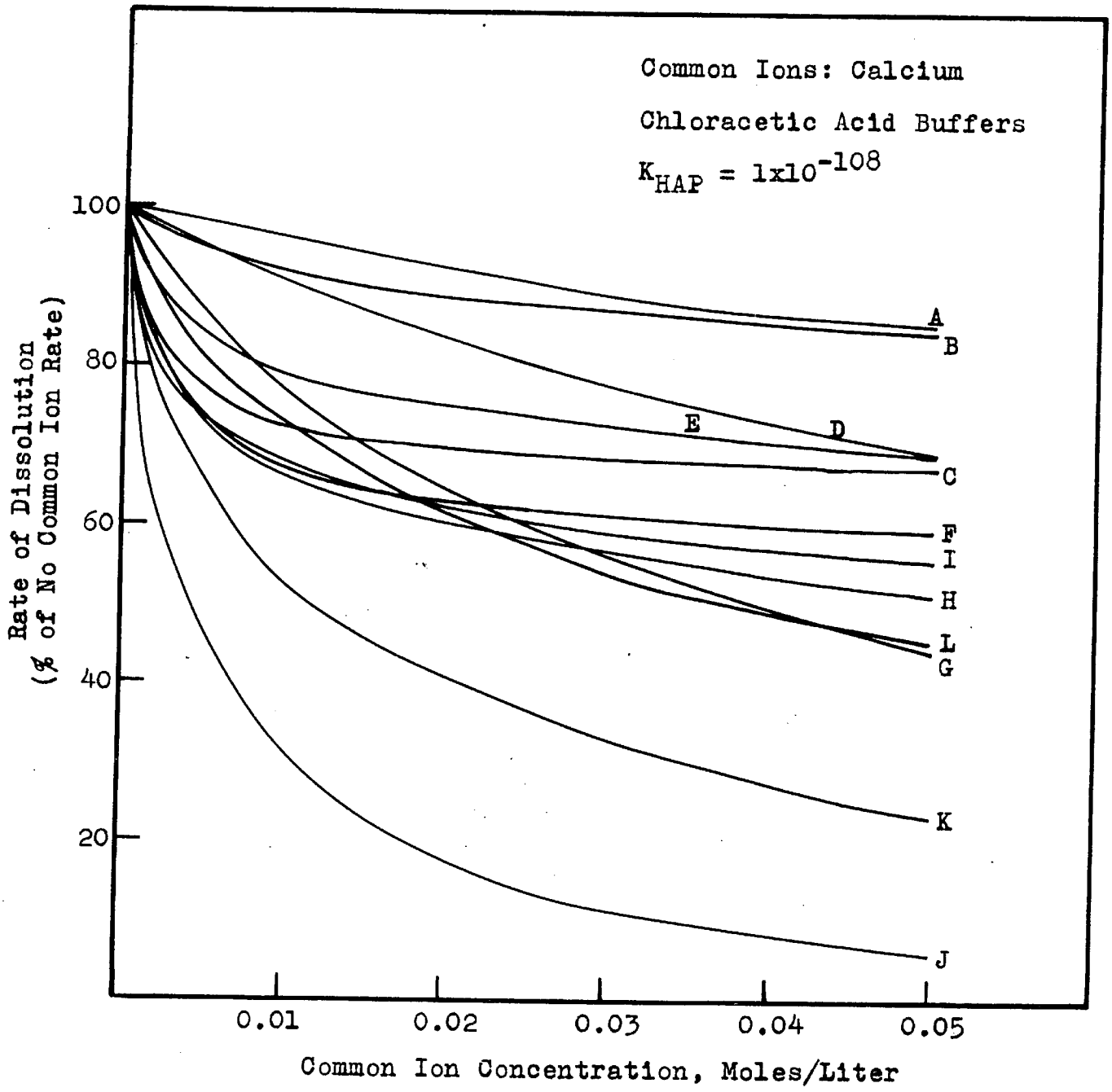

Fifure 26.- Effects of Calcium Ions on Theoretical Dissolution Rates in Chloracetic Acid Buffers. $K_{HAP} = 1x10^{-108}$. See Table 3 for decoding the curves.

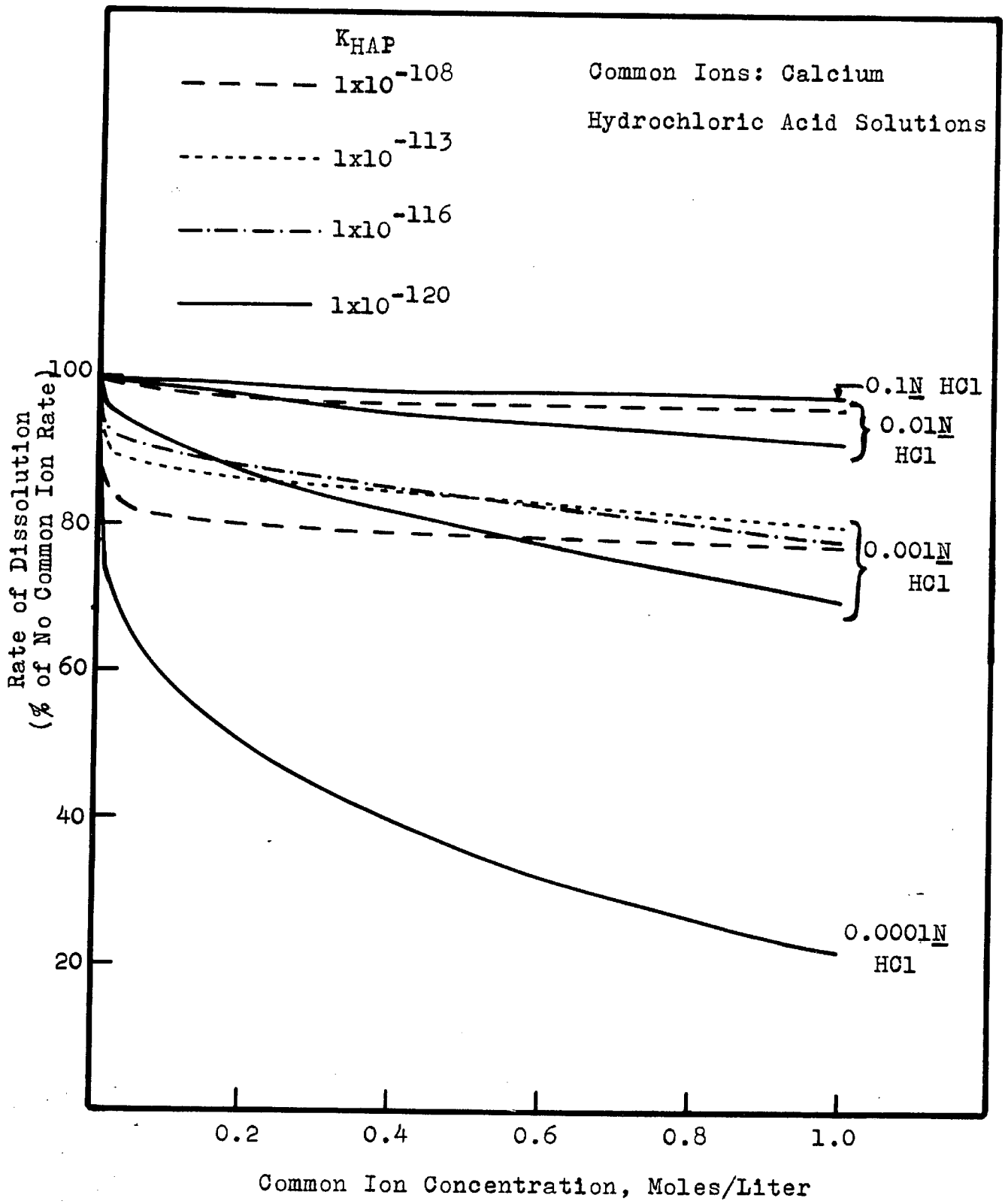

Figure 27.- Effects of Calcium Ions on Theoretical Dissolution Rates in Hydrochloric Acid Solutions. Different K_{HAP} values were used as indicated.

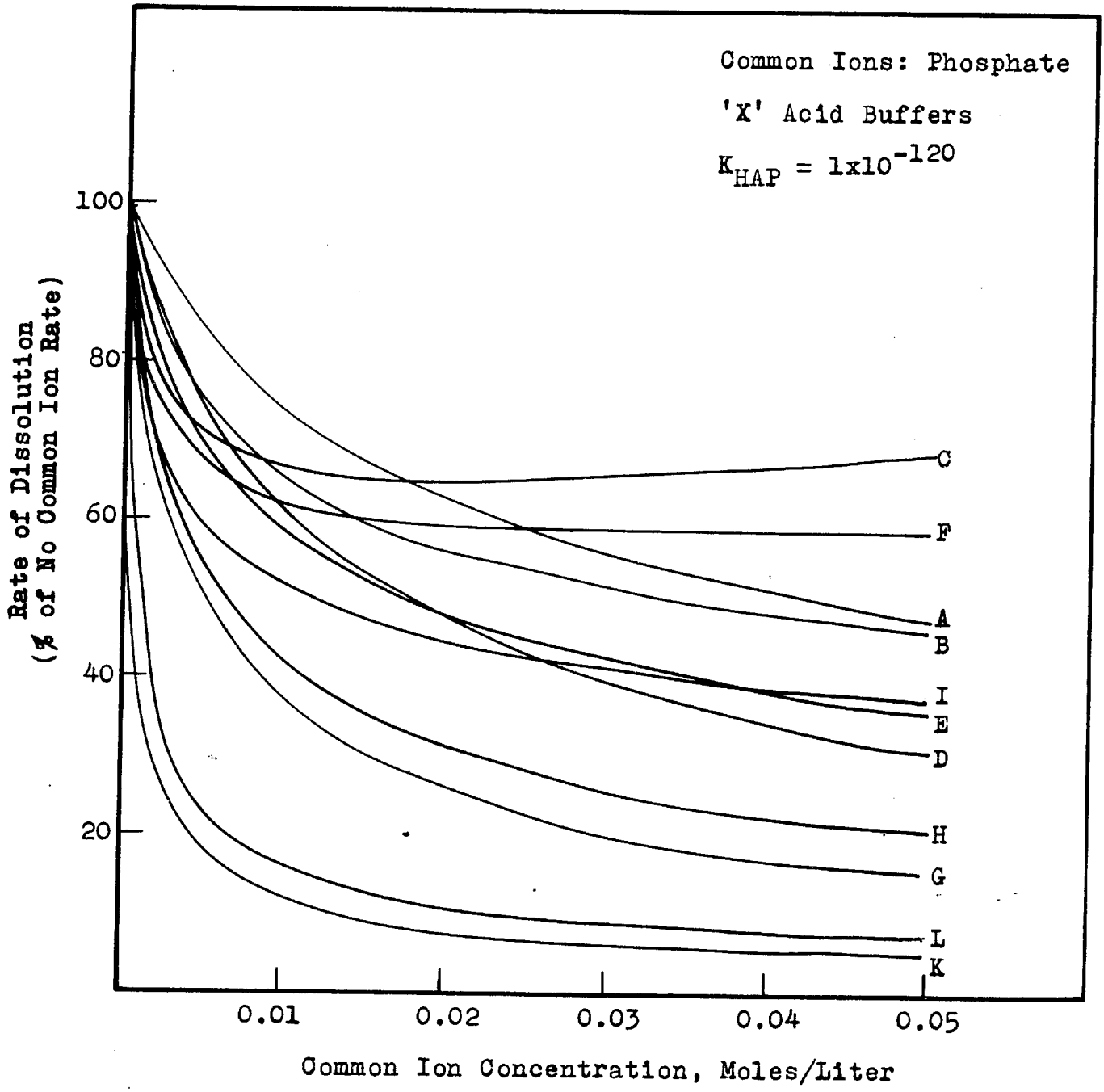

Figure 28.- Effects of Phosphate Ions on Theoretical Dissolution Rates in 'X' Acid Buffers. $K_{HAP} = 1x10^{-120}$. See Table 3 for decoding the curves.

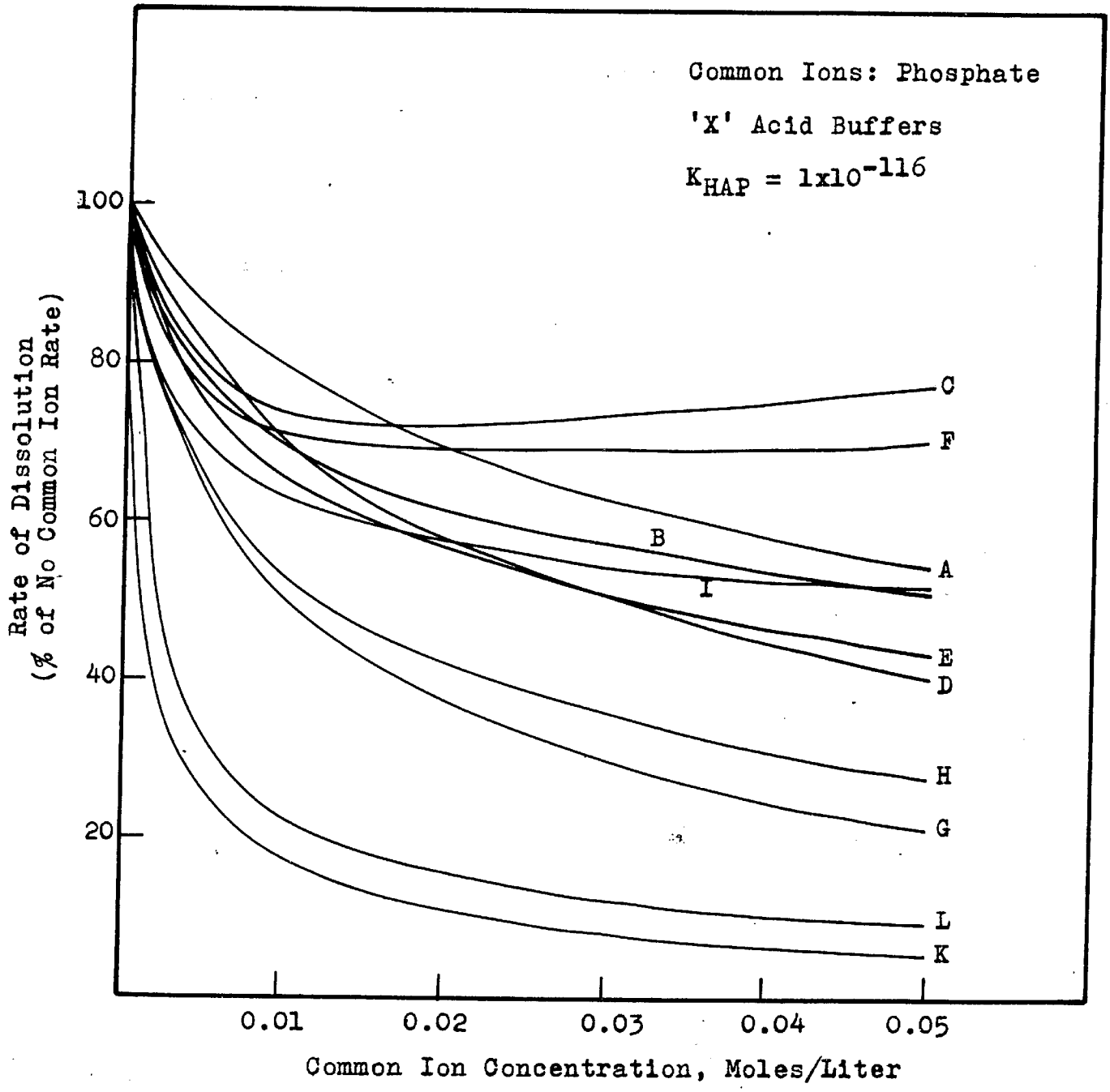

Figure 29.- Effects of Phosphate Ions on Theoretical Dissolution Rates in 'X' Acid Buffers. $K_{HAP} = 1x10^{-116}$. See Table 3 for decoding the curves.

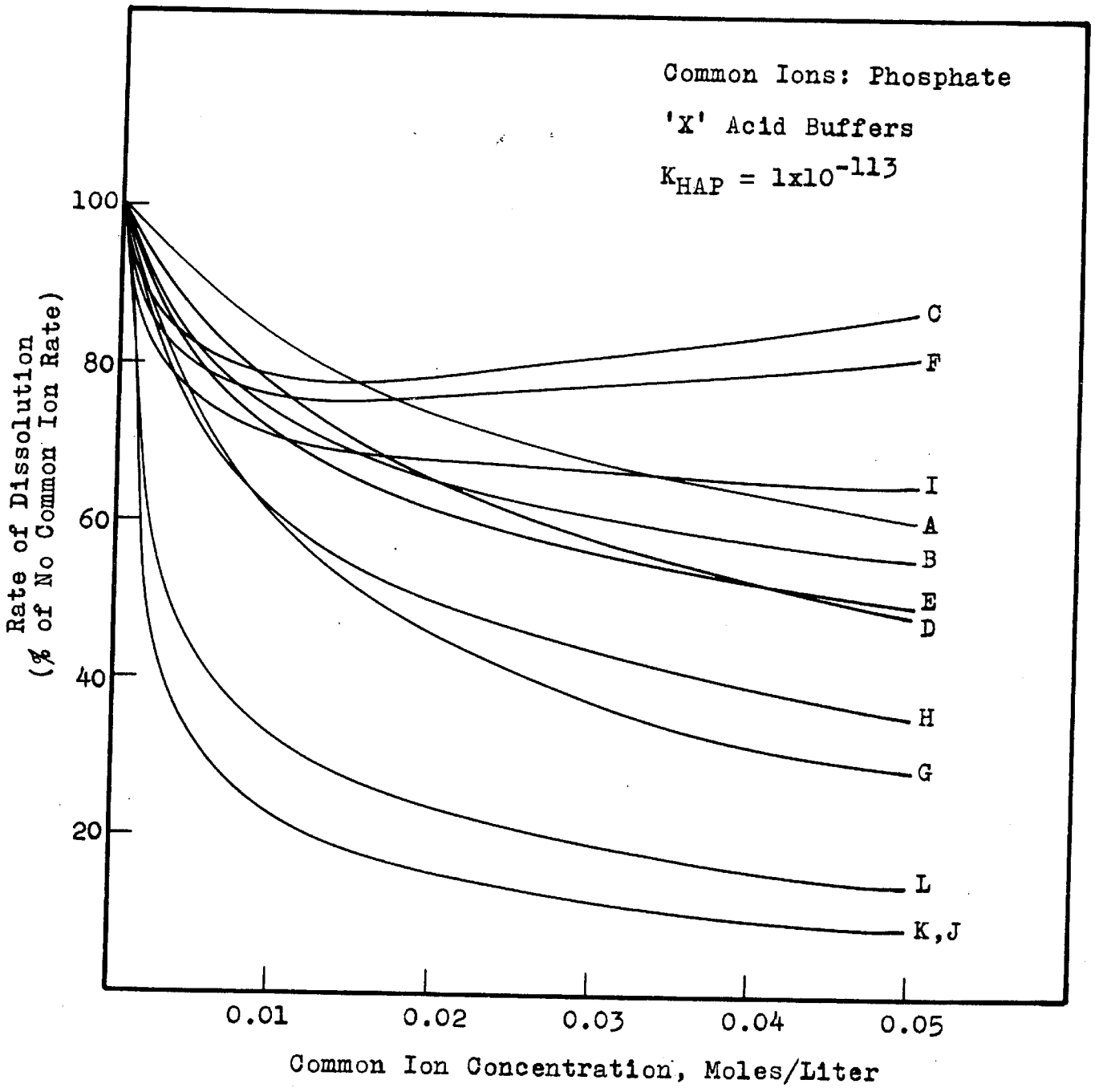

Figure 30.- Effects of Phosphate Ions on Theoretical Dissolution Rates in 'X' Acid Buffers. $K_{HAP} = 1x10^{-113}$. See Table 3 for decoding the curves.

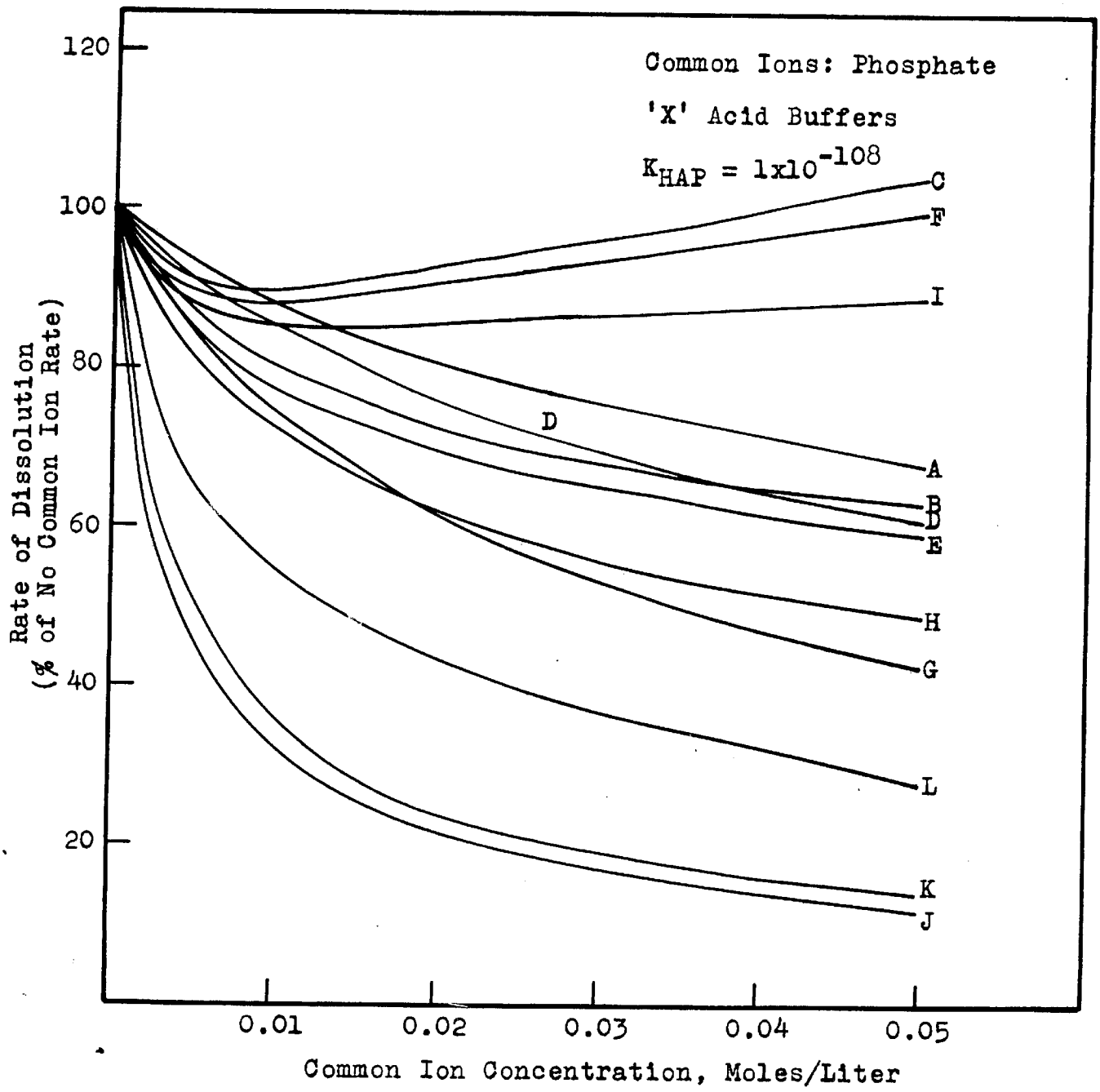

Figure 31.- Effects of Phosphate Ions on Theoretical Dissolution Rates in 'X' Acid Buffers. $K_{HAP} = 1x10^{-108}$. See Table 3 for decoding the curves.

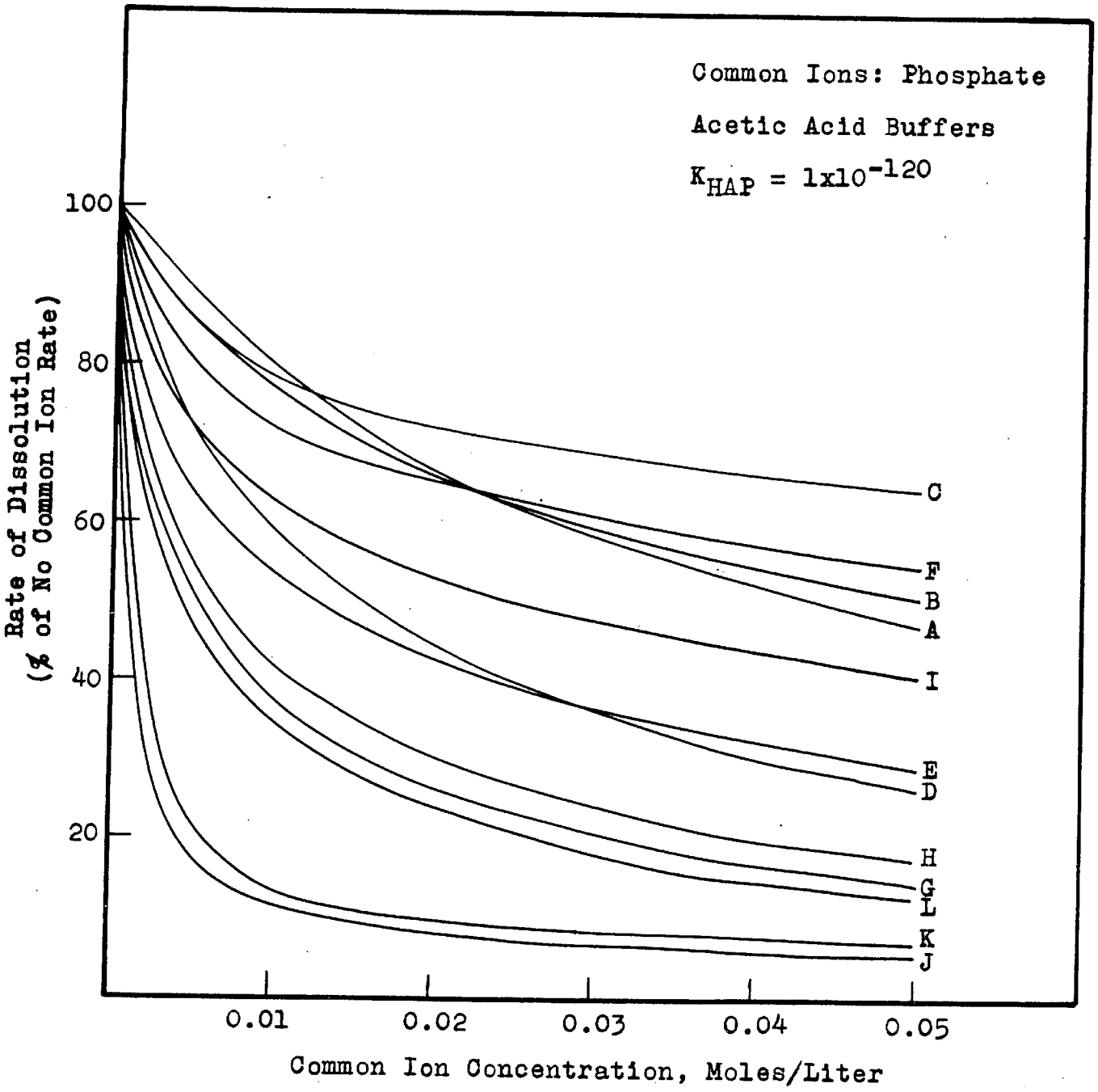

Figure 32.- Effects of Phosphate Ions on Theoretical Dissolution Rates in Acetic Acid Buffers. $K_{HAP} = 1x10^{-120}$. See Table 3 for decoding the curves.

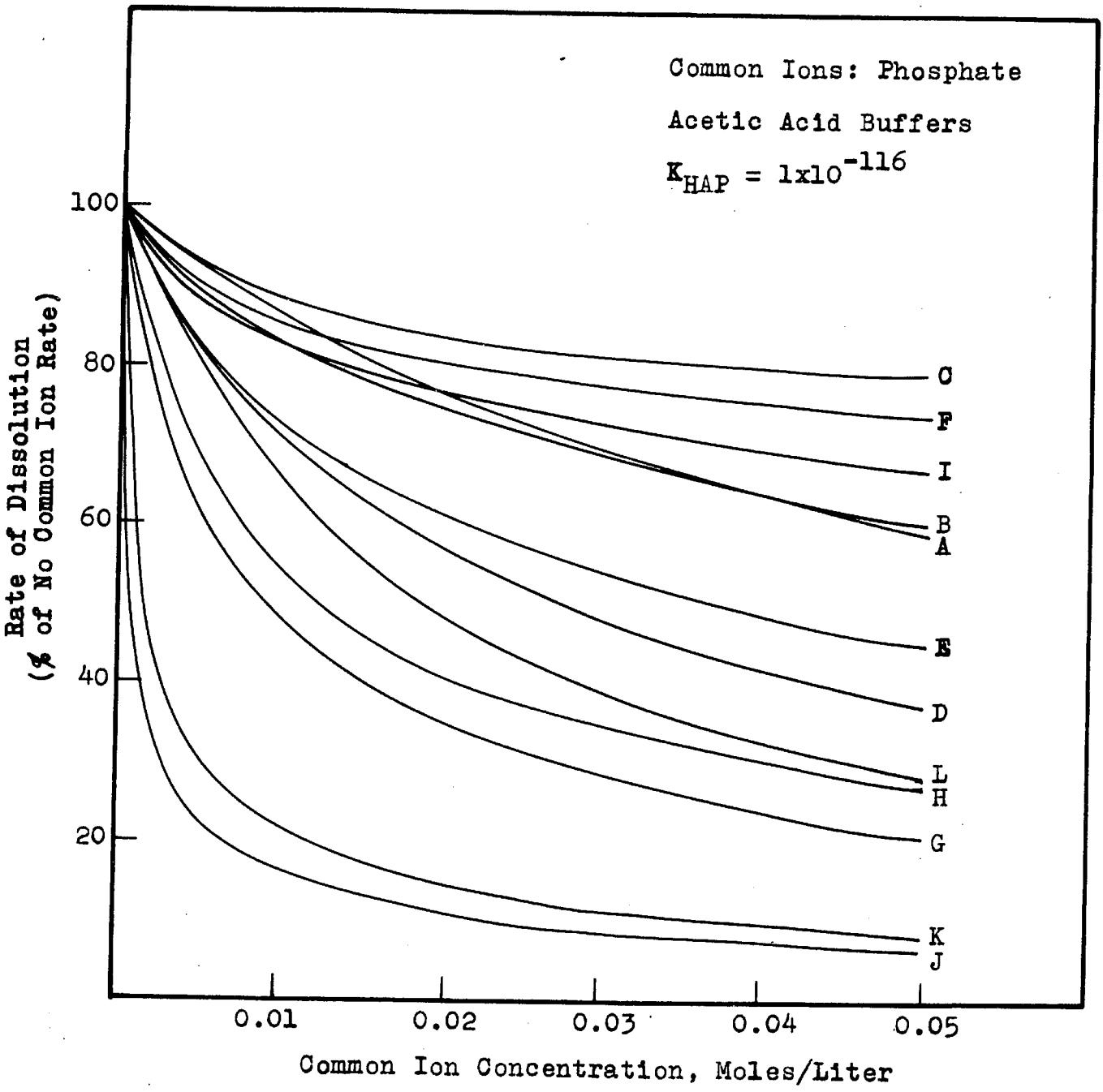

Figure 33.- Effects of Phosphate Ions on Theoretical Dissolution Rates in Acetic Acid Buffers. $K_{HAP} = 1x10^{-116}$. See Table 3 for decoding the curves.

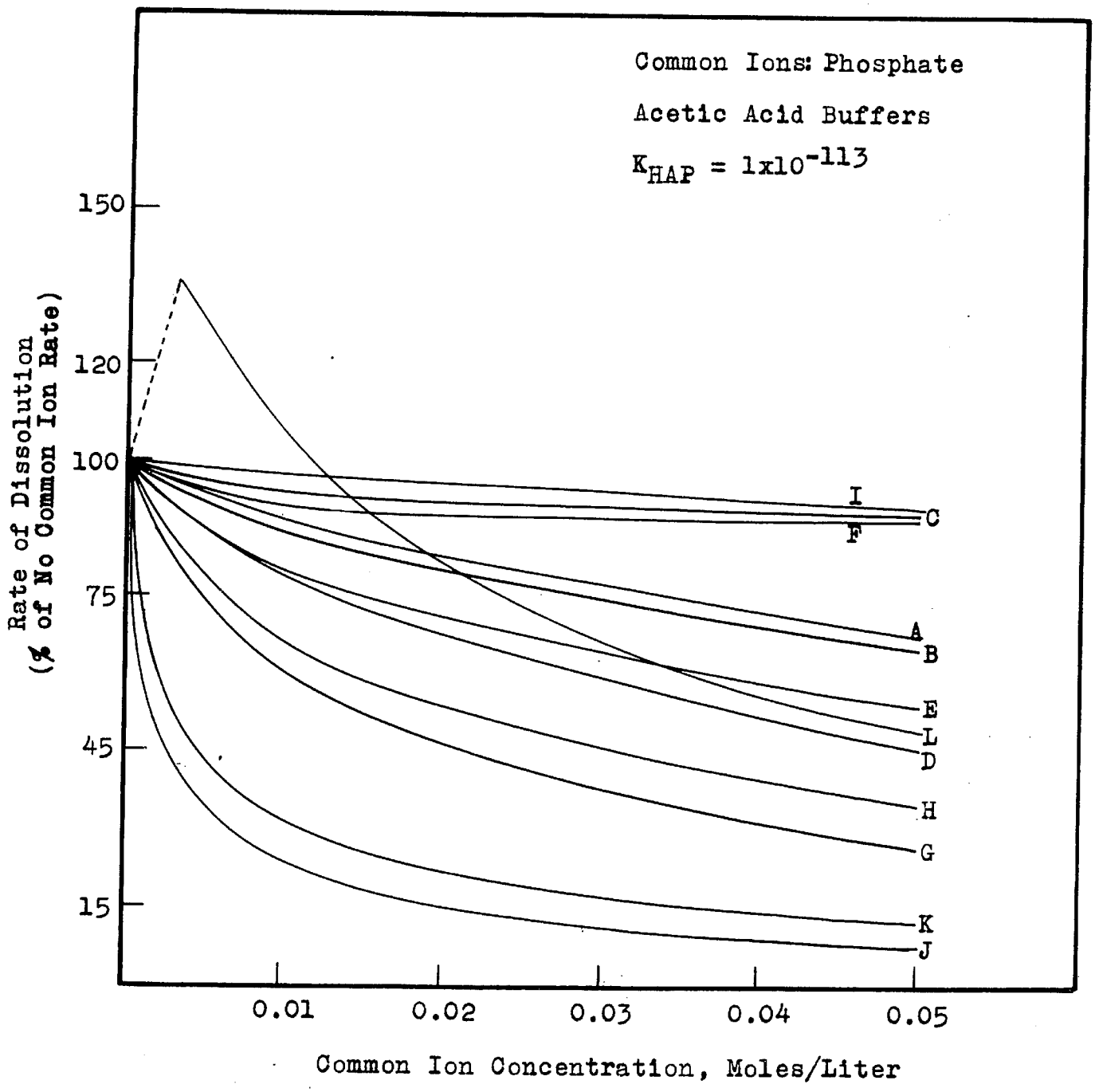

Figure 34.- Effects of Phosphate Ions on Theoretical Dissolution Rates in Acetic Acid Buffers. $K_{HAP} = 1x10^{-113}$. See Table 3 for decoding of the curves.

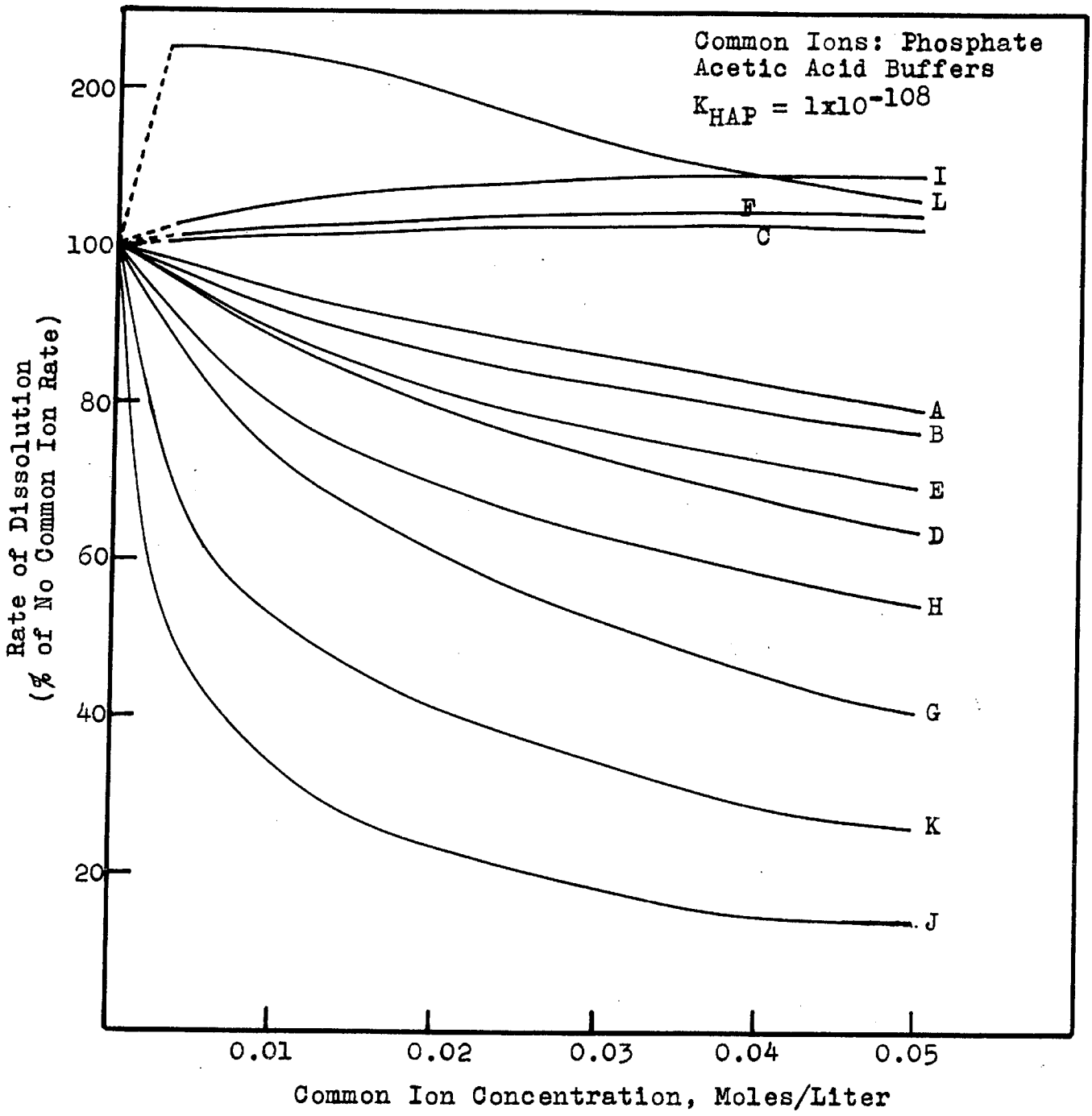

Figure 35.- Effects of Phosphate Ions on Theoretical Dissolution Rates in Acetic Acid Buffers. $K_{HAP} = 1x10^{-108}$. See Table 3 for decoding the curves.

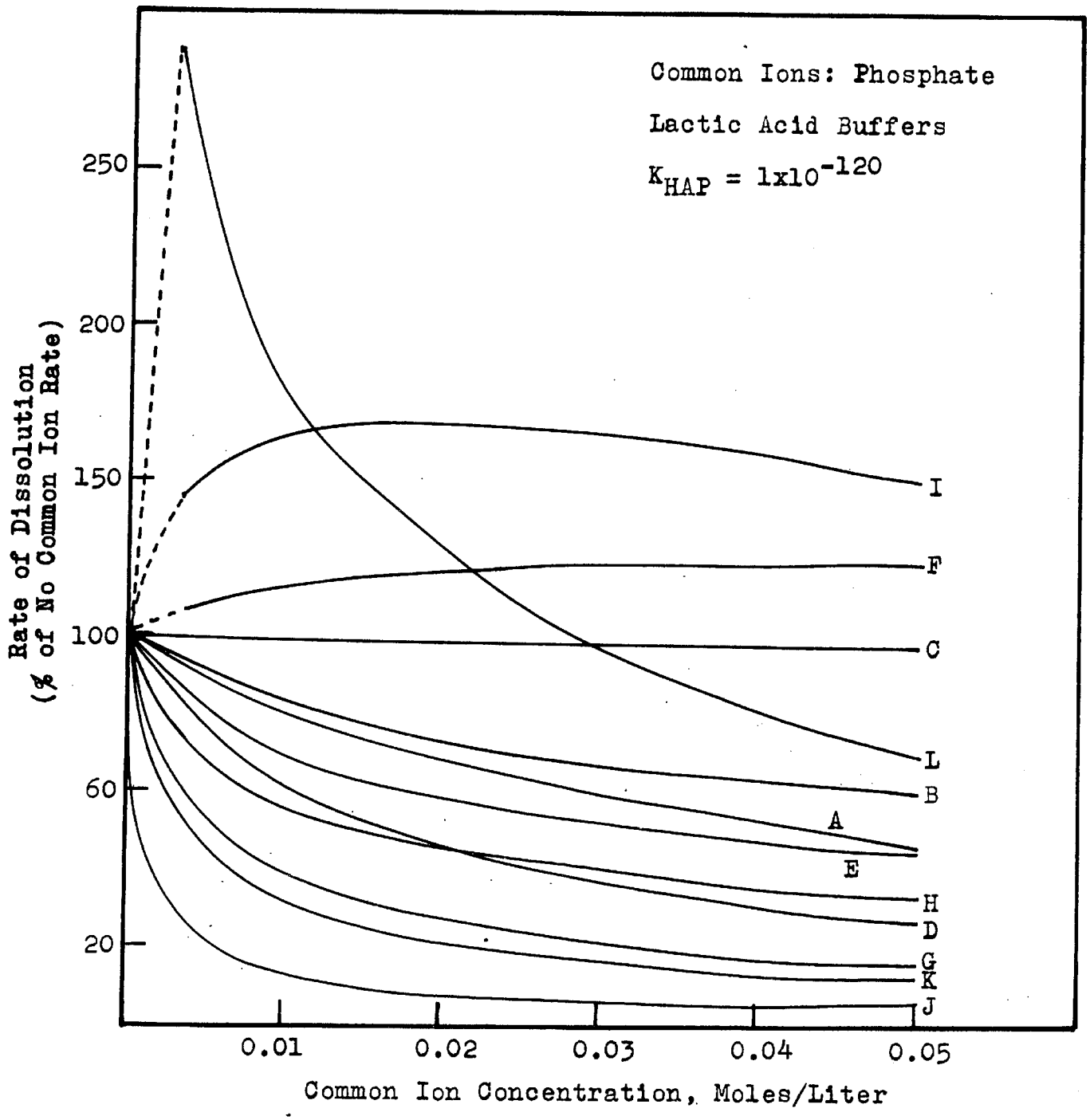

Figure 36.- Effects of Phosphate Ions on Theoretical Dissolution Rates in Lactic Acid Buffers. $K_{HAP} = 1x10^{-120}$. See Table 3 for decoding the curves.

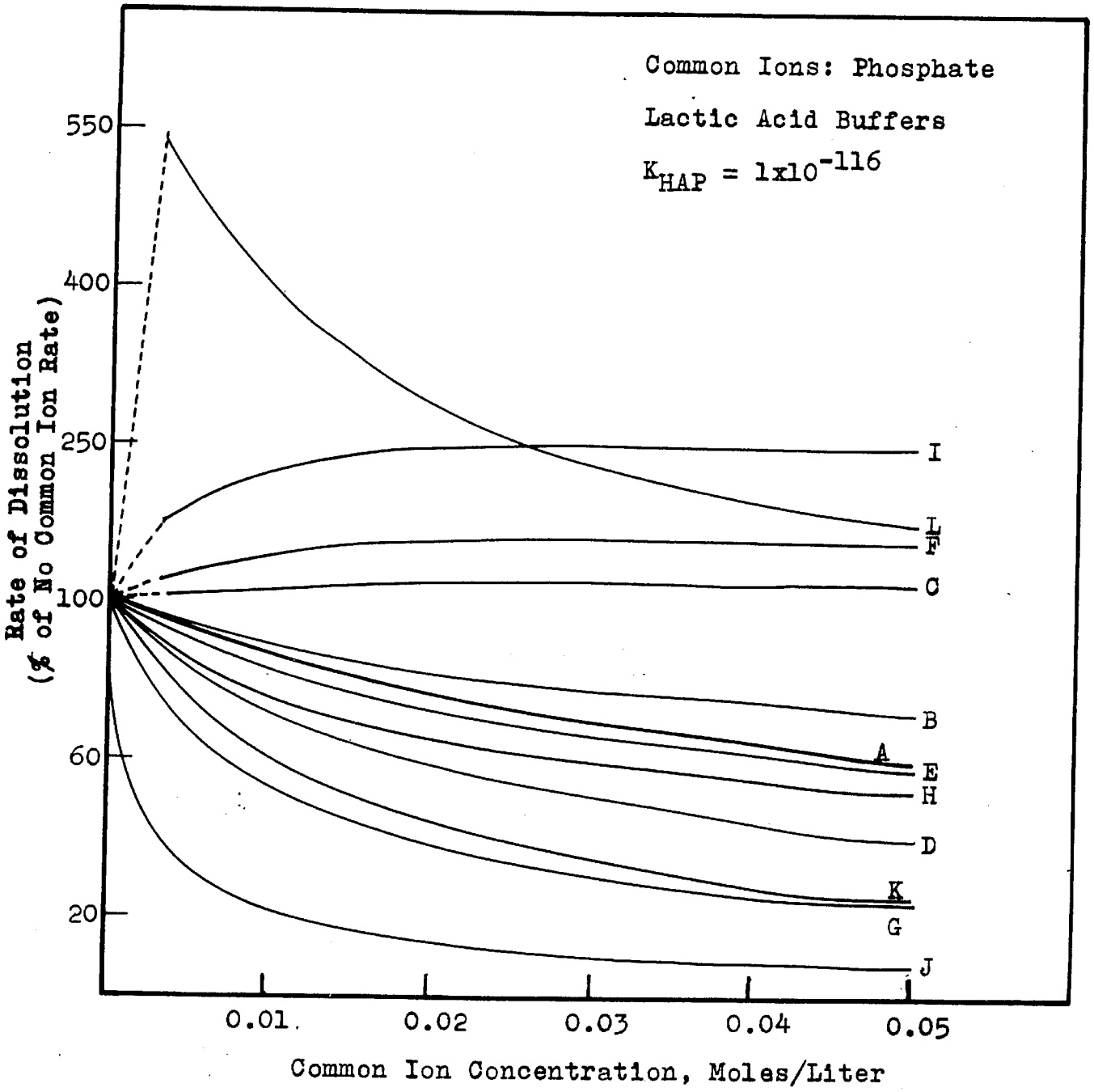

Figure 37.- Effects of Phosphate Ions on Theoretical Dissolution Rates in Lactic Acid Buffers. K_{HAP} = 1x10^{-116}. See Table 3 for decoding the curves.

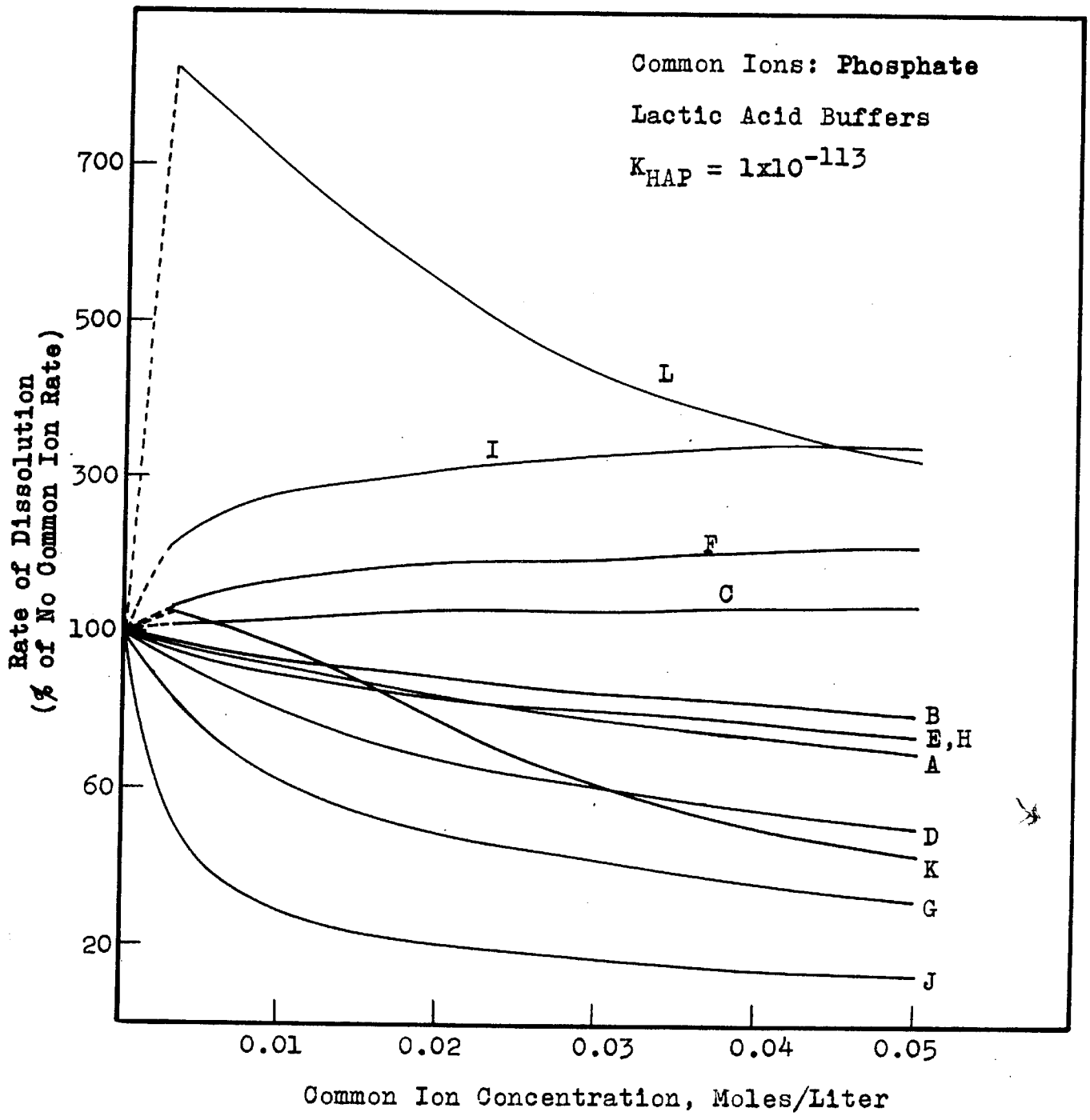

Figure 38.- Effects of Phosphate Ions on Theoretical Dissolution Rates in Lactic Acid Buffers. $K_{HAP} = 1x10^{-113}$. See Table 3 for decoding the curves.

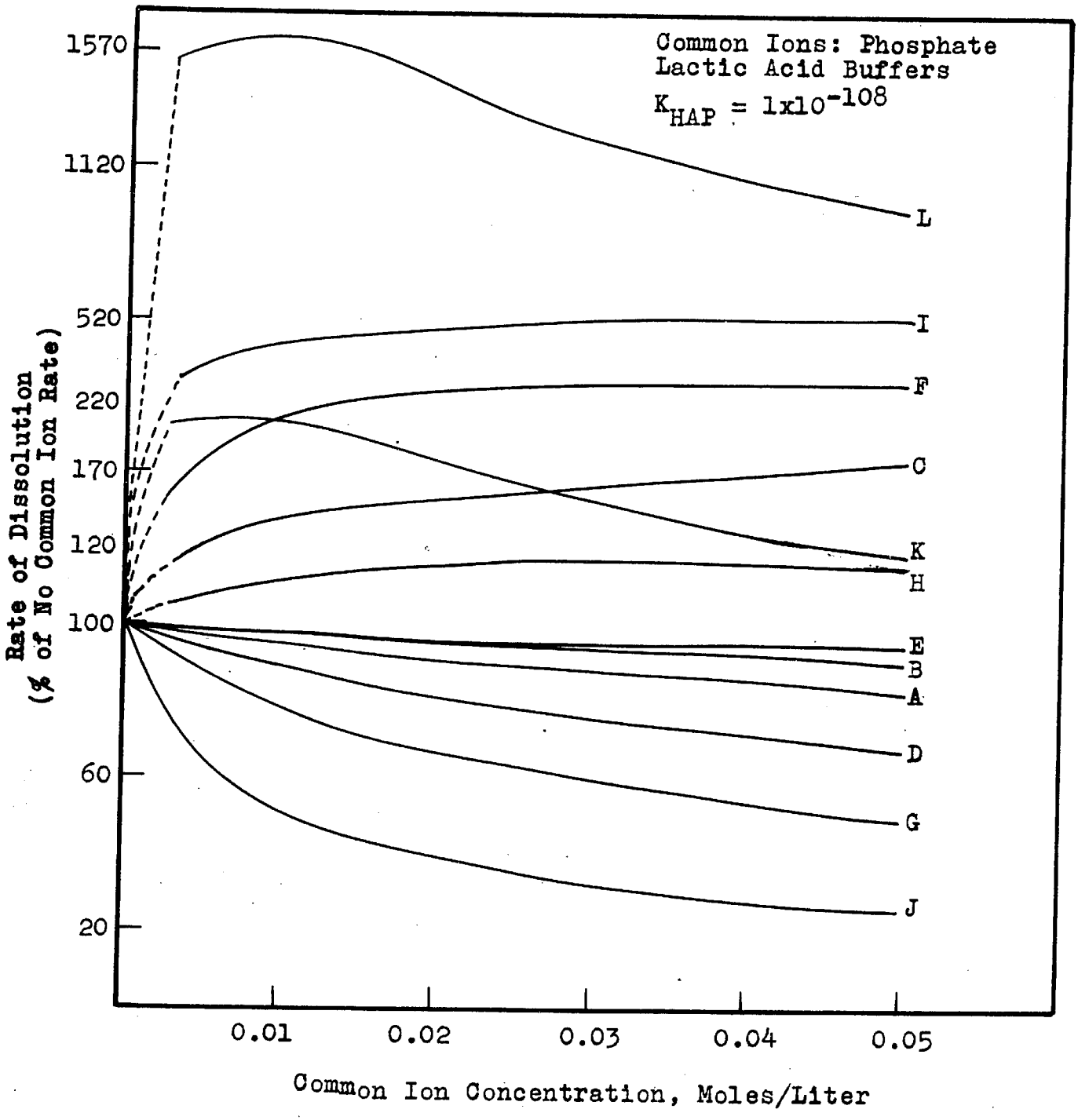

Figure 39.- Effects of Phosphate Ions on Theoretical Dissolution Rates in Lactic Acid Buffers. $K_{HAP} = 1x10^{-108}$. See Table 3 for decoding the curves.

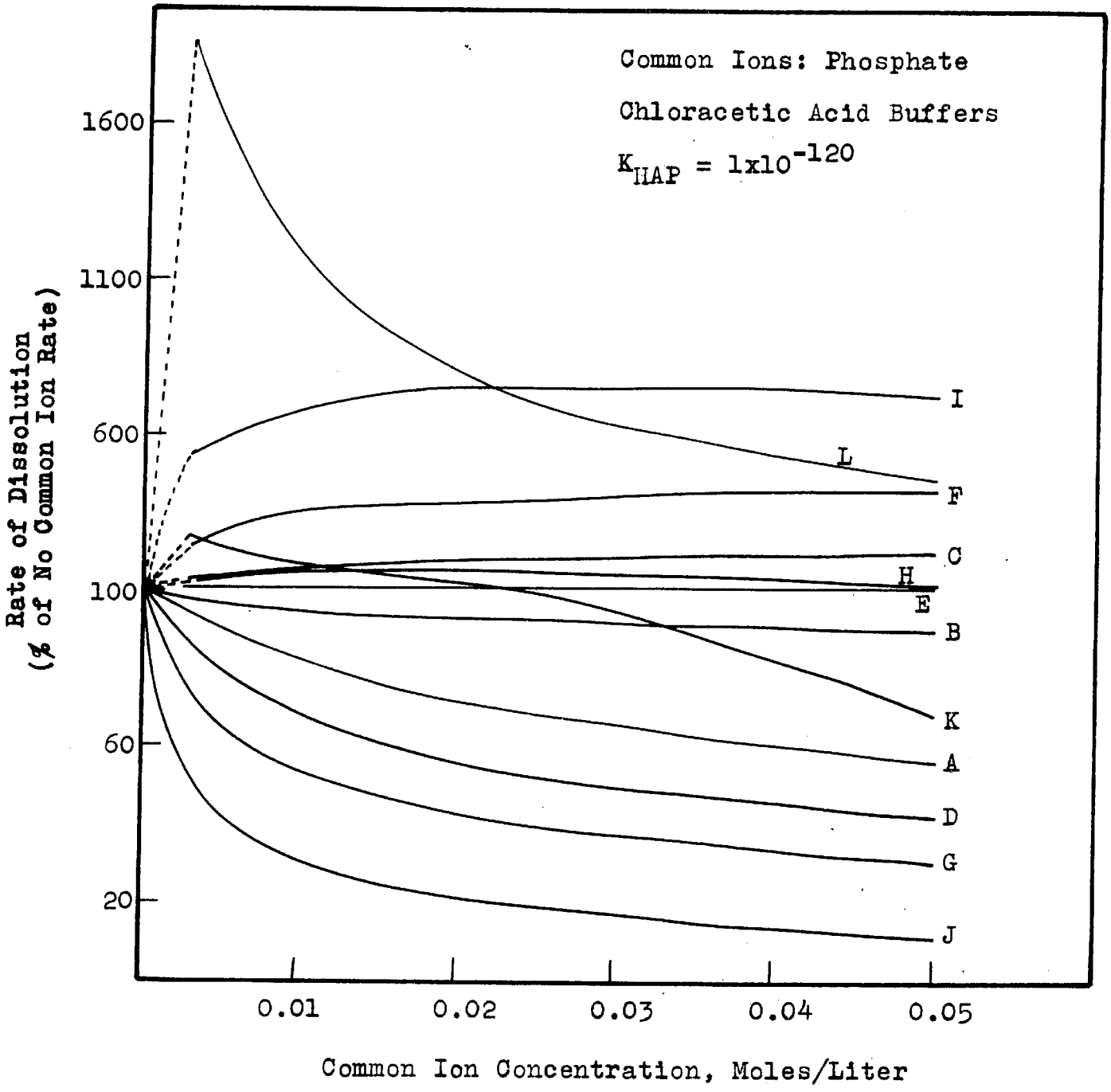

Figure 40.- Effects of Phosphate Ions on Theoretical Dissolution Rates in Chloracetic Acid Buffers. $K_{HAP} = 1x10^{-120}$. See Table 3 for decoding the curves.

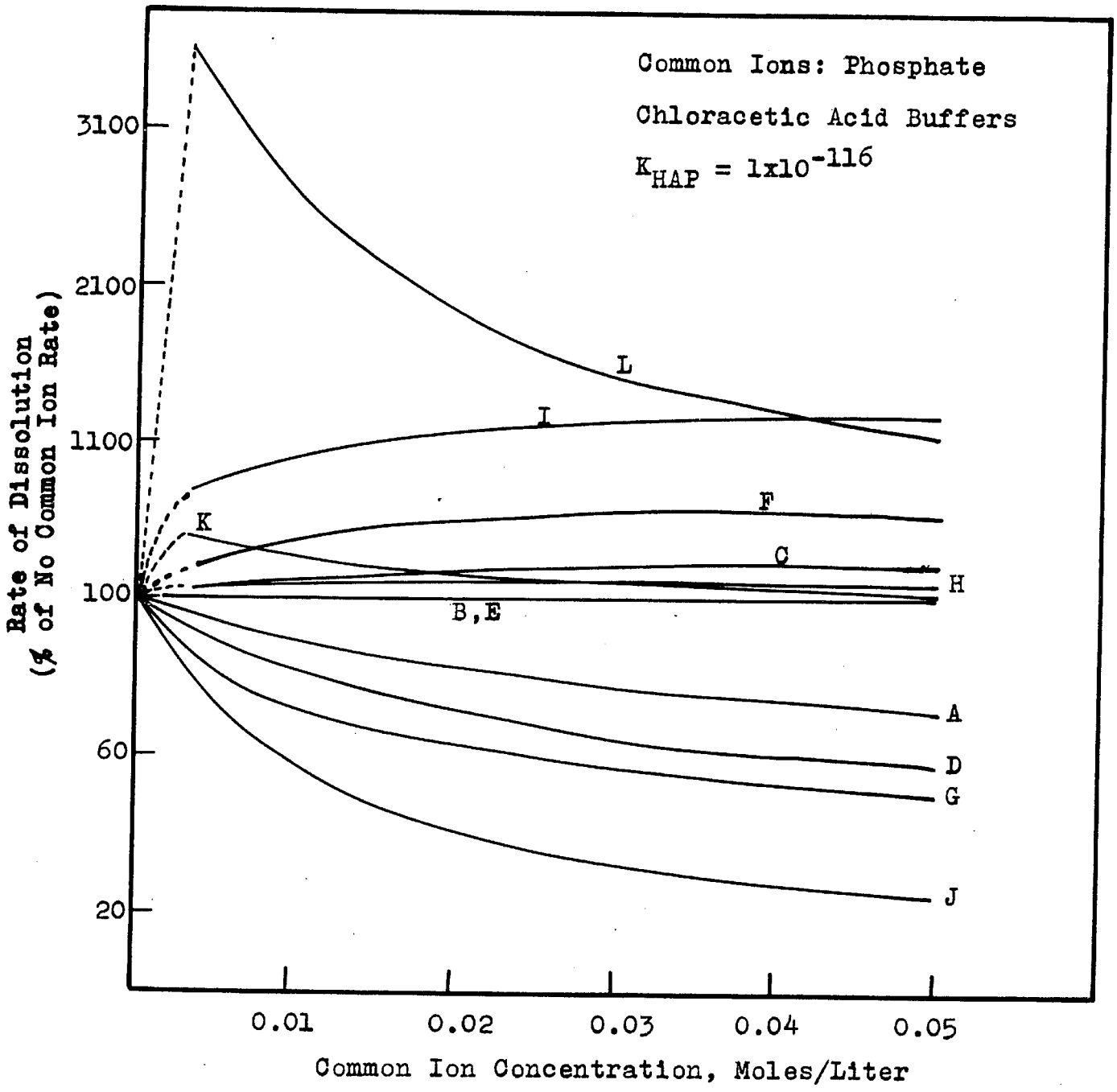

Figure 41.- Effects of Phosphate Ions on Theoretical Dissolution Rates in Chloracetic Acid Buffers. $K_{HAP} = 1x10^{-116}$. See Table 3 for decoding the curves.

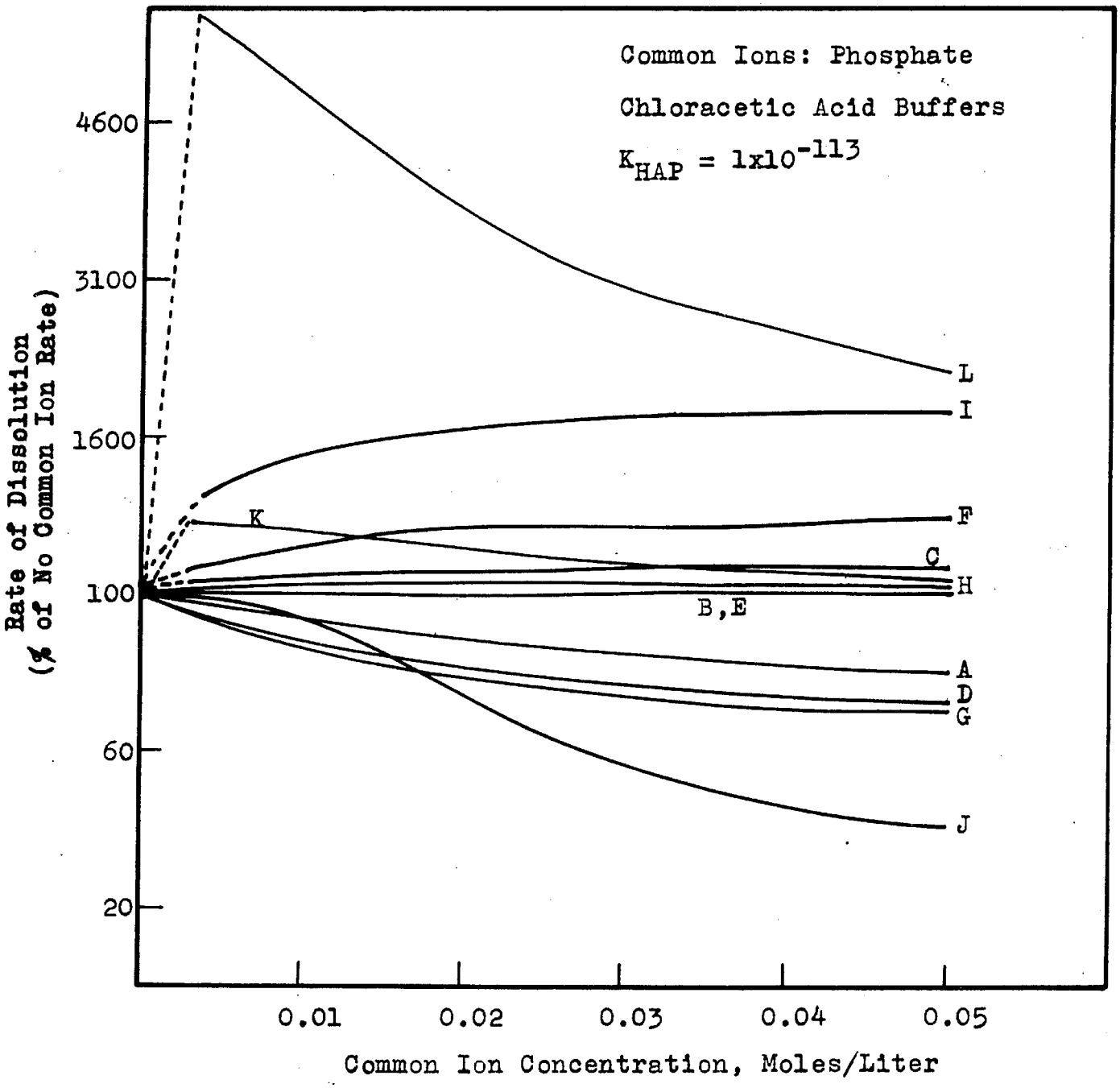

Figure 42.- Effects of Phosphate Ions on Theoretical Dissolution Rates in Chloracetic Acid Buffers. $K_{HAP} = 1x10^{-113}$. See Table 3 for decoding the curves.

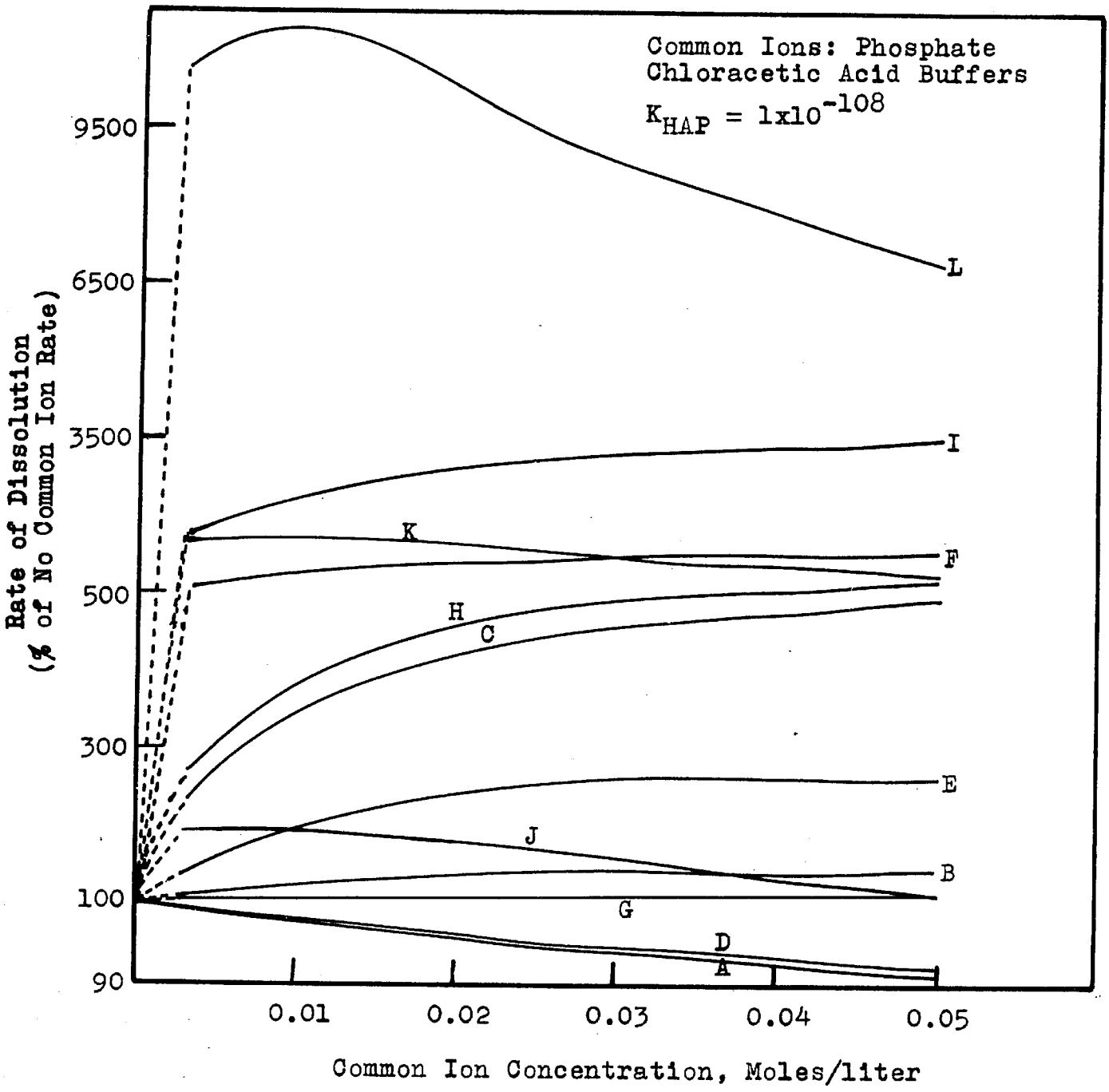

Figure 43.- Effects of Phosphate Ions on Theoretical Dissolution Rates in Chloracetic Acid Buffers. $K_{hap} = 1x10^{-108}$. See Table 3 for decoding the curves.

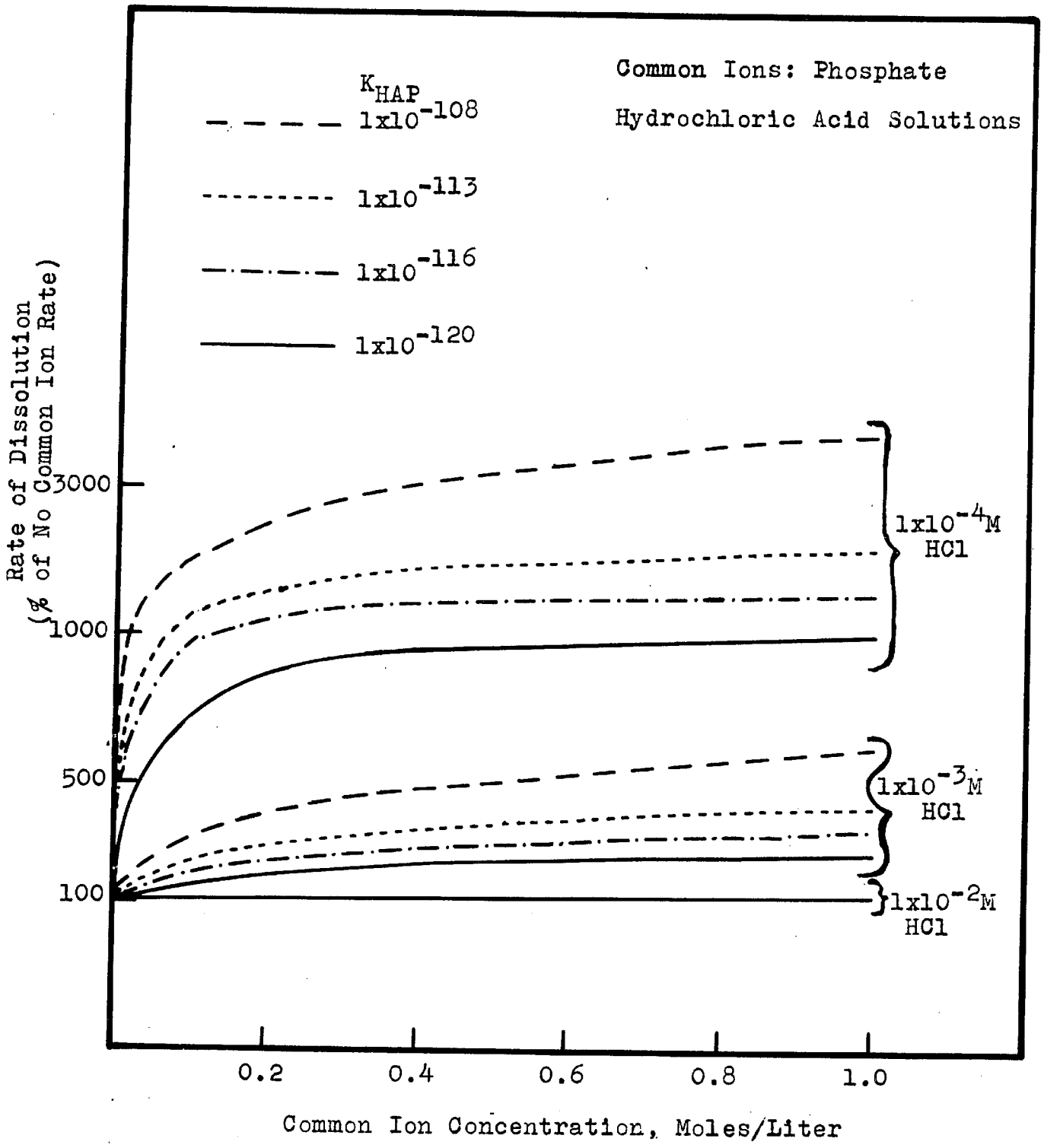

Figure 44.- Effects of Phosphate Ions on Theoretical Dissolution Rates in Hydrochloric Acid. Several K_{HAP} values were used as indicated.

Study in the Presence of Calcium Ions-- Results of this study are presented as plots of dissolution rates, calculated as % of Gh for no common ion versus calcium ion concentration, in Figures 11 to 27, for various acids at various pH values and total buffer concentrations and at different K_{HAP} values as indicated.

Generally, the effect of increasing the K_{HAP} value is a decrease in the common ion effect. Also it seems that relative effect of calcium ions on decreasing the rate, within any one acid and one K_{HAP} value, depends upon:

a). pH of the buffer,

b). Total buffer concentration of the buffer,

and c). Calcium ion concentration.

This can be typically exemplified by Figure 15, in which at pH 4.0 at low concentration of calcium ions, the order of effectiveness in reducing rates increases with decreasing the total buffer concentration. However, at higher calcium ion concentration this effect tends to reverse gradually, and finally at the concentration of 5×10^{-2} Moles per Liter the order of effectiveness is completely reversed. It is also observed that calcium ion concentration at which this reversal occurs decreases with increasing the pH. Thus, at pH 6.0, the reversal has occurred prior to the range of calcium ion concentration for which the calculations were made. Within one acid, an increase in the K_{HAP} value increases the reversal range of calcium ion concentration at all pH values. At one K_{HAP} value, as K_A is increased,

i.e., acid with higher dissociation constant is used, this reversal occurs at lower calcium ion concentration range. Considering one acid, one K_{HAP} value and one buffer concentration, an increase in the pH increases the effectiveness of the calcium common ion.

Figure 27 shows effect of calcium common ions in hydrochloric acid solutions. Here, increasing the concentration of hydrochloric acid decreases the common ion effect at fixed K_{HAP} value. However, at very low common ion concentration and at a fixed hydrochloric acid concentration, increasing the K_{HAP} value tends to increase the common ion effect sharply, but this effect levels off earlier at higher common ion concentrations.

Study in the Presence of Phosphate Ions-- Results of phosphate common ion study are presented in Figures 28-43, in various acids, at various pH values and total buffer concentrations, and at different K_{HAP} values as indicated.

Figure 28 shows that, for 'X' acid buffer ($K_A=1x10^{-6}$), at pH 6.0 where the $[B^-]_h/[HB]_h$ ratio is 1.0 (i.e., at maximum buffer capacity), the pattern followed for phosphate common ion effectiveness is similar to that for calcium ions. But $[B^-]_h/[HB]_h$ ratio decreases from 0.1 to 0.0316 to 0.01 as pH is decreased from 5.0 to 4.5 to 4.0 respectively, for this acid buffer. This means decreased buffer capacity, which decreases the effect of the phosphate common ion because added phosphate ions now may have

a significant role to act as hydrogen ion donors in addition to their common ion effect. Buffer capacity is also lowered as total buffer concentration is lowered. Thus, it can be seen in Figure 28 that, at pH 4.0 and $[TB]_h$ = 0.005 Moles per Liter, there is antagonistic action in phosphate common ion effect as phosphate ion concentration is increased. This antagonistic effect contributes to the increase of the dissolution rate. This is plausible, since the added phosphate ions can increase the total buffer capacity of the acid solution. The antagonistic effect is sufficient to overcome the common ion effect when the buffer capacity contribution from the original acid buffer is small. Thus, as a net result negative common ion effect is observed (curve C, Figure 28).

As a general rule, in any one acid buffer, increasing the K_{HAP} decreases the phosphate common ion effect at all pH values and at all buffer concentrations and the negative phosphate common ion effect becomes more pronounced (Figures 29-31).

In the case of the acetate buffer ($K_A=2.2\times10^{-5}$), the ratio $[B^-]_h/[HB]_h$ is 0.22 for pH 4.0, 0.675 for pH 4.5, 2.2 for pH 5.0, and 22.0 for pH 6.0. Buffer capacity is decreased by going far away from the pK_A value of the buffer on both sides. Figure 32 does not show any sign of antagonistic phosphate ion effect, but as K_{HAP} is increased (Figures 33-35) curve L starts to inflate showing sign of antagonistic phosphate effect at low concentrations of

phosphate ions. In Figure 34, this effect is increased to the extent that the dissolution rate in the presence of phosphate ions is even greater than the no common ion rate. At $K_{HAP} = 1x10^{-108}$, as shown in Figure 35, buffers at pH 4.0, $[TB]_h$=0.005 Moles/Liter (curve C); pH 4.5, $[TB]_h$=0.005 Moles/Liter (curve F); and pH 5.0, $[TB]_h$=0.005 Moles/Liter (curve I) overcome the normal phosphate common ion behavior and display negative common ion effect.

For lactic acid buffers ($K_A=2.0x10^{-4}$), the ratio $[B^-]_h/[HB]_h$ is 2.0, 6.33, 20.0, and 200.0 for pH = 4.0, 4.5, 5.0, and 6.0, respectively. According to Figure 36, for lactic acid buffers, higher the pH and lower the total buffer concentration more pronounced is the antagonistic phosphate ion effect.

For chloracetic acid buffers ($K_A=1.9x10^{-3}$), the ratio $[B^-]_h/[HB]_h$ is 19.0, 60.1, 190.0, and 1900.0 for pH = 4.0, 4.5, 5.0, and 6.0, respectively. Accordingly, similar to previous but much more pronounced antagonistic phosphate ion effects are seen in Figures 40-43.

Figure 44 shows similar effects in hydrochloric acid solutions. With smaller concentrations of hydrochloric acid and large values of K_{HAP}, the antagonistic phosphate ion effect is larger.

EXPERIMENTAL

Synthetic Hydroxyapatite Samples

For a number of reasons, it was decided to use more than one sample of hydroxyapatite obtained from different sources. Firstly, the solubility behavior of hydroxyapatite has not been adequately characterized. This is presumably due, to the large specific surface areas associated with most conveniently prepared samples leading to nonstoichiometric surface ionic ratios under different solution conditions (24), and to the tendency of foreign ions to substitute into the apatite lattice. Thus the reported values for the solubility product of hydroxyapatite, K_{HAP}, varies from $1x10^{-120}$ to $1x10^{-110}$. Secondly, a number of investigators (10-14) have employed commercial hydroxyapatite samples for studies designed to seek out the basic enamel mineral reactions under different conditions. It is thus desirable to have some indication of the variability among samples from different sources or from different methods of preparation with regard to demineralization rates.

The four samples of synthetic hydroxyapatite used at various stages of experiments will be referred to as A, C, P, and R. Sample A was obtained from the Victor Chemical Works.*

---

* Stauffer Chemical Co., Victor Division, Chicago, Ill.

Samples P, R, and C were prepared in the laboratory in the following manner.

Preparation of Synthetic Hydroxyapatite Samples C, P and R

Basically, the procedure of Egan, Wakefield, and Elmore (31) was followed in the preparation of the sample P. One liter of 0.20 Moles/Liter calcium nitrate and one liter of 0.12 Moles/Liter monobasic ammonium phosphate were added simultaneously, during a 15 minute period, with continuous bubbling of nitrogen into a 5-gallon carboy containing 12 liters of distilled water placed on a steam bath. The distilled water obtained from a stainless steel still was redistilled from a glass still and the double distilled water thus obtained was used throughout this study. Then, 500 ml. of 1.0 Molar ammonium hydroxide was added dropwise over a period of six hours. The resulting precipitate was stirred for another twelve hours by continuous bubbling of nitrogen and then allowed to settle. The precipitate was washed by decantation with distilled water, filtered, and dried at 105°C for 72 hours. Experimental yield was 18.5 Gm. (i.e., 92.5% of theoretical yield).

Sample C was the same as sample C used by Higuchi et al. (21). It was prepared by rapid precipitation procedure, in which 500 ml. each of 0.4 Molar calcium nitrate and 0.24 Molar monobasic ammonium phosphate were added together during a 30 minute period to a 4-Liter flask containing one liter of distilled water and 30 ml. of concentrated

ammonium hydroxide maintained at 90-95°C. The resulting precipitate was digested for one hour at the same temperature, and then it was allowed to cool. The precipitate was washed, filtered and dried in the same way as described for sample P. Experimental yield by this procedure was 19.0 Gm. which is 95% of the theoretical yield.

In the case of sample R, labelled calcium was used during its preparation. To 250 ml. of 0.4 Molar calcium nitrate solution 0.1 ml. of $Ca^{45}Cl_2$ in hydrochloric acid (amounting to approximately one millicurie radioactivity) was added and mixed properly. This solution of calcium nitrate containing homogeneously mixed tagged calcium ions, and 250 ml. of 0.24 Molar monobasic ammonium phosphate solution were added dropwise over a period of two hours to one liter of distilled water containing 15 ml. of concentrated ammonium hydroxide in a 4-Liter three necked flask. Nitrogen was continuously bubbled throughout this operation. Temperature was maintained at 95°C. ± 2°C. The precipitate was allowed to stir for another 12 hours by nitrogen bubbling and then it was cooled, washed, filtered, and dried in the same manner as described for the previous preparations. Experimental yield for this preparation was 9.5 Gm. which amounts to 95% of the theoretical yield.

The analytical data for these samples are given in Table 4 in terms of percent hydroxyapatite calculated by assuming that calcium or phosphate is present as $Ca_{10}(PO_4)_6(CH)_2$ only. These were obtained by the analytical

TABLE 4

Composition of Samples

Sample	% HAP by Phosphate Analysis	% HAP by Calcium Analysis	Ca/PO_4 Molar Ratio
A	95.0	92.2	1.612
C	96.0	92.0	1.600
P	102.1	98.1	1.600
R	95.5	91.3	1.590
Enamel*	94.8	87.2	1.532

* The enamel sample used in this study contained 73 ppm Fluoride.

methods described later. The values represent the average of 3-5 determinations. The precision of the results in these instances was about ±1% for both the calcium and phosphate analyses.

All samples gave the characteristic diffraction peaks for hydroxyapatite. These determinations were made on the Siemens Crystalloflex IV X-ray diffractometer. Infrared spectra showed peaks for ionic carbonate in samples A and C.

Powdered Tooth Enamel

The procedure for efficient grinding of tooth enamel was described by Hefferren and Higuchi (32). Extracted human teeth were cleaned to remove roots, decayed portions, and pulp. These were ground (32) in a Model-M Fitz Mill* using a No. 60 mesh sizing screen. Following the grinding step, the powder obtained was screened, and the fraction collected between 100 and 200 mesh screen sizes was retained. Then the enamel was separated from the dentin by the flotation procedure described by Manly and Hodge (33) using bromoform as the suspending medium. The separated particles then were given several rinses with acetone, dried overnight in air at room temperature, and finally dried in an oven for one hour at 105°C.

---

* W. J. Fitzpatrick Co., Chicago, Illinois.

Preparation of Buffers

Acetate buffers at the pH and total buffer concentrations indicated in the figures were prepared by mixing calculated amounts of acetic acid and sodium acetate of the same molarity. Lactate buffers were made similarly. Since concentrated lactic acid contains polymers of lactic acid, diluted lactic acid solution was allowed to age for one month and then this solution was used to make various strengths of lactic acid and sodium lactate on the basis of titratable acid.

After mixing the free acid, and its sodium salt the pH was measured using the Beckman Model G pH-meter. Calculated weight of sodium chloride was added whenever it was necessary to obtain a 0.5 Molar sodium chloride concentration in the final solution. The pH was adjusted to the value originally calculated by adding dropwise very concentrated sodium hydroxide or hydrochloric acid solution whichever was necessary. Sodium chloride was incorporated in buffers so that one can have essentially unchanged ionic strength in solution when dissolution rate of synthetic hydroxyapatite or enamel is studied in it. The dissolution rate thus obtained then can be compared with the dissolution rate in the same buffer made without adding sodium chloride where the ionic strength of the solution will be continuously increasing as the solid dissolves.

For the common ion study, buffers were made with

double the total buffer strength than desired and then the calculated aliquots of calcium chloride or sodium dihydrogen phosphate of known strength were added together with the calculated amount of sodium chloride whenever needed. The buffers were then diluted to double their initial volumes to get the desired total buffer concentrations and common ion concentrations. The pH was adjusted as before to the value originally desired.

Assay for Phosphate

Phosphate concentrations were determined by the method of Gee, Domingues and Deitz (34). The reagents used in the assay were prepared as follows.

a). Acid Ammonium Molybdate Solution: 500 ml. of 4% ammonium molybdate solution in distilled water was mixed with 500 ml. of 50% sulfuric acid. The mixed reagent was stored under refrigeration when not in use and was stable for at least two months.

b). Chlorostannous Acid Solution: 5% stannous chloride solution in 8 Normal hydrochloric acid was prepared and stored in dark. Aliquots of this solution, depending upon the need, were diluted 20 times with distilled water daily.

Known aliquots of standard phosphate solution and unknown solution were pipetted into 50-ml. volumetric flasks. Distilled water was added to make approximately 40 ml. volume in each flask. Then 2 ml. of acid ammonium

molybdate reagent and 1 ml. of chlorostannous acid reagent were pipetted into each flask and volume was made to 50 ml. with distilled water. The absorbance of the blue color obtained as a result of the reduction of the phospho-ammonium molybdate complex by chlorostannous acid reagent, was measured exactly after 15 minutes using the Spectronic 20 Colorimeter* at a wavelength of 720 millimicrons against distilled water as a blank. Reagent blank was also measured against distilled water which always gave zero absorbance. Absorbance-concentration relationship obeyed Beer's law upto 80 micrograms of phosphate. The least squares slope of the absorbance-concentration plot was used to calculate the amount of hydroxyapatite in solution assuming that $Ca_{10}(PO_4)_6(OH)_2$ was the phase of solid which contributed all the phosphate in the solution. Precision of this method was about ±1%.

Assay for Calcium

Chemical Analysis

Calcium was analyzed according to the method of Lancina and West (35). The principle of this procedure is that the selective colorimetric reagent, Calcichrome [cyclotris-7-(1-azo-8-hydroxynaphthalene-3,6-disulfonic acid)], forms a complex with calcium ions at pH 12.0,

---

* Bausch and Lomb Inc., Rochester, New York.

having the wavelength of maximum absorbance at 510 millimicrons, while that of the reagent itself is at 615 millimicrons. The reagents used in this procedure were as follows:

a). Glycine-Sodium Hydroxide Buffer: 4.0 Gm. of sodium hydroxide, 2.34 Gm. of sodium chloride and 3.002 Gm. of glycine were dissolved in distilled water to make one liter of the buffer.

b). Calcichrome Reagent: 0.2% Calcichrome* was prepared in distilled water, daily as required.

Aliquots of calcium standard solution and unknown samples containing calcium ions between 2 and 70 micrograms were pipetted into 50-ml. volumetric flasks. Then 5.0 ml. of the Calcichrome reagent and 5.0 ml. of the glycine-sodium hydroxide buffer were pipetted into each of the volumetric flask and volume was made to 50 ml. with distilled water. Reagent blank was carried through in the same way. After waiting for one hour, the absorbance of the complex formed was measured against the reagent blank using the Spectronic 20 Colorimeter at the wavelength of 510 millimicrons. Absorbance-concentration relationship obeyed Beer's law up to 70 micrograms of calcium in solution. The least squares slope of the standard Beer's plot was used to calculate the amount of hydroxyapatite in solution assuming the stoichiometric dissolution. Precision of the calcium analysis by this procedure was about ± 3%.

*Obtained from Burdick Jackson Laboratories, Muskegon, Mich.

Radioactivity Determination

Radioactivity in the liquid samples obtained from dissolution rate runs of the synthetic hydroxyapatite sample R, containing tagged calcium, was determined in the following manner.

A known weight of the sample R was dissolved in a minimum amount of concentrated hydrochloric acid and the solution was diluted to one liter with distilled water. A one ml. aliquot of this solution was used as standard and the count obtained for this was taken as the standard. Dioxane phosphor was prepared by dissolving 7.0 Gm. PPO (2,5-diphenyloxazole*, Scintillation grade), 0.05 Gm. POPOP ((1,4-bis-2,5-phenyloxazolyl)-benzene*, Scintillation grade) and 50 Gm. naphthalene in p-dioxane (spectroquality) to make one liter of solution. To this solution 100 ml. of distilled water was added and mixed well. Ten ml. of this dioxane phosphor was pipetted into screw capped vials to which one ml. aliquots of unknown samples and standard samples were added. Contents of the vials were counted on a Tri-Carb liquid scintillation counter* in duplicate. Average counts were then used to calculate the amount of hydroxyapatite in solution, assuming the stoichiometric dissolution.

---

* Packard Instrument Co., Inc., La Grange, Illinois.

Procedure for Determination of Solubility

Different weights varying from 2.0 mg. to 100.0 mg. of the hydroxyapatite samples A and P and the powdered enamel were transferred to Neutraglas ampoules. Twenty ml. of acetate buffer of known pH and total buffer concentration was pipetted into each ampoule. The ampoules were then sealed and rotated in a constant temperature water bath maintained at 30.0°C. ± 0.1°C. for 54 and 114 hours. Then, at the end of each time interval, the contents of each ampoule were filtered through 0.24 micron membrane filters* using the syringe-Swinny adapter assembly. The filtrate obtained from each ampoule was assayed for phosphate and calcium.

Procedure for the Synthetic Hydroxyapatite Dissolution Rate Experiments

Tablets of synthetic hydroxyapatite, 0.5 inch in diameter, were made using the Carver Laboratory Press at 75,000 p.s.i. The tablets then were ground lightly in a glass mortar and sieved dry, through the No. 80 and 100 mesh screens. The portion retained by the No.100 mesh screen was used in the experiments. For the radioactive sample R, the grinding and sieving step was carried out in a plastic bag to avoid contamination.

---

* Millipore Filter Corp., Bedford, Mass.

One hundred milligram of these granules was transferred into a 250-ml. volumetric flask clamped to the arm of a Burrell Wrist-action shaker so that the lower portion of the flask was immersed in a water bath maintained at 30.0° ±0.1°C. Then 200 ml. of the buffer, in which the dissolution rate was to be studied, and which was equilibrated at the temperature of the water bath, was introduced into the flask, and the shaker was turned on. The shaker amplitude was adjusted to keep the granule particles just suspended in the medium. These agitation conditions were maintained constant for all runs. A timer was initiated with the starting of the shaker. Five-milliliter samples were withdrawn at predetermined times with a syringe-filter assembly. The syringe-filter assembly consisted of a glass filter stick (maximum pore size of 4-8 microns) connected by means of a piece of Tygon tubing to the inlet of a B.D.* automatic valve attached to a 50-ml. syringe. The outlet of the valve was connected to a piece of latex rubber tubing which dipped back into the solution. This arrangement permitted sampling and then rinsing out the line before the next sample was taken. All samples were collected in premarked screw-capped tubes. The samples were assayed for phosphate. Calcium analysis was performed in selected samples.

---

* Becton, Dickinson and Company, Rutherford, N. J.

Procedure for the Enamel Dissolution Rate Experiments

Exactly 100 mg. of the enamel powder was run in a manner the same as the granulated synthetic hydroxyapatite samples.

Results of the Experimental Study

Solubility Study

The solubility of hydroxyapatite varies with the solid to solvent ratio (24). In view of this, solubility experiments were carried out on some of the samples. Figure 45 shows the results of the solubility experiments with the synthetic hydroxyapatite samples A and P and with the powdered enamel in acetate buffer having pH 6.0 and 0.2 Molar total buffer concentration. Figure 46 shows similar results in acetate buffer, having pH 5.7 and 0.2 Molar total buffer concentration, which also contained 0.5 Molar sodium chloride. Since negligible differences were observed between the 54-hour and 114-hour solubilities, only the results of the later time period are reported. The results are plotted as the amount of hydroxyapatite dissolved in 20 ml. of buffer at equilibrium *versus* amount of solid originally put in the same volume of the buffer. Excess of solid still remained in the liquid at equilibrium even when only 5.0 mg. of solid was added initially. As it can be observed from these figures , the solubility increases

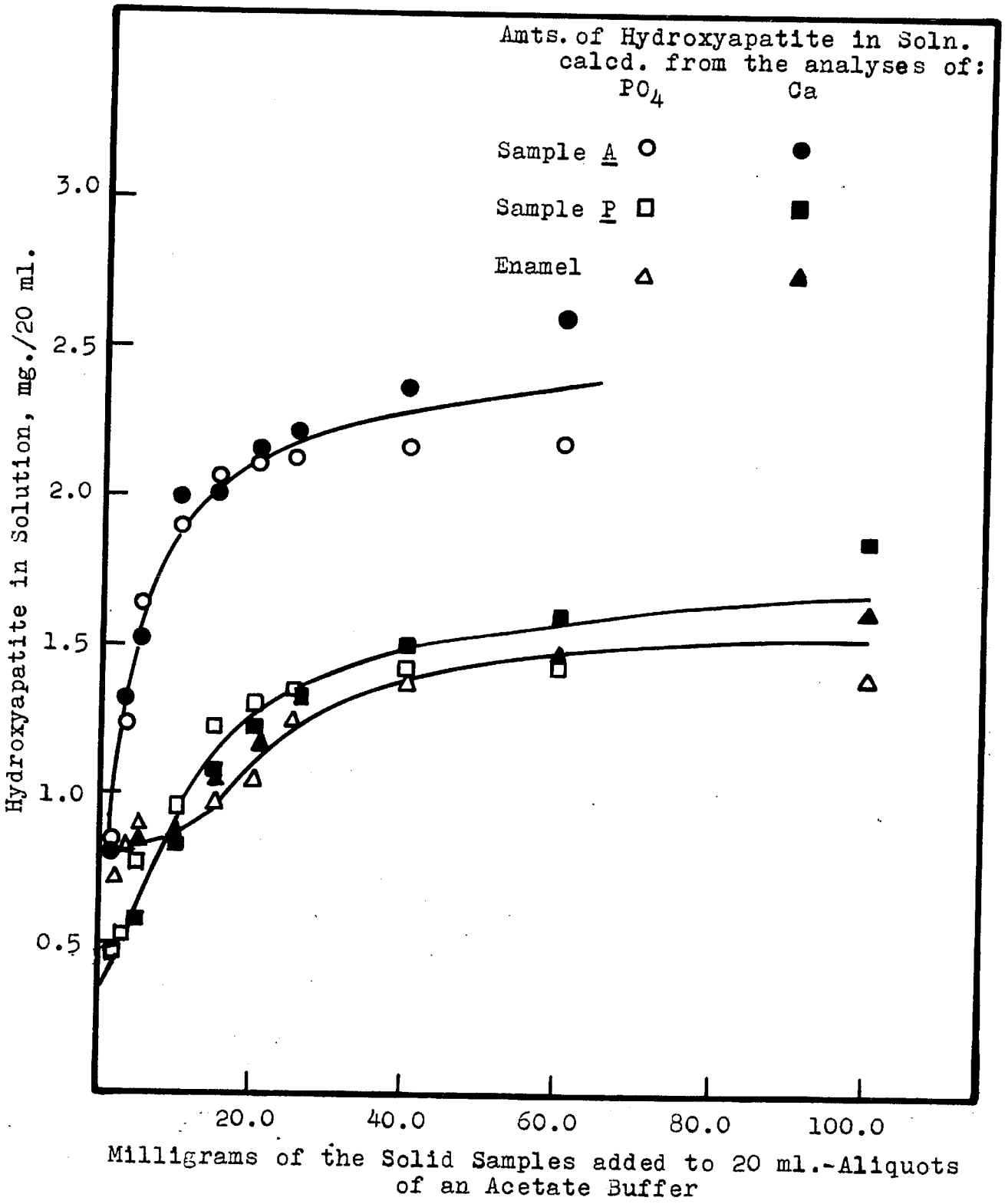

Figure 45.- Solubilities of Synthetic Hydroxyapatite Samples A and P and Enamel as a Function of Amount of the Solids exposed to 20 ml.-Aliquots of 0.2M Acetate Buffer pH 6.0 for 114 Hours (at 30°C.).

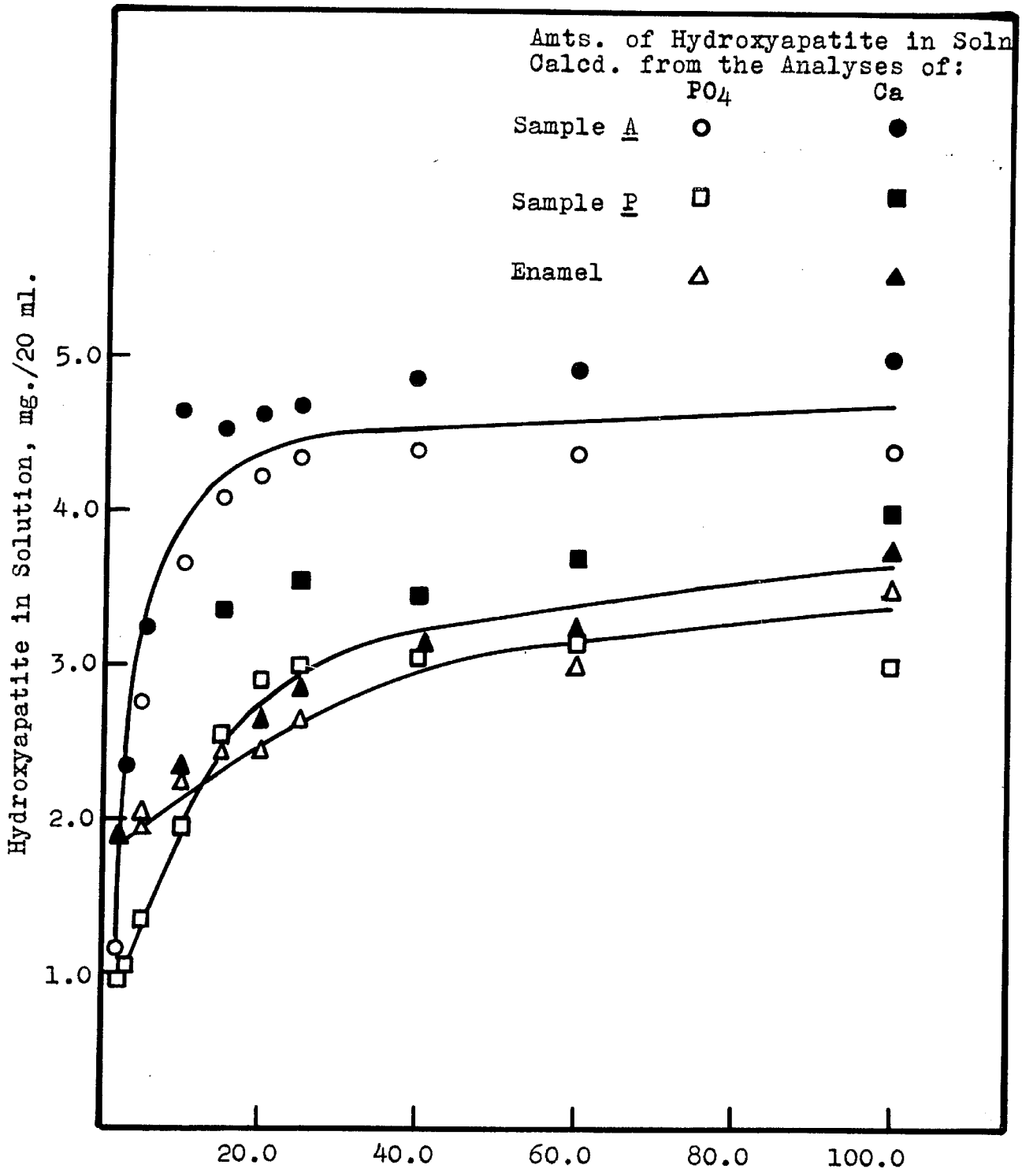

Figure 46.- Solubilities of Synthetic Hydroxyapatite Samples A and P and Enamel as a Function of Amount of the Solids exposed to 20 ml.-Aliquots of 0.2M Acetate Buffer pH 5.7 containing 0.5M Sodium Chloride for 114 Hours (at 30°C.).

as the solid to buffer ratio is increased and it tends to level off at high solid to buffer ratios for all the three samples. However, solubility of hydroxyapatite sample A is significantly greater than those of hydroxyapatite sample P and powdered enamel, while the solubility behavior of the latter two show a remarkable similarity. The difference between samples A and P may be due to the presence of carbonate in the commercially obtained sample A.

Dissolution Rate Study in the Absence of Common Ions

In order to compare the experimental rates with the theoretical rates described earlier, dissolution rate experiments were carried out with the synthetic hydroxyapatite samples A and P, and the powdered enamel in acetic acid and lactic acid buffers. The pH and buffer concentration of each buffer and whether the buffer contained 0.5 Molar sodium chloride is indicated in Figures 47-52. Similar experiments were also carried out with the sample C in addition to the above three , in dilute hydrochloric acid, ranging in concentrations from 0.001 Normal to 0.01 Normal, with ionic strength adjusted to 0.5 by the addition of sodium chloride.

The data (see Appendix I) obtained was initially plotted as the amount of hydroxyapatite in solution versus time. The amount of hydroxyapatite in solution was calculated on the basis of phosphate analysis assuming stoichiometric dissolution. Calcium analyses of the liquid

samples were carried out in most of the dissolution runs at alternate time intervals. When the initial dissolution rates were estimated according to the procedure described below, it was observed that essentially the same rates were obtained based on either of the analysis.

Procedure for the Estimation of the Initial Dissolution Rates-- Initial dissolution rates were estimated from the plots of amount of hydroxyapatite in solution as a function of time. Whenever possible, slopes were taken at the point where 10% of the solid had dissolved. These were then corrected for the reduction in driving force for dissolution estimated from the amount dissolved at that time and the amount in solution at equilibrium i.e., the solubility.

But when there were not enough data points to cover the region upto 10% of the solid dissolved, slopes were taken at 5% of the solid dissolved and corrected as before. Or the initial rates were estimated directly involving a method of manual extrapolation of the data points to the abscissa and estimating the initial slopes.

Figures 47-52 show the initial rates thus obtained for the synthetic samples and enamel in the acetate and lactate buffers as indicated. Similarly, Figure 53 shows the plot of the initial rates as a function of hydrochloric acid concentrations. Circles in all these figures represent the estimated experimental rates. It seems that the synthetic

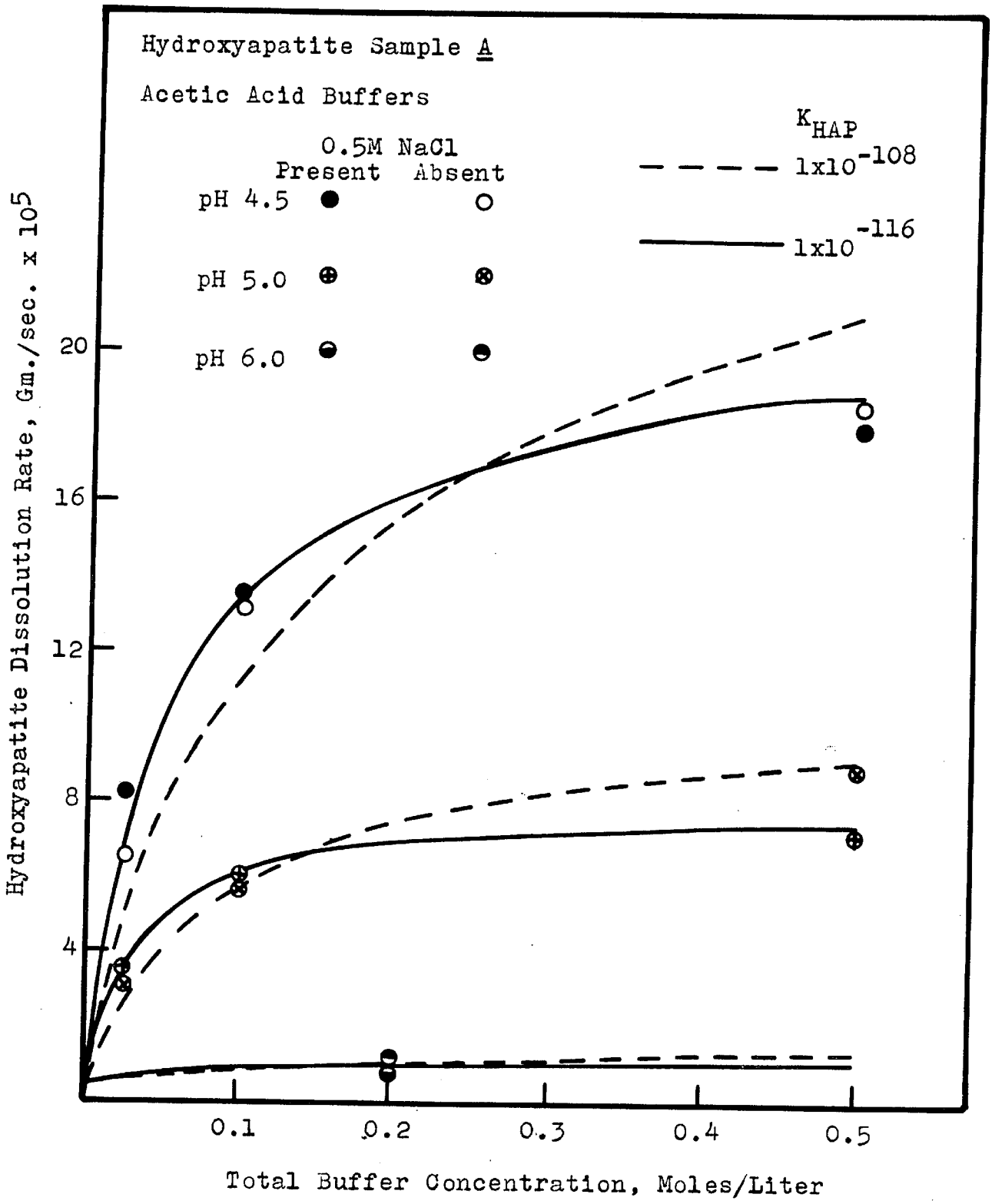

Figure 47.- Initial Dissolution Rates of Synthetic Hydroxyapatite Sample A in Acetic Acid Buffers with and without the Presence of 0.5M NaCl as a Function of $[TB]_h$ and pH. Circles are experimental data. Curves are Theory (Equations 3 and 4) with the indicated K_{HAP} values. The h' values used to obtain this fit are given in Appendix III.

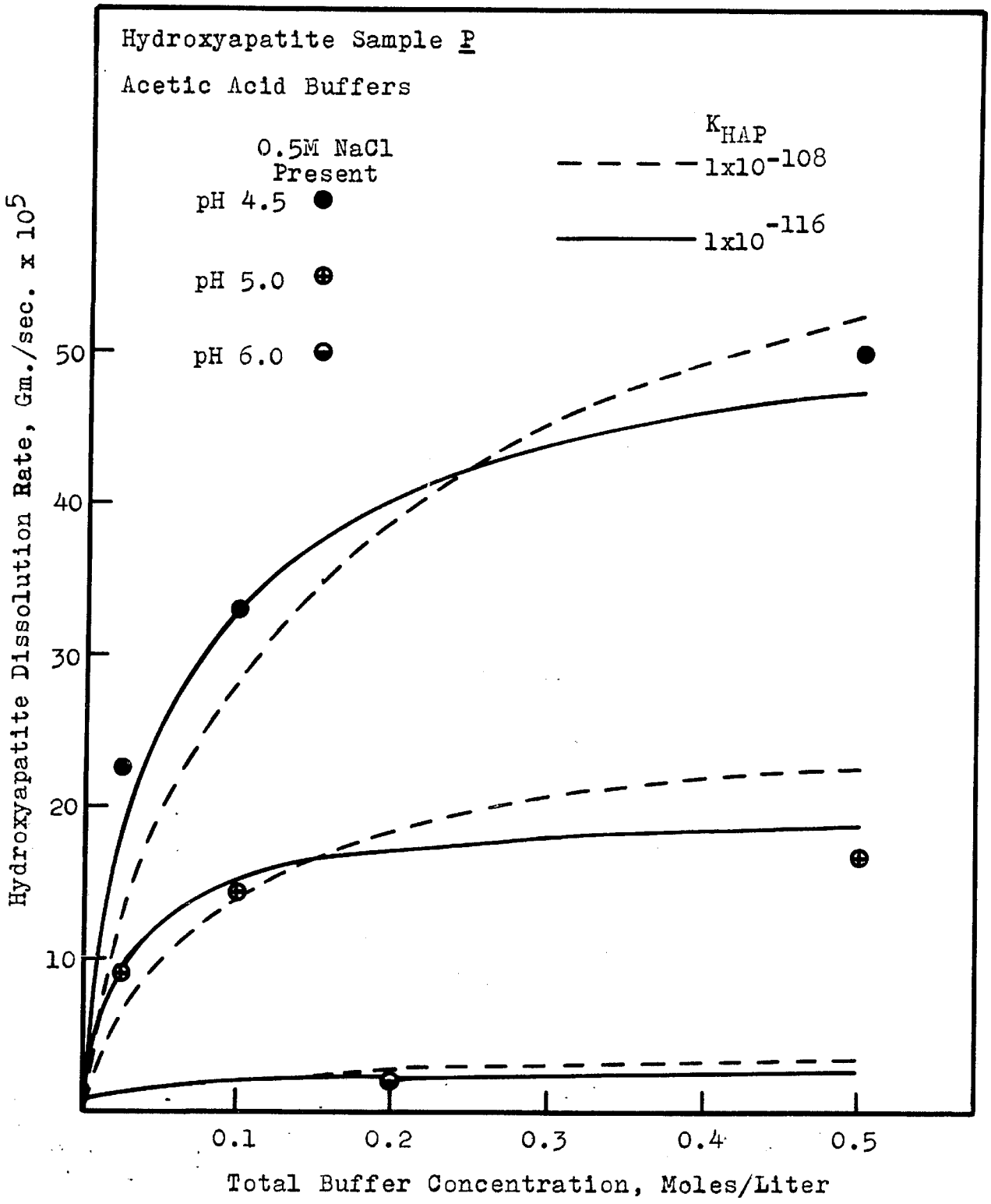

Figure 48.- Initial Dissolution Rates of Synthetic Hydroxyapatite Sample P in Acetic Acid Buffers with the Presence of 0.5M NaCl as a Function of $[TB]_h$ and pH. Circles are experimental data. Curves are Theory (Equations 3 and 4) with the indicated K_{HAP} values. The h' values used to obtain this fit are given in Appendix III.

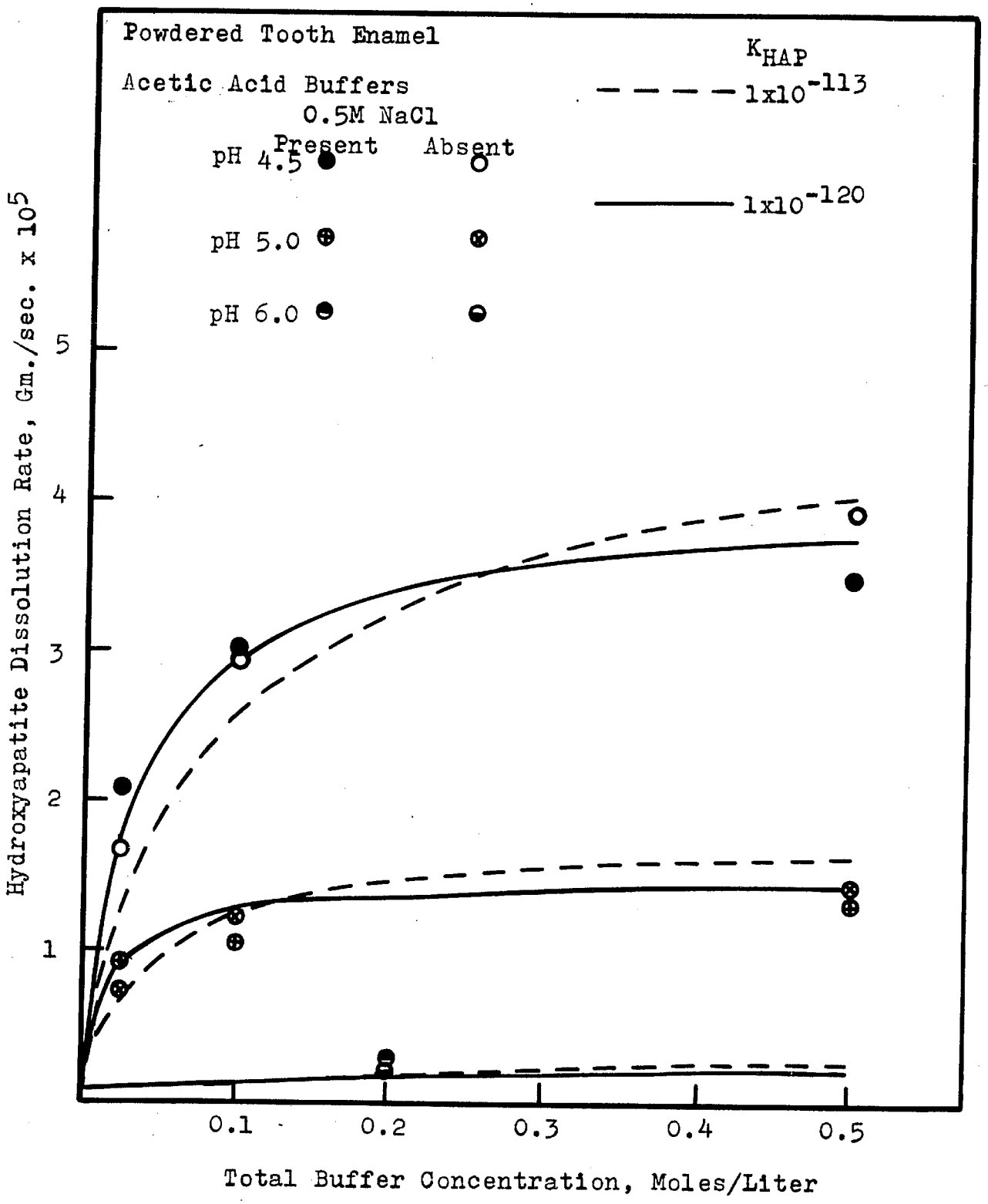

Figure 49.- Initial Dissolution Rates of Powdered Tooth Enamel in Acetic Acid Buffers with and without the Presence of 0.5M NaCl as a Function of $[TB]_h$ and pH. Circles are experimental data. Curves are Theory (Equations 3 and 4) with the indicated K_{HAP} values. The h' values used to obtain this fit are given in Appendix III.

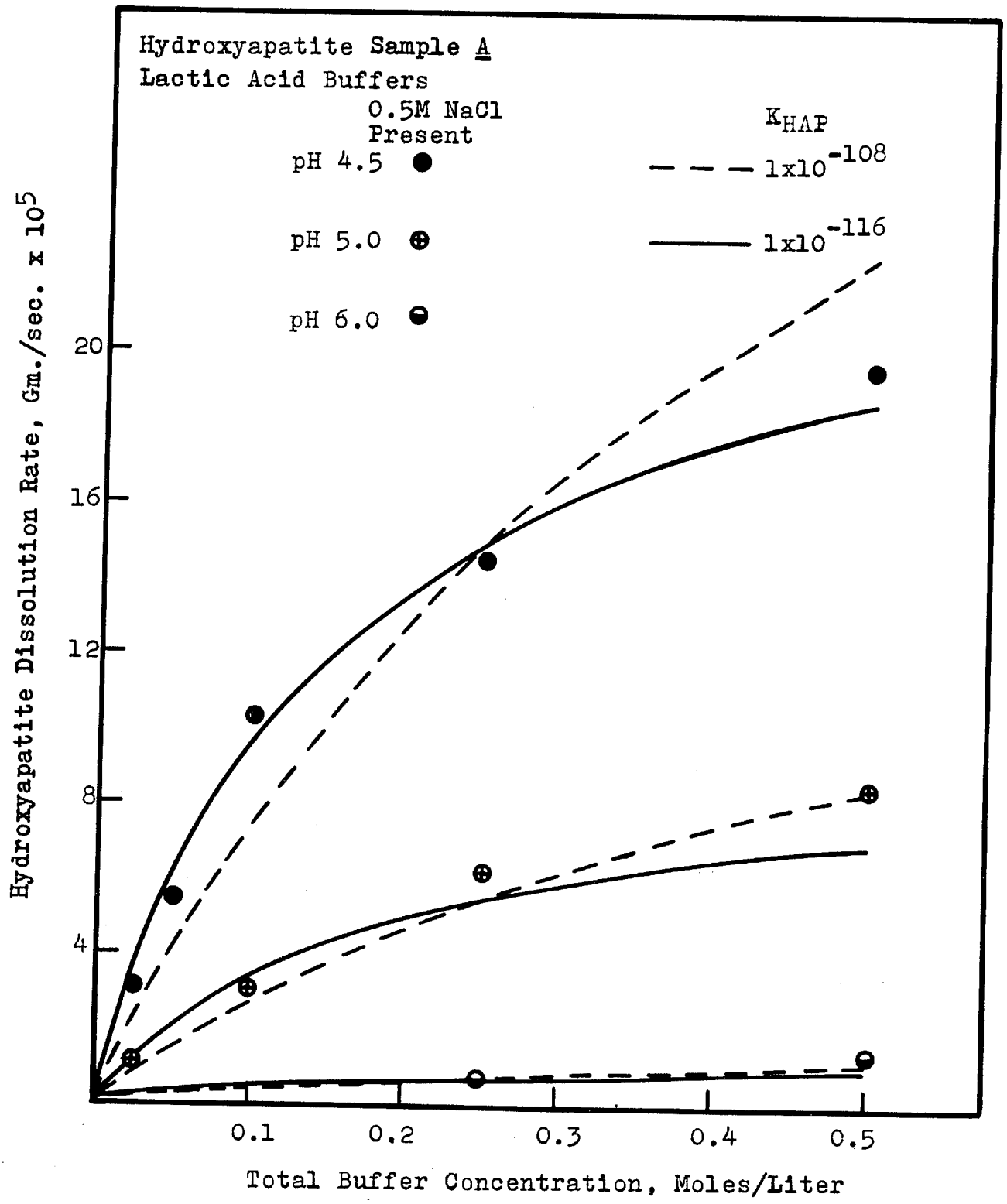

Figure 50.- Initial Dissolution Rates of Synthetic Hydroxyapatite Sample A in Lactic Acid Buffers with the Presence of 0.5M NaCl as a Function of $[TB]_h$ and pH. Circles are experimental data. Curves are Theory (Equations 3 and 4) with the indicated K_{HAP} values. The h' values used to obtain this fit are given in Appendix III.

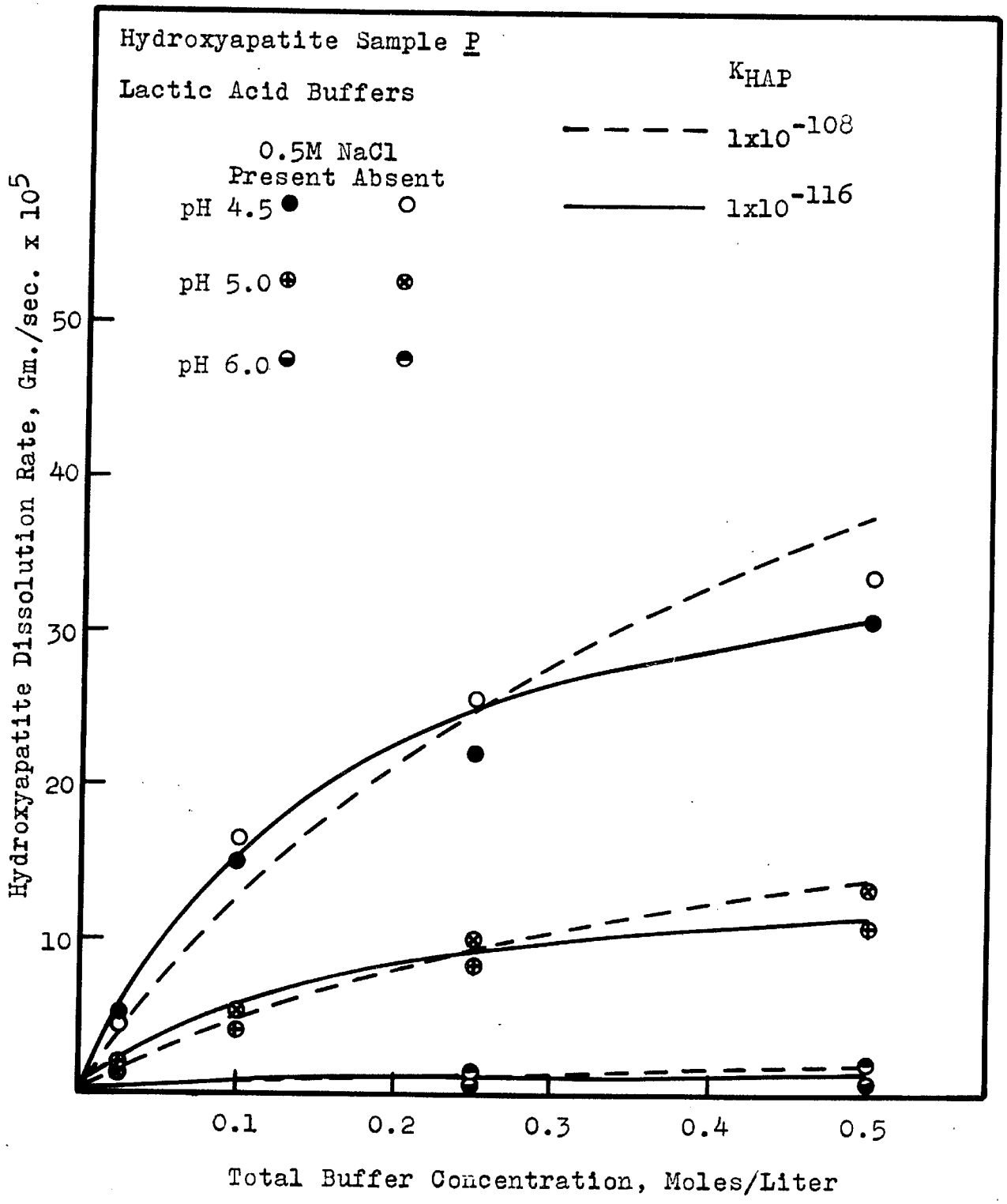

Figure 51.- Initial Dissolution Rates of Synthetic Hydroxyapatite Sample P in Lactic Acid Buffers with and without the Presence of 0.5M NaCl as a Function of $[TB]_h$ and pH. Circles are experimental data. Curves are Theory (Equations 3 and 4) with the indicated K_{HAP} values. The h' values used to obtain this fit are given in Appendix III.

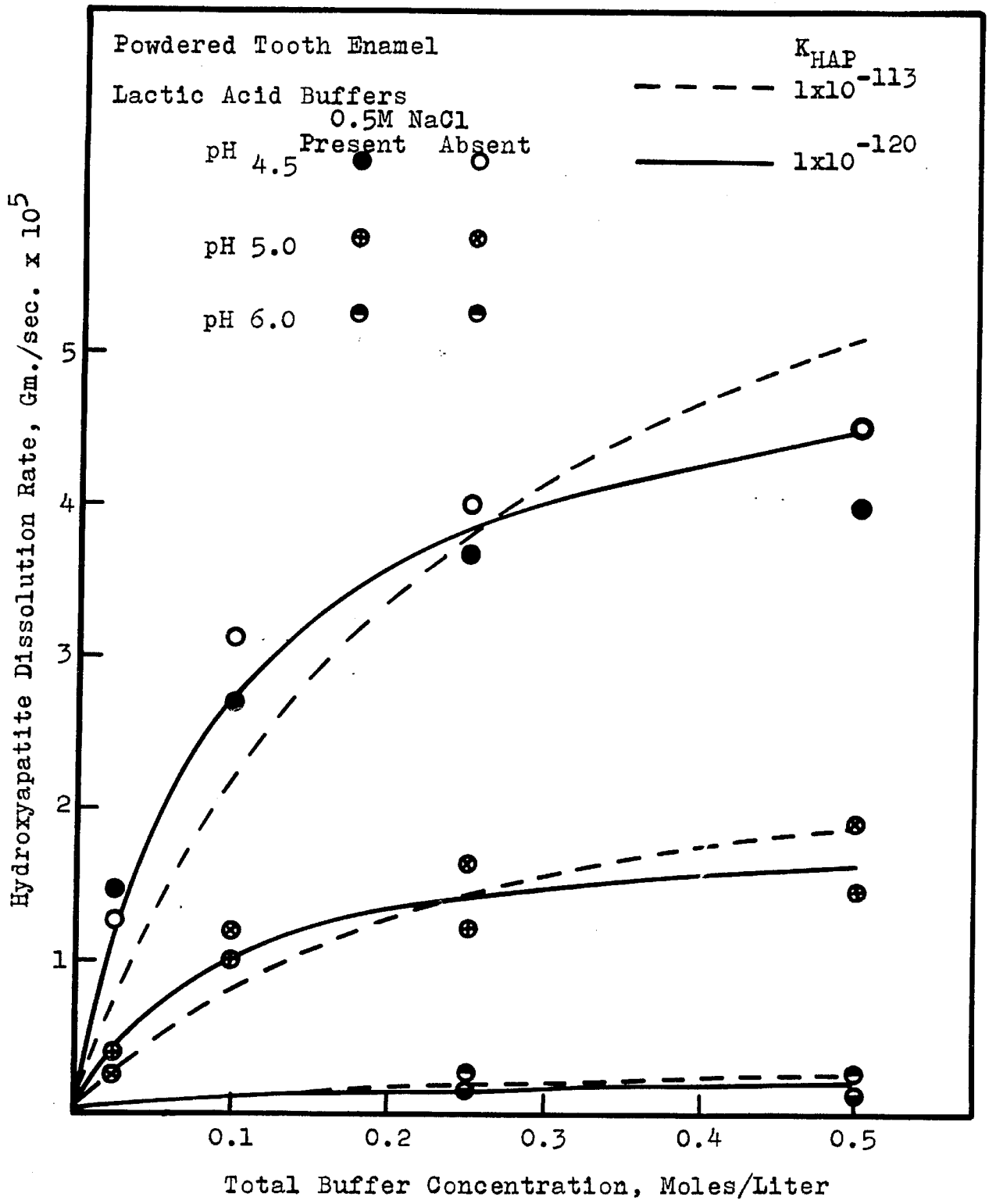

Figure 52.- Initial Dissolution Rates of Powdered Tooth Enamel in Lactic Acid Buffers with and without the Presence of 0.5M NaCl as a Function of $[TB]_h$ and pH. Circles are experimental data. Curves are Theory (Equations 3 and 4) with the indicated K_{HAP} values. The h' values used to obtain this fit are given in Appendix III.

hydroxyapatite sample P dissolves at almost twice the rate of the sample A, in both the acetate and lactate buffers as well as in the hydrochloric acid solutions. Whereas enamel dissolves much more slowly (about 1/4th the rate of the sample A) in the acetate and lactate buffers, but its rate of dissolution in the hydrochloric acid solutions is comparable to that of the samples A and C. As it can be seen from these plots, whenever the "swamping" electrolyte, sodium chloride, was used at low buffer concentrations (0.025 Molar), the effect was to increase the rate. However, at high buffer concentrations (0.1-0.5 Molar), the effect of the added electrolyte was to decrease the rate in both the acetic and lactic acid buffers.

Comparison of the Experimental Initial Rates with the Theory-- The closed curves in Figures 47-52 represent theory based on equations 3 and 4 (case I) with the hydroxyapatite solubility product, K_{HAP}, value as indicated in the figures. For each set of data represented by each figure (i.e., all the three pH values and all the buffer concentrations), a single hydrodynamic constant, h, value was selected to give the best visual fit as shown in each of the figures by the closed curves.

The broken curves in the Figures 47-52 correspond to the theory based on the same equations but with different K_{HAP} values. These curves were fitted to the data in the same manner as before, requiring different h values.

Comparisons of the synthetic mineral data with the theory indicate that the theory with a K_{HAP} value in the range of $1x10^{-116}$ to $1x10^{-113}$ appears to give better agreement. In the case of the enamel data, the theory with a K_{HAP} value in the range of $1x10^{-120}$ to $1x10^{-118}$ seems to give better fit. This is true for the results obtained in the acetate as well as in the lactate buffers. Also it can be noticed that, in both buffers, the effect of the "swamping" electrolyte is to lower the value of the best-fit K_{HAP}.

Figure 53 shows a linear relationship between initial dissolution rates and hydrochloric acid concentrations as predicted by the theory (see Figure 8). The fact that each of the samples gave different slopes may be indicative of the varying surface areas of the samples used.

Dissolution Rate Study in the Presence of Common Ions

Again from the plots of the amount of hydroxyapatite in solution as a function of time in acetate and lactate buffers, pH 4.5 and 0.05 Molar total buffer concentration, containing 0.003-0.05 Molar calcium or phosphate ions, initial dissolution rates were estimated employing the same technique as before. Only phosphate analysis was performed in the case of buffers containing calcium ions, except when sample R was studied. In this latter case only calcium was assayed by radioactivity determination. When the rate was studied in the buffers containing phosphate ions, only

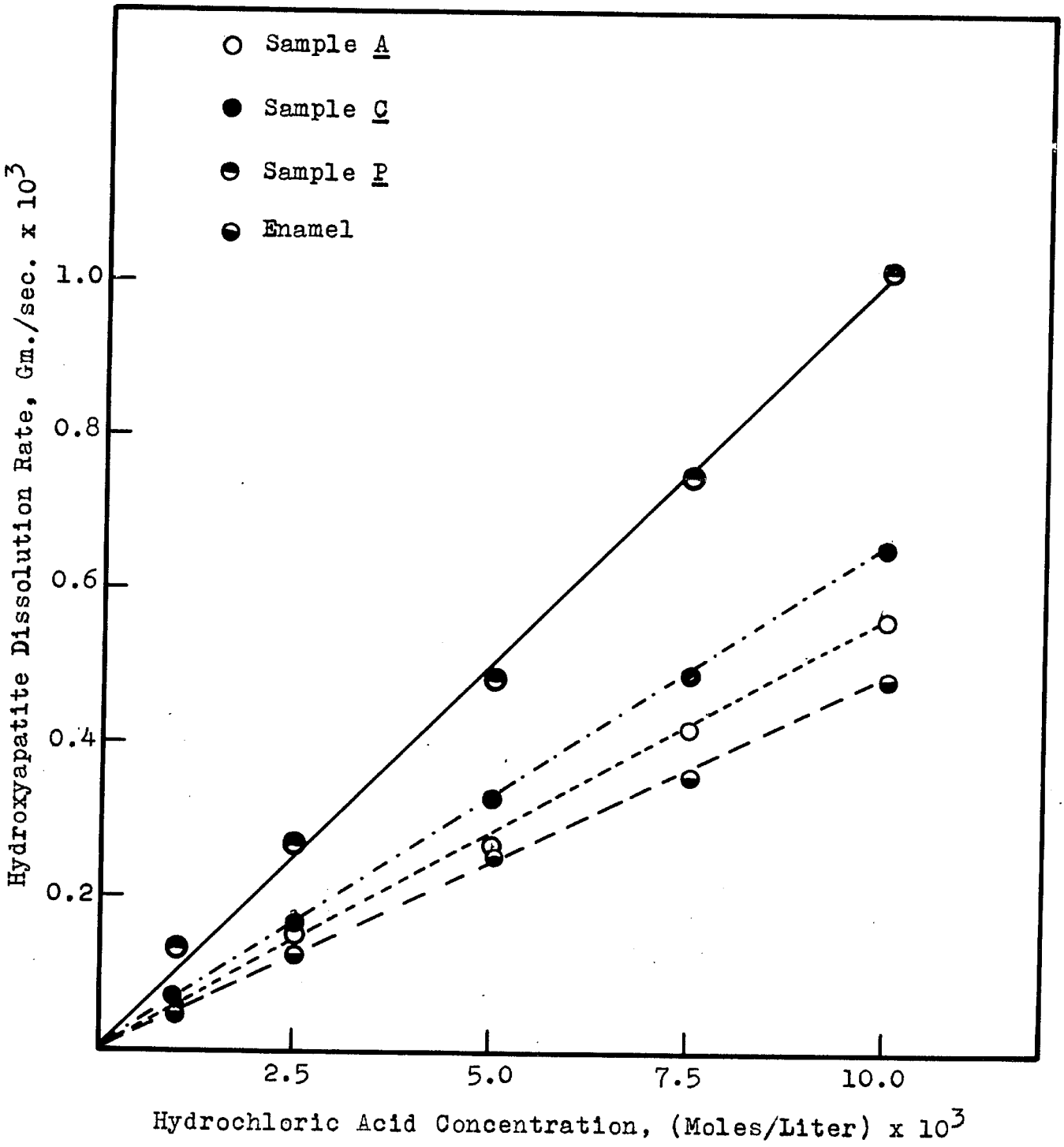

Figure 53.- Dissolution Rates of Synthetic Hydroxyapatite Samples and Enamel as a Function of Hydrochloric Acid (containing 0.5M Sodium Chloride) concentration (at 30°C.).

calcium was analyzed. The reason for analyzing only one ion is that, when the buffer is initially flooded with a large concentration of either calcium or phosphate ions one can not accurately analyze small increases in calcium or phosphate respectively, due to the dissolution of the solid sample.

Comparison of the Experimental Initial Dissolution Rates with the Theory-- The results of this study are plotted as % of no common ion rate versus common ion concentration as shown in Figures 54-57. The circles represent the experimental results obtained with the indicated mineral samples and the curves represent the theory corresponding to the equations 3 and 4 with different K_{HAP} values as indicated in each figure.

It should be noted here that these theoretical curves represent the theory without any assumption regarding h, because it cancels out when the % of no common ion rate [common ion rate x 100/no common ion rate] is calculated.

From the comparisons between the theory and experimental data it appears that enamel data in acetate and lactate buffers containing calcium and phosphate ions would fit well to the theory with a K_{HAP} value somewhere in the range of $1x10^{-118}$ to $1x10^{-122}$. In acetate buffers containing calcium ions, data for the samples A and R would fit to the theory with a K_{HAP} value between $1x10^{-113}$ and $1x10^{-116}$ (Figure 54), while the sample P data in the same

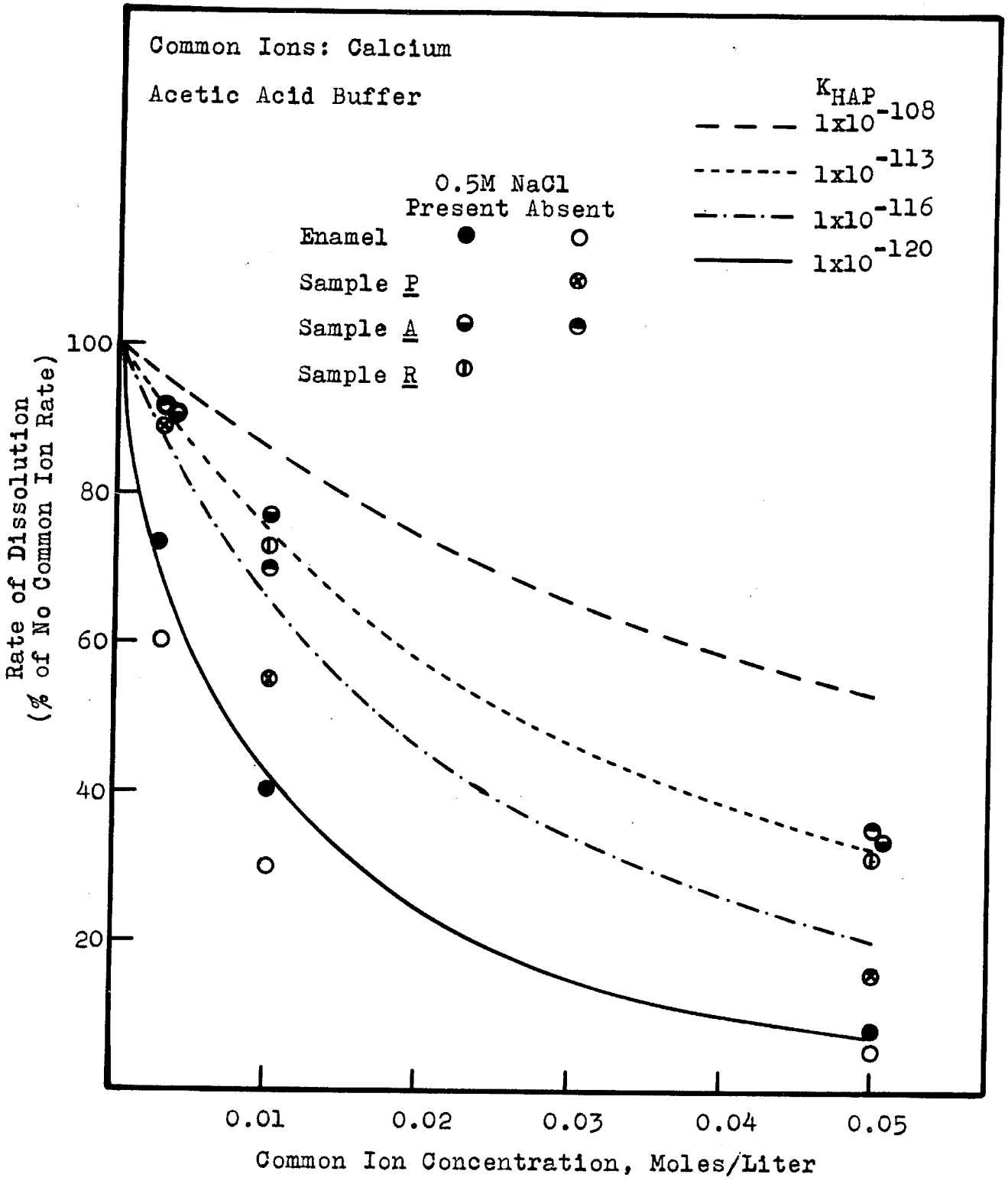

Figure 54.- Effects of the Calcium Ions on the Initial Dissolution Rates of Synthetic Hydroxyapatite Samples and Enamel in a 0.05M Acetate Buffer pH 4.5 with and without the Presence of 0.5M NaCl. Circles are experimental data. Curves are Theory (Equations 3 and 4) with the indicated K_{HAP} values.

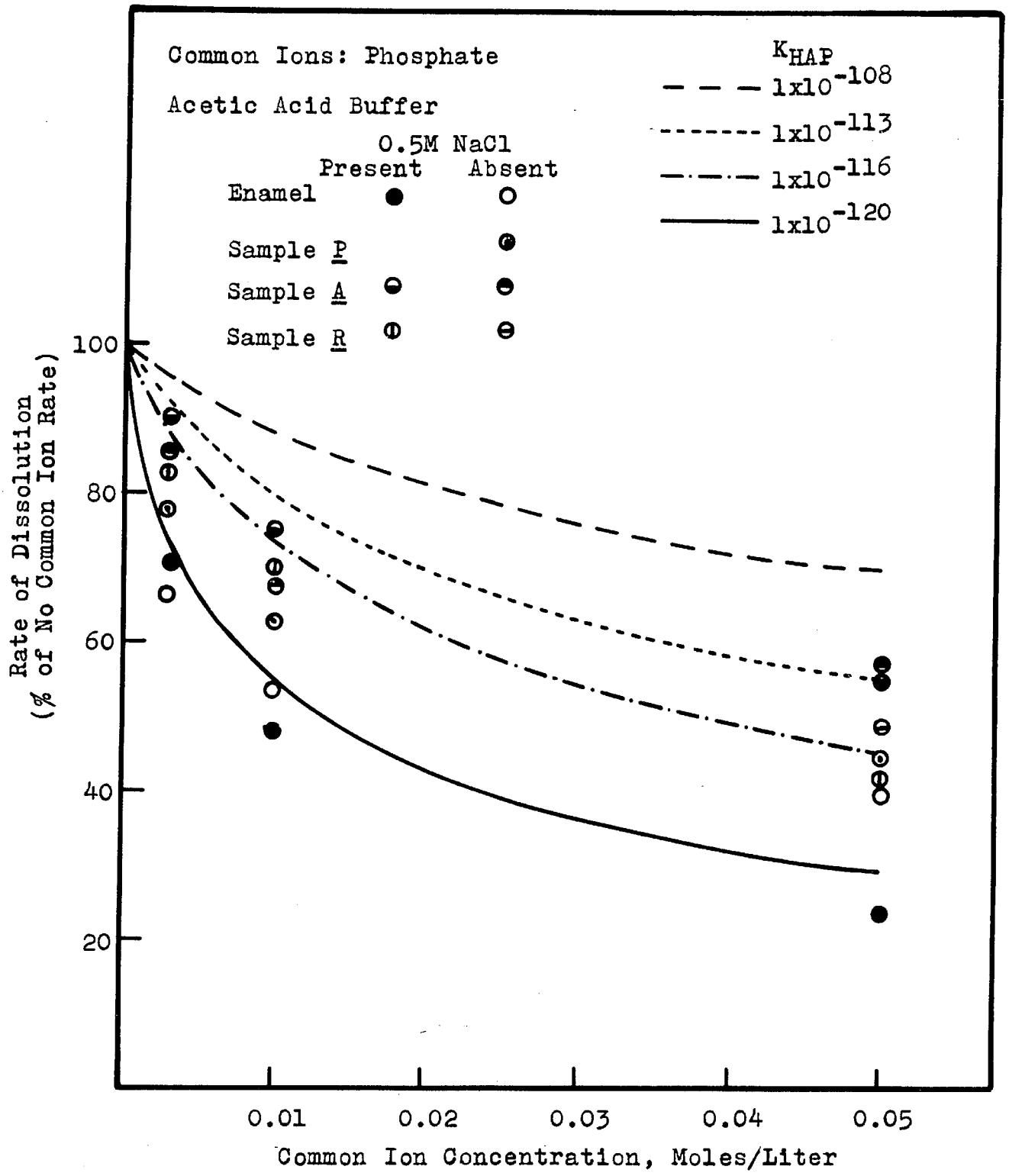

Figure 55.- Effects of the Phosphate Ions on the Initial Dissolution Rates of Synthetic Hydroxyapatite Samples and Enamel in a 0.05M Acetate Buffer pH 4.5 with and without the Presence of 0.5M NaCl. Circles are experimental data. Curves are Theory (Equations 3 and 4) with the indicated K_{HAP} values.

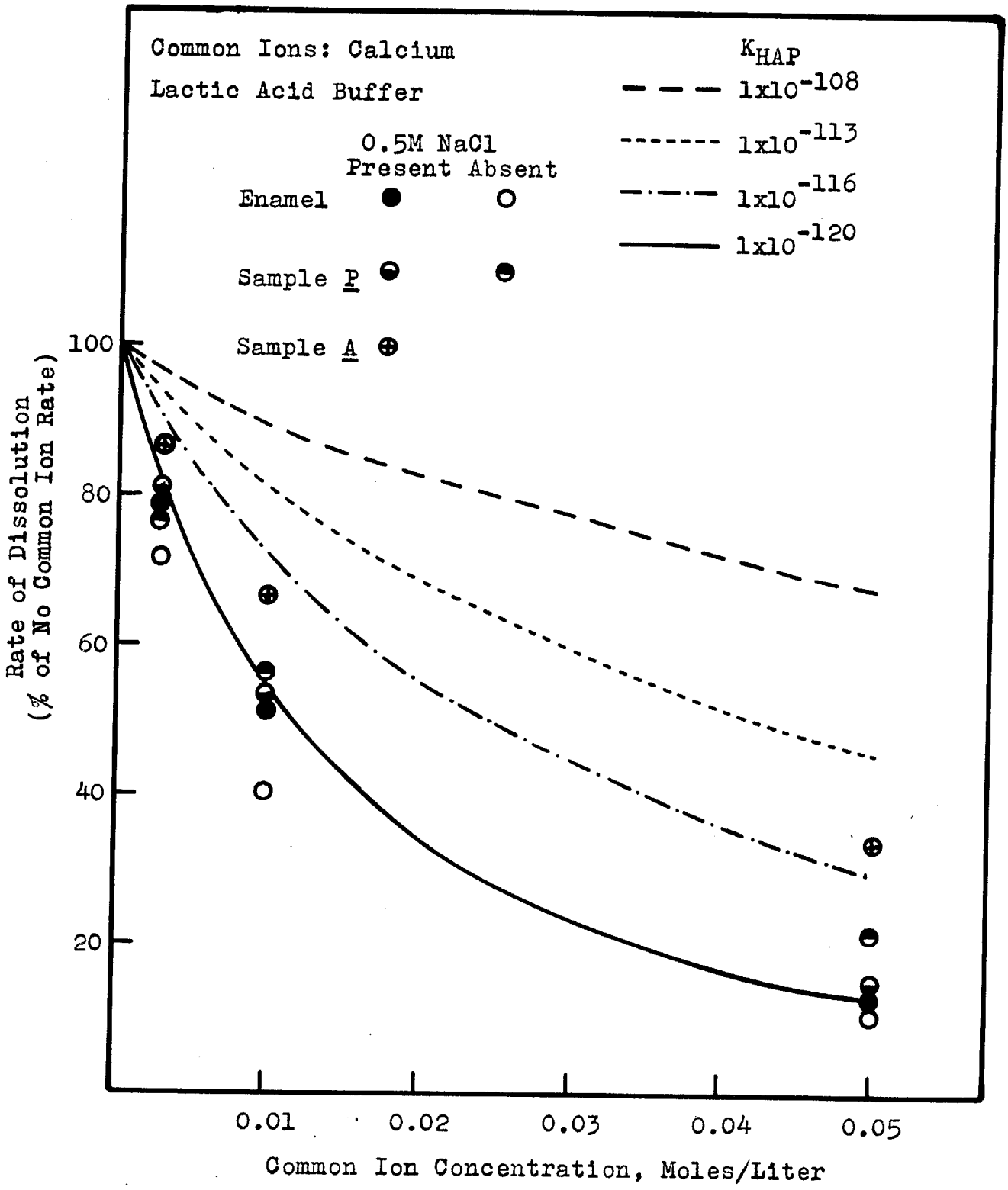

Figure 56.- Effects of the Calcium Ions on the Initial Dissolution Rates of Synthetic Hydroxyapatite Samples and Enamel in a 0.05M Lactate Buffer pH 4.5 with and without the Presence of 0.5M NaCl. Circles are experimental data. Curves are Theory (Equations 3 and 4) with the indicated K_{HAP} values.

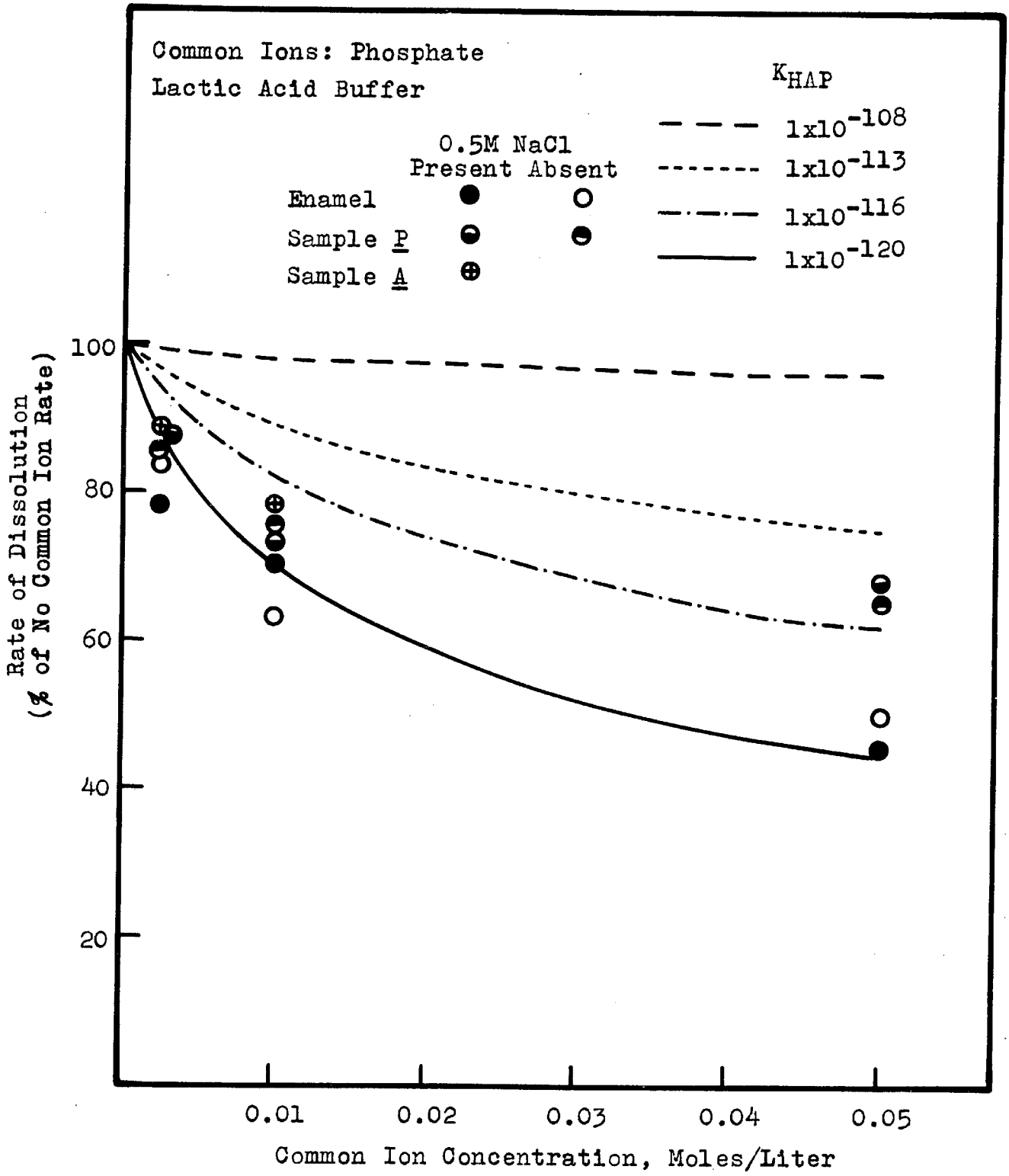

Figure 57.- Effects of the Phosphate Ions on the Initial Dissolution Rates of Synthetic Hydroxyapatite Samples and Enamel in a 0.05M Lactate Buffer pH 4.5 with and without the Presence of 0.5M NaCl. Circles are experimental data. Curves are Theory (Equation 3 and 4) with the indicated K_{HAP} values.

buffers would fit somewhere between K_{HAP} values $1x10^{-120}$ and $1x10^{-116}$. In lactate buffers containing calcium ions, the sample A data fit to the theory with $K_{HAP} = 1x10^{-116}$ and the sample P data appear to fit to the theory with $K_{HAP} = 1x10^{-120}$ (Figure 56), which is also true for the results in the lactate buffers containing phosphate ions (Figure 57). In the case of acetate buffers containing phosphate ions, the sample P data fell between the theory with K_{HAP} values $1x10^{-120}$ and $1x10^{-116}$ (Figure 55), while data for the samples A and R lie near the theory with $K_{HAP} = 1x10^{-116}$.

DISCUSSION

Equilibrium Constants

In the present study all equilibrium constants employed are concentration equilibrium constants. These were obtained from the thermodynamic values by correcting for ionic strength effects with appropriate activity coefficients, as discussed earlier. The values given in Tables 1 and 2 are for 25°C., whereas the present study was conducted at 30°C. It was decided that estimations of the temperature corrections were unwarranted in view of the uncertainties in the values of the activity coefficients. Furthermore, in a comparative study like this, where only the relative rates were considered, the expected small temperature effects should cancel out or could be absorbed in the hydrodynamic factor h.

The estimated concentration equilibrium constants for acetic and lactic acid (Table 2) are justified by experimentally determined values as shown in Appendix II.

The Meaning of the h value in the Comparison of the Theoretical and Experimental Dissolution Rates

All the theoretical demineralization rates of enamel in this study are presented as the product Gh. Here, G is the stoichiometric dissolution rate in Moles $Ca^{2+}/cm.^2/sec.$,

and h is the hydrodynamic factor constant having a unit of centimeter. Hence, Gh has the units of Moles Ca^{2+}/cm./sec.

Because the true surface areas of the 80-100 mesh granules of the synthetic hydroxyapatite (HAP) samples and 100-200 mesh particles of powdered enamel were not known, the experimental rates were expressed as Gm.HAP dissolved/sec.

In order to be able to compare the theoretical rates with the experimental rates it was necessary to have both the rates in the same units. However, since h is also an unknown, the only way one can make the comparison is on a relative basis. All Gh values were first multiplied with a factor, f, to convert the Moles Ca^{2+}/cm./sec. units into the Gm.HAP/cm./sec. units. The factor f is (Mol.Wt.HAP)/(No. of Ca^{2+} Moles/Mole of HAP). These new values of Gh were again multiplied with an another factor, h', which is constant for any one set of the experimental data (Figures 47-52). This factor h' is SA/h, where SA is the effective surface area of 100 mg. of the granulated mineral sample in question and h has the usual meaning. Both SA and h are unknowns. For any one set of the data (Figures 47-52), a single value of the factor h' was selected to obtain the best visual fit of the experimental rates to the theoretical rates. The h' values used for each set of the data are tabulated in Appendix III.

It should be noted, that in making a comparison of the experimental rates in the presence of common ions with the

theoretical rates, there is no need for the h' factor. Since this factor cancels out, the ratios ((common ion rate x100)/(no common ion rate)) calculated from the experimental and theoretical rates are directly comparable.

Granulated Synthetic Hydroxyapatite Samples versus Powdered Enamel

It is possible that the synthetic minerals prepared by different methods might have different crystal size distributions, and hence different surface areas. It is conceivable that synthetic hydroxyapatite samples with different surface areas may differ in their properties of compressibility and ability to form compact masses upon compression. Hence, the granules obtained from such different samples after compression may have different porosities. It is believed that upon compression, samples with larger surface areas would form a more compact mass with less porosity; the reverse would be true for the samples with smaller surface areas.

Preliminary experiments (36) on surface area measurements have shown that before the granulation step sample A had a bigger surface area than sample P. This in view of the above suggests that granules of sample P might be more porous than those of sample A.

In dissolution rate studies, porous granules may contribute to increased initial dissolution rates due to the dissolution of the crystals not only from the surface

region but also from the bulk part of the granules. In such cases effective surface areas should be important in determining the initial dissolution rates.

In view of this, the higher initial dissolution rates of the synthetic mineral P in the weak acid buffers can be partly explained on the basis of the larger effective surface area available for the dissolution. The mineral sample A, which might have a smaller effective surface area, dissolved at about one half the rate of sample P in the same buffers. Since enamel particles, consisting of compact masses of large hydroxyapatite crystals embedded in an organic matrix, dissolved at the slowest rate in the weak acid buffers, one might conclude that there is a very small effective surface area involved in the enamel dissolution process as compared to the synthetic minerals.

However, in hydrochloric acid the initial dissolution rates of enamel were comparable to those of sample A, while sample P dissolved at higher rates. Since strong acids are completely dissociated in dilute solutions, a large pool of hydrogen ions is available to dissolve the surface crystals. In view of this, only the surface region of the granules or solid particles would be important in determining the dissolution rates. Sample A and enamel might have comparable areas in the surface region of their granules and particles respectively. Sample P might have a little larger surface area in the surface region of its granules or there might be a small amount of surface detachment of the primary crystals in the surface region of the granules of sample P

during the dissolution rate experiments to give higher initial dissolution rates in strong acids.

Stoichiometry of Hydroxyapatite Samples

The chemical analyses of the hydroxyapatite samples and the powdered enamel (Table 4) indicate that the samples vary in stoichiometry, the Ca/PO_4 molar ratio. Many investigators (37, 38) have suggested that calcium phosphates intermediate in stoichiometry between apatite (Ca/PO_4 molar ratio = 1.667) and dicalcium phosphate (Ca/PO_4 molar ratio = 1.000) involve:

a) solid solutions of these two as end members,

b) defect-apatite structures,

c) isomorphic replacement of calcium ions of apatite by hydrogen ions

or d) solids whose compositions have been altered by absorption of other ions or by other changes in the Ca/PO_4 ratio in the surface.

Solubility Product of Hydroxyapatite

The solubility products of hydroxyapatite can be calculated from the solubilities (Figures 45-46) of the synthetic mineral samples and the enamel. Because the solubility varies with the amount of solid, one would expect different solubility product values depending upon which point on the solubility curve is selected. Table 5 shows the results of such calculations. It is remarkable

TABLE 5

Calculated Values of K_{HAP}

From Solubility Experiments, Figure 45

(Amt. Solid)/ (Buffer Volm.) Ratio mg./ml.	Enamel and Sample P			Sample A		
	Exp'l $K^6_{3P} x K^2_w / K_{HAP}$	Exp'l K_{HAP}		Exp'l $K^6_{3P} x K^2_w / K_{HAP}$	Exp'l K_{HAP}	
		Concn.	Thermdyn.		Concn.	Thermdyn.
10/20	4.8×10^{11}	2.3×10^{-110}	2.7×10^{-120}	3.0×10^{7}	3.7×10^{-106}	3.6×10^{-116}
50/20	4.3×10^{7}	2.6×10^{-106}	2.4×10^{-116}	7.1×10^{3}	1.5×10^{-102}	4.2×10^{-112}

to note that the values of the solubility product calculated from the solubility experiments are very close to the values which gave good fit to the dissolution rate data for the enamel and the hydroxyapatite samples A and P.

In the literature, various reasons have been cited for this abnormal solubility behavior of hydroxyapatite. Rootare, Deitz, and Carpenter (24) have reported such behavior and have suggested that when hydroxyapatite is immersed in water the terminal phosphate ions of the solid undergo hydrolysis as shown below and a surface complex is formed:

a) $Ca_{10}(PO_4)_6(OH)_2 = 4[Ca_2(HPO_4)(OH)_2] + 2Ca^{2+} + 2HPO_4^{=}$
Surface Complex

b) $Ca_2(HPO_4)(OH)_2 = 2Ca^{2+} + HPO_4^{=} + 2OH^-$

This surface complex rapidly covers the exposed surface of the solid, which might have different solubility.

Another explanation comes from Posner, Perloff, and Diorio (38) that hydrogen ions diffuse inside the crystal lattice of hydroxyapatite when it is exposed to water. These hydrogen ions then substitute for calcium ions in the lattice structure. Thus, starting from true hydroxyapatite one can have the following compositions in the surface unit cells of the crystals having different solubility behavior: $Ca_{10}(PO_4)_6(OH)_2$; $Ca_9H_2(PO_4)_6(OH)_2$; - - - - -; and $Ca_6H_8(PO_4)_6(OH)_2$.

Biological Significance

A unique feature of dental caries is the subsurface demineralization phenomena. This is sometimes referred to as "white spot" formation. A "white spot" or a "softened" zone may exceed a thousand microns showing subsurface loss of minerals extending almost to the full depth of the enamel. Despite this subsurface demineralization, a thin zone along the enamel surface may be surprisingly intact. The relative resistance of the thin surface enamel layer to demineralization is attributed to a less soluble surface structure.

Pigman, Brasher, and Koulourides (39) have studied enamel "softening" resulting from an exposure of extracted human tooth to artificially grown plaques in several sugars. An artificial mouth was used for this purpose. Weak acids generated by bacterial-enzymatic breakdown of the sugars were responsible for the enamel "softening".

Soni and Brudevold (40) have duplicated <u>in vitro</u> the subsurface demineralization pattern of carious lesions in enamel by employing weak buffers (0.01-0.001 Molar pH 4-5) as decalcifying agents. They observed that as the buffer becomes weaker and the pH higher, the longer it takes for visible lesions ("white spots") to develop and the thicker will be the apparently normal surface layer over the lesion. Strong acids at low pH are, on the other hand, known to demineralize surface enamel, thus, producing cavities

rather than subsurface dissolution. In this context, the results of the present theoretical study with weak acid buffers and with hydrochloric acid tend to signify the same thing. The experimental results also show that in strong acids (e.g., hydrochloric acid) there is negligible difference in the dissolution rates between various synthetic minerals and enamel. While the dissolution rates vary widely in weak acid buffers. The solubility results indicate that there are variations in solubilities not only among various samples but also within the same samples.

Thus, the variations in hydroxyapatite solubilities may be related to the subsurface demineralization of enamel. It is suggested that mineral in the surface layer of enamel might have smaller solubilities and there may be a gradient of increasing solubility as one moves into the inner layers. Thus, more soluble mineral can preferentially dissolve away in weak acid buffers forming "white spots", while in stronger acids such as hydrochloric acid subsurface demineralization may not be observed because surface mineral would dissolve as fast as subsurface mineral. Theoretical results (Figure 8) show this indifference to solubility products in hydrochloric acid, while a great dependence of dissolution rates (Ghs) on solubility products in weak acid buffers is evident in Figures 4-7.

SUMMARY

1. Theoretical dissolution rates of enamel have been computed employing the "hydroxyapatite model" in which it was assumed that $Ca_{10}(PO_4)_6(OH)_2$ is the thermodynamically governing phase in enamel. The rates were obtained as a function of hydrogen ion concentration, total buffer concentration, dissociation constant of buffer acid (K_A), solubility product of hydroxyapatite (K_{HAP}), diffusion coefficients of various species, and common ion concentration.

2. It is revealed that small changes in the diffusion coefficient value of hydrogen ions do not alter the theoretical rates in the case of acetic acid ($K_A = 2.2 \times 10^{-5}$), while increasing the value of diffusion coefficient of hydrogen ions increased the rates to a much greater extent in the case of strong acids (e.g., hydrochloric acid, K_A = very large).

3. The theoretical dissolution rate-total buffer concentration relationship becomes more and more linear with increasing values of the acid dissociation constant.

4. The effect of increasing the K_{HAP} value is to increase the dissolution rate, and in the presence of

common ions, to decrease the effectiveness of the common ions. However, the degree of the rate increase by increasing K_{HAP} diminishes as stronger acids are used.

5. The theoretical model predicts that calcium and phosphate ions are effective as common ions. And it also predicts that in the case of buffers with very low buffer capacities phosphate ions might act to increase the dissolution rate (i.e., show an antagonistic phosphate ion effect).

6. Attempts have been made to verify the model experimentally. For this purpose dissolution rates of several synthetic hydroxyapatite samples and powdered enamel have been experimentally determined in acetate and lactate buffers with and without the presence of common ions, and in hydrochloric acid solutions. Effects of added neutral electrolyte have been also studied. Solubility studies on some of the mineral samples have been carried out in acetate buffer as a function of the amount of the solid added in a constant volume of the buffer solution.

7. The solubility study has revealed that the solubility of enamel and hydroxyapatite samples increases as a function of the amount of the solid originally added.

8. Comparison of the theory with the experimental rates

showed that the enamel data fitted to the theory with K_{HAP} values between $1x10^{-118}$ and $1x10^{-122}$. The laboratory made synthetic hydroxyapatite data fitted to the theory with K_{HAP} values between $1x10^{-116}$ and $1x10^{-120}$, while the commercial synthetic mineral fitted to the theory with a K_{HAP} value in the range of $1x10^{-113}$- $1x10^{-116}$. These K_{HAP} ranges were found to correlate with the experimentally obtained values from the solubility experiments for the respective samples.

9. Biological significance of the theoretical and the experimental results is discussed.

APPENDIX I

Experimental Data for Dissolution Rates of Synthetic Hydroxyapatite Samples and Powdered Tooth Enamel In Acetate and Lactate Buffers and In Hydrochloric Acid Solutions

Rate of Dissolution of Synthetic Hydroxyapatite Sample A

In Acetic Acid Buffers

In the Absence of Common Ions

Time Seconds	pH 4.5							
	0.025M		0.05M		0.1M		0.5M	
	0.5M NaCl	No NaCl	0.5M NaCl	No NaCl	0.5M NaCl	No NaCl	0.5M NaCl	No NaCl
	Amts* of Hydroxyapatite Dissolved in 200 ml. Buffer, Gm.x10^3							
100	10.7;12.1	8.8;10.5	17.2;20.0	11.6;10.5	16.3;16.0	15.1;15.9	19.3;22.5	19.9;21.2
300	23.2; --	19.1; --	37.0;39.5	25.7;24.5	33.2; --	31.6; --	40.5; --	41.8; --
500	31.9;35.8	26.8;30.2	48.9;50.3	35.8;28.9	44.8;45.4	42.9;55.3	56.4;59.3	58.3;57.8
700	38.8; --	32.5; --	56.3;60.1	44.3;35.7	52.2; --	52.1; --	62.6; --	68.6; --
900	43.3;52.0	37.3;41.1	64.9;67.9	50.5;44.0	57.7;58.8	57.9;58.6	73.0;77.6	78.8;74.1
1100	47.8; --	40.3; --	68.6; --	54.7;46.1	63.3; --	61.5; --	76.7; --	79.9; --

*The first number in each column is obtained from phosphate analysis and the second number is obtained from calcium analysis.

Rate of Dissolution of Synthetic Hydroxyapatite Sample A

in Acetic Acid Buffers

In the Absence of Common Ions

Time Seconds	pH 5.0					
	0.025M		0.1M		0.5M	
	0.5M NaCl	No NaCl	0.5M NaCl	No NaCl	0.5M NaCl	No NaCl
	Amts.*of Hydroxyapatite Dissolved in 200ml. Buffer, Gm.x10^3					
100	5.6; 7.9	4.7; 6.2	8.7; 9.7	7.7; 7.9	10.9;12.1	11.6; 6.9
300	12.0; --	10.3; --	18.7; --	17.9; --	22.5; --	24.1; --
500	17.0;20.0	14.6;16.4	25.3;27.4	25.2;26.5	31.9;33.6	34.7;28.7
700	20.5; --	18.6; --	31.7; --	31.2; --	40.5; --	42.1; --
900	23.2;27.5	21.4;24.0	36.1;36.7	35.6;37.0	44.3;47.5	47.6;49.6
1100	25.2; --	23.6; --	39.9; --	39.0; --	51.1; --	52.1; --

*The first number in each column is obtained from phosphate analysis and the second number from calcium analysis.

Rate of Dissolution of Synthetic Hydroxyapatite Sample A

In Lactate Buffers

In the Absence of Common Ions

Time Seconds	pH 4.5			
	0.025M	0.1M	0.25M	0.5M
	0.5M NaCl			
	Amts.* of Hydroxyapatite Dissolved in 200 ml. Buffer, Gm.x10^3			
100	--	12.6;17.5	16.0;20.7	28.7;30.0
300	12.3;14.6	26.9; --	38.3; --	54.9; --
500	--	37.5;46.0	52.9;62.1	72.8;75.6
600	18.8; --	--	--	--
700	--	44.4;--	63.3; --	83.1; --
900	22.9;27.6	50.3;60.0	71.2;80.9	89.4;83.4
1100	--	55.2; --	77.5; --	91.6; --
1200	26.3; --	--	--	--
1500	28.1;34.8	--	--	--
1800	30.1; --	--	--	--

*The first number in each column is obtained from phosphate analysis and the second number from calcium analysis.

Rate of Dissolution of Synthetic Hydroxyapatite Sample A

In Lactic Acid Buffers

In the Absence of Common Ions

Time Seconds	pH 5.0			
	0.025M	0.1M	0.25M	0.5M
	0.5M NaCl			
	Amts.* of Synthetic Hydroxyapatite Dissolved in 200ml. Buffer, Gm.x10^3			
100	--	5.4; 8.5	8.9;10.6	12.1;14.8
300	6.1; 1.4	11.2; --	18.6; --	26.7; --
500	--	15.8;20.1	26.9;30.1	38.5;39.9
600	9.4; --	--	--	--
700	--	19.2; --	32.2; --	46.0; --
900	11.4; --	21.5;28.4	36.8;41.1	52.4;55.5
1100	--	24.2; --	40.4; --	58.4; --
1200	12.7; --	--	--	--
1500	13.9;10.3	--	--	--
1800	14.7; --	--	--	--

*The first number in each column is obtained from phosphate analysis and the second number from calcium analysis.

Rate of Dissolution of Synthetic Hydroxyapatite Sample A

In Acetic and Lactic Acid

Buffers In the Absence of Common Ions

Time Seconds	Acetate Buffers		Lactate Buffers			
	pH 6.0					
	0.2M		0.25M		0.5M	
	0.5M NaCl	No NaCl	0.5M NaCl	No NaCl	0.5M NaCl	No NaCl
	Amts.* of Hydroxyapatite Dissolved in 200 ml. Buffer, Gm.x10^3					
300	5.0; 5.3	5.1; --	5.4; 5.7	--	6.8; 8.8	--
600	7.5; --	7.3; --	7.4; --	--	10.2; --	--
900	9.0; 9.0	9.0; 8.4	9.1;10.3	--	12.6;13.9	--
1200	10.5; --	10.7; --	10.2; --	--	14.1; --	--
1500	11.6;11.4	12.0;11.2	11.1;13.3	--	15.6;18.0	--
1800	12.4; --	12.9; --	11.9; --	--	16.7; --	--

*The first number in each column is obtained from phosphate analysis and the second number fron calcium analysis.

Rate of Dissolution of Synthetic Hydroxyapatite Sample P

In Acetic Acid Buffers

In the Absence of Common Ions

Time Seconds	pH 4.5			
	0.025M	0.05M	0.1M	0.5M
	0.5M NaCl	No NaCl	0.5M NaCl	0.5M NaCl
	Amts.* of Hydroxyapatite Dissolved in 200 ml. Buffer, Gm.x10^3			
100	23.2;26.4	14.9;13.6	29.5;28.5	37.2;32.7
300	39.0; --	27.6;25.3	50.7; --	59.4; --
500	46.9;49.6	36.7;27.9	61.4;58.8	70.1;64.4
700	51.6; --	43.5;32.2	67.3; --	76.1; --
900	54.4;58.0	48.1;36.0	71.4;67.7	78.9;74.6
1100	56.9; --	51.9;40.1	73.9; --	81.2; --

*The first number in each column is obtained from phosphate analysis and the second number from calcium analysis.

Rate of Dissolution of Synthetic Hydroxyapatite Sample P

In Acetic Acid Buffers

In the Absence of Common Ions

Time Seconds	pH 5.0			pH 6.0	
	0.025M	0.1M	0.5M	0.2M	
	No NaCl	No NaCl	No NaCl	0.5M NaCl	No NaCl
	Amts* of Hydroxyapatite Dissolved in 200 ml. Buffer, Gm.x10^3				
100	12.1;14.6	14.6;15.8	18.0;12.1	--	--
300	20.1; --	27.1; --	33.3;33.5	5.9; 4.9	5.2; --
500	24.3;27.1	32.9;32.4	38.8; --	--	--
600	--	--	--	8.0;8.1	7.6; --
700	26.7; --	36.5; --	44.7; --	--	--
900	28.6;31.3	38.6;37.8	47.9;47.5	9.4; 9.4	9.1; --
1100	29.7; --	40.6; --	51.8; --	--	--
1200	--	--	--	10.1; --	10.3; --
1500	--	--	--	10.6; --	11.1; --
1800	--	--	--	11.2; --	11.8; --

*The first number in each column is obtained from phosphate analysis and the second from calcium analysis.

Rate of Dissolution of Synthetic Hydroxyapatite Sample P

In Lactic Acid Buffers

In the Absence of Common Ions

Time Seconds	pH 4.5							
	0.025M		0.1M		0.25M		0.5M	
	0.5M NaCl	No NaCl	0.5M NaCl	No NaCl	0.5M NaCl	No NaCl	0.5M NaCl	No NaCl
	Amts.* of Hydroxyapatite Dissolved in 200 ml. Buffer, Gm.x10^3							
100	--	--	14.9;18.9	16.6;19.8	18.8;23.5	23.2;23.5	25.9;30.0	29.4;29.9
300	15.9;17.2	15.9;15.5	29.6; --	32.8; --	36.8; --	44.5; --	48.9; --	53.9; --
500	--	--	38.4;42.5	43.0;48.5	46.6;50.8	59.5;61.7	64.3;62.3	70.9;68.9
600	22.4; --	22.4; --	--	--	--	--	--	--
700	--	--	44.9; --	50.5; --	55.6; --	67.0; --	72.9; --	78.3; --
900	26.2;27.4	27.6;27.8	49.9;55.8	55.8;63.2	59.6;63.9	72.0;77.3	79.2;82.3	85.2;87.3
1100	--	--	55.7; --	60.3; --	65.6; --	76.7; --	82.6; --	89.7; --
1200	28.6; --	30.4; --	--	--	--	--	--	--
1500	30.5;33.8	32.9;33.8	--	--	--	--	--	--
1800	32.1; --	33.9; --	--	--	--	--	--	--

*The first number in each column is obtained from phosphate analysis and the second number from calcium analysis.

Rate of Dissolution of Synthetic Hydroxyapatite Sample P

In Lactic Acid Buffers

In the Absence of Common Ions

Time Seconds	pH 5.0							
	0.025M		0.1M		0.25M		0.5M	
	0.5M NaCl	No NaCl	0.5M NaCl	No NaCl	0.5M NaCl	No NaCl	0.5M NaCl	No NaCl
	Amts.* of Hydroxyapatite Dissolved in 200 ml. Buffer, Gm.x10^3							
100	--	--	8.3;11.1	8.7;10.1	11.1;11.5	12.8;13.2	14.1;18.5	15.9;16.7
300	8.6; 3.6	8.2;14.4	14.1; --	15.4; --	19.6; --	22.7; --	25.9; --	30.7; --
500	--	--	17.6;20.3	19.8;21.8	25.3;24.8	29.6;29.5	34.6;35.9	40.5;40.0
600	11.8; --	10.6; --	--	--	--	--	--	--
700	--	--	20.6; --	22.9; --	29.5; --	34.1; --	40.6; --	47.4; --
900	13.3; 7.5	12.0;18.6	22.2;25.1	25.1;27.6	33.1;33.6	37.8;39.2	44.6;46.2	52.0;54.3
1100	--	--	23.7; --	26.9; --	37.0; --	41.1; --	49.2; --	56.2; --
1200	14.4; --	12.6; --	--	--	--	--	--	--
1500	14.9;10.3	13.4;20.3	--	--	--	--	--	--
1800	15.4; --	14.0; --	--	--	--	--	--	--

*The first number in each column is obtained from phosphate analysis and the second number from calcium analysis.

Rate of Dissolution of Powdered Tooth Enamel

In Acetic Acid Buffers

In the Absence of Common Ions

Time Seconds	pH 4.5							
	0.025M		0.05M		0.1M		0.5M	
	0.5M NaCl	No NaCl	0.5M NaCl	No NaCl	0.5M NaCl	No NaCl	0.5M NaCl	No NaCl
	Amts* of Hydroxyapatite Dissolved in 200 ml. Buffer, Gm.x10^3							
100	--	--	5.7; 7.1	4.5; 2.7	--	--	--	--
300	9.0; 8.3	6.9; 8.2	13.4;13.6	11.1; 8.4	10.3; 9.8	11.5;11.5	10.3;11.2	12.8;12.5
500	--	--	20.3;21.4	16.7;13.5	--	--	--	--
600	15.7; --	10.8; --	--	--	18.4; --	19.0; --	17.8; --	22.2; --
700	--	--	25.5;27.2	21.7;18.9	--	--	--	--
900	21.4;21.1	14.6;15.3	29.5;30.0	25.0;22.5	25.4;23.2	26.3;28.4	25.4;22.5	31.4;27.9
1100	--	--	33.7;33.5	28.2;25.5	--	--	--	--
1200	25.7; --	17.6; --	--	--	30.0; --	29.9; --	31.3; --	37.0; --
1500	29.0;30.9	19.8;20.9	--	--	35.0;34.7	35.1;34.6	36.8;34.7	43.7;44.3
1800	31.7; --	22.0; --	--	--	38.1; --	38.2; --	40.2; --	47.0; --

*The first number in each column is obtained from phosphate analysis and the second number from calcium analysis.

Rate of Dissolution of Powdered Tooth Enamel

In Acetic Acid Buffers

In the Absence of Common Ions

Time Seconds	pH 5.0					
	0.025M		0.1M		0.5M	
	0.5M NaCl	No NaCl	0.5M NaCl	No NaCl	0.5M NaCl	No NaCl
	Amts.*of Hydroxyapatite Dissolved in 200 ml. Buffer, Gm.x10^3					
300	--	--	5.8; 5.8	5.6; 4.7	4.2; --	5.8; --
500	7.3; 8.5	6.1; 6.6	--	--	--	--
600	--	--	9.1; --	9.6; --	8.2; 8.4	10.1; --
900	--	--	12.2;12.2	12.9;11.6	11.0; --	14.4; --
1000	11.0; --	9.6; --	--	--	--	--
1200	--	--	14.2; --	15.7; --	14.2; --	17.4; --
1500	13.2;14.0	12.0;12.1	16.3;16.6	18.2;19.6	16.5;15.8	20.9; --
1800	--	--	18.2; --	19.8; --	18.8; --	23.7; --
2000	14.6; --	13.4; --	--	--	--	--
2500	15.9;17.7	14.7;15.6	--	--	--	--
3000	16.7; --	15.5; --	--	--	--	--

*The first number in each column is obtained from phosphate analysis and the second number from calcium analysis.

Rate of Dissolution of Powdered Tooth Enamel

in Lactic Acid Buffers

In the Absence of Common Ions

Time Seconds	pH 4.5							
	0.025M		0.1M		0.25M		0.5M	
	0.5M NaCl	No NaCl	0.5M NaCl	No NaCl	0.5M NaCl	No NaCl	0.5M NaCl	No NaCl
	Amts* of Hydroxyapatite Dissolved in 200 ml. Buffer, Gm.x10^3							
100	--	--	--	--	--	--	5.1; 5.6	6.4; 4.6
300	--	--	9.0; 5.1	10.8; 7.8	10.6;17.9	11.3; 8.8	11.3; --	14.5; --
500	--	--	--	--	--	--	17.1;22.2	23.0;21.8
600	--	--	16.8; --	19.5; --	18.6; --	22.0; --	--	--
700	--	--	--	--	--	--	22.7; --	29.2; --
900	--	--	23.1;21.8	26.6;24.8	26.3;30.1	28.8;27.4	29.0;28.9	36.1;35.6
1000	15.8;17.2	14.1;13.8	--	--	--	--	--	--
1100	--	--	--	--	--	--	33.5; --	39.4; --
1200	--	--	29.0; --	32.4; --	31.0; --	37.2; --	--	--
1500	--	--	33.0;37.8	37.4;37.2	36.0;43.3	42.0;49.9	--	--
1800	--	--	37.2; --	42.3; --	40.7; --	49.7; --	--	--
2000	22.4; --	22.2; --	--	--	--	--	--	--
3000	25.6;28.6	26.8;28.3	--	--	--	--	--	--
4000	28.3; --	29.1; --	--	--	--	--	--	--
5000	29.3;32.2	30.5;32.6	--	--	--	--	--	--
6000	30.4; --	32.0; --	--	--	--	--	--	--

*The first number in each column is obtained from phosphate analysis and the Second number is obtained from calcium analysis.

Rate of Dissolution of Powdered Tooth Enamel

in Lactic Acid Buffers

In the Absence of Common Ions

Time Seconds	pH 5.0							
	0.025M		0.1M		0.25M		0.5M	
	0.5M NaCl	No NaCl	0.5M NaCl	No NaCl	0.5M NaCl	No NaCl	0.5M NaCl	No NaCl
	Amts.* of Hydroxyapatite Dissolved in 200 ml. Buffer, Gm.x10^3							
300	--	--	--	--	4.5; 7.1	5.9; 5.7	5.3; 6.3	8.3; 9.8
500	--	--	6.3; 7.2	6.8; 7.9	--	--	--	--
600	--	--	--	--	8.1; --	10.2; --	9.5; --	13.4; --
900	--	--	--	--	11.5;13.3	14.2;13.7	13.2;12.9	18.8;18.6
1000	7.8; --	6.4;11.3	10.9; --	11.9; --	--	--	--	--
1200	--	--	--	--	14.5; --	18.1; --	16.7; --	23.7; --
1500	--	--	14.2;15.9	16.1;16.9	17.4;18.1	21.1;24.7	20.2;22.2	28.2;29.5
1800	--	--	--	--	19.5; --	23.7; --	23.2; --	31.7; --
2000	10.8; --	9.2; --	16.8; --	19.3; --	--	--	--	--
2500	--	--	18.7;21.1	21.4;23.7	--	--	--	--
3000	12.0;10.0	10.7;11.0	19.9; --	23.3; --	--	--	--	--
4000	12.7; --	11.5; --	--	--	--	--	--	--
5000	12.8;11.5	11.9;12.2	--	--	--	--	--	--
6000	13.2; --	12.2; --	--	--	--	--	--	--

* The first number in each column is obtained from phosphate analysis and the second number from calcium analysis.

Rate of Dissolution of Powdered Tooth Enamel

In Acetate and Lactate

Buffers In the Absence of Common Ions

--

Time Seconds	Acetate Buffers		Lactate Buffers			
	pH 6.0					
	0.2M		0.25M		0.5M	
	0.5M NaCl	No NaCl	0.5M NaCl	No NaCl	0.5M NaCl	No NaCl
	Amts.*of Hydroxyapatite Dissolved in 200ml. Buffer, Gm.x10^3					
1000	2.2; --	2.6;2.4	3.4; 2.7	3.8; 3.6	3.2; --	4.5; 5.1
2000	3.1; --	3.7; --	5.0; --	5.8; --	5.3; --	7.4; --
3000	3.3; --	4.5;4.3	6.0; 5.3	7.0; 6.7	6.9; --	9.3; 9.8
4000	3.8; --	5.0; --	6.9; --	7.9; --	8.2; --	11.0; --
5000	4.1; --	5.4; --	7.5; 6.8	8.6; 9.3	9.1; --	12.0;13.3
6000	4.4; --	5.8; --	7.9; --	9.2; --	9.7; --	13.2; --

*The first number in each column is obtained from phosphate analysis and the second number from calcium analysis.

Rate of Dissolution of Synthetic Hydroxyapatite Samples and Enamel

In Lactic Acid Buffers

In the Absence of Common Ions

Time Seconds	Sample A	Enamel		Sample P					
	0.05M pH 4.5	0.05M pH 4.5		0.05M pH 4.5		0.025M pH 6.0		0.5M pH 6.0	
	0.5M NaCl	0.5M NaCl	No NaCl	0.5M NaCl	No NaCl	0.5M NaCl	No NaCl	0.5M NaCl	No NaCl
	Amts.* of Hydroxyapatite Dissolved in 200 ml. buffer, Gm.x10^3								
100	7.6	2.8	3.5	11.6	11.9	--	--	--	--
	9.1	2.4	2.6	12.2	11.3	--	--	--	--
300	16.3	7.0	8.6	20.7	22.9	5.8	6.7	6.8	9.5
	19.2	6.9	7.1	21.6	22.7	5.3	5.4	7.8	9.7
600	--	--	--	--	--	7.4	8.5	9.2	12.8
	--	--	--	--	--	--	--	--	--
500	23.2	11.0	12.6	26.6	31.3	--	--	--	--
	24.8	11.0	14.8	25.7	31.7	--	--	--	--
700	28.9	15.0	16.9	30.6	38.3	--	--	--	--
	31.0	14.9	17.0	29.4	36.6	--	--	--	--
900	33.1	17.6	20.5	33.9	40.3	8.0	9.8	10.6	14.6
	34.1	18.4	20.7	32.0	38.7	8.4	9.9	10.6	14.4
1100	36.1	20.6	23.8	36.2	43.6	--	--	--	--
	37.4	21.6	24.7	35.0	41.5	--	--	--	--
1200	--	--	--	--	--	8.9	10.7	11.6	16.5
	--	--	--	--	--	--	--	--	--
1500	--	--	--	--	--	9.8	11.4	12.7	17.7
	--	--	--	--	--	10.1	10.1	13.3	17.4
1800	--	--	--	--	--	10.5	12.0	13.8	18.6
	--	--	--	--	--	--	--	--	--

*The first number in each column is obtained from phosphate analysis and the second number from calcium analysis.

Rate of Dissolution of Synthetic Hydroxyapatite Sample A

in Hydrochloric Acid Solutions

Containing 0.5M NaCl

Time Seconds	0.001N		0.0025N		0.005N		0.0075N		0.01N	
	Amts. of Hydroxyapatite Dissolved in 200 ml. Solution, Gm.x10^3									
	PO_4	Ca	PO_4	Ca	PO_4	Ca	PO_4	Ca	PO_4	Ca
100	6.6	6.6	14.8	15.5	26.0	19.9	36.7	38.1	47.4	35.5
300	11.4	--	27.2	--	48.7	43.4	65.6	67.2	80.5	68.9
500	13.1	--	32.0	--	57.6	48.4	78.5	81.9	90.0	78.6
700	14.0	--	34.1	--	61.6	55.2	83.0	85.7	94.2	82.5
900	14.4	--	35.0	--	64.9	59.0	87.9	92.1	94.7	92.5
1100	14.7	--	35.9	--	66.9	62.7	90.2	96.6	95.6	82.8
3600	16.3	--	37.7	--	71.4	63.6	95.6	97.5	95.6	82.8
14 Hrs.	17.0	--	38.5	--	73.4	--	96.1	--	98.9	82.8

Ca-- Calcium was analyzed; PO_4-- Phosphate was analyzed.

Rate of Dissolution of Synthetic Hydroxyapatite Sample P

in Hydrochloric Acid Solutions

Containing 0.5M NaCl

Time Seconds	0.001N		0.0025N		0.005N		0.0075N		0.01N	
	Amts. of Hydroxyapatite Dissolved in 200 ml. Solution, Gm.x10^3									
	PO_4	Ca	PO_4	Ca	PO_4	Ca	PO_4	Ca	PO_4	Ca
100	12.8	12.2	27.2	22.2	48.4	48.6	65.7	58.4	78.1	66.5
300	14.4	14.1	34.7	38.7	69.3	67.1	88.2	73.9	94.6	95.4
500	14.8	14.9	35.5	38.7	74.2	71.6	93.6	--	97.8	92.1
700	15.1	15.3	35.7	41.6	74.2	--	96.2	--	99.8	--
900	15.4	15.7	35.7	42.0	75.7	--	97.9	--	99.8	96.6
1100	15.4	16.2	35.7	--	75.7	--	98.8	--	99.8	97.9
3600	15.8	16.5	35.9	--	75.9	74.7	99.3	--	99.8	--
14 Hrs.	16.4	17.0	36.4	--	76.8	--	99.3	--	101.8	100.6

Ca-- Calcium was analyzed; PO_4-- Phosphate was analyzed.

Rate of Dissolution of Synthetic Hydroxyapatite Sample C

in Hydrochloric Acid Solutions

Containing 0.5M NaCl

Time Seconds	0.001N		0.0025N		0.005N		0.0075N		0.01N	
	Amts. of Hydroxyapatite Dissolved in 200 ml. Solution, Gm.x10^3									
	PO_4	Ca	PO_4	Ca	PO_4	Ca	PO_4	Ca	PO_4	Ca
100	6.9	7.4	16.2	18.0	33.0	34.9	42.3	42.2	53.8	54.6
300	11.5	12.8	28.4	26.8	56.4	51.0	73.0	69.3	85.0	85.2
500	12.7	13.7	31.6	31.5	64.3	60.0	84.8	83.0	92.7	94.8
700	13.6	14.9	33.1	33.8	68.4	62.2	90.9	90.7	95.0	97.6
900	13.7	15.4	33.7	34.4	70.3	64.8	91.7	94.4	96.1	--
1100	14.0	16.2	34.1	34.4	71.4	66.9	94.2	94.4	97.5	--
3600	15.5	16.0	35.5	35.0	74.4	66.9	97.6	96.1	97.5	100.4
14 Hrs.	16.3	17.4	35.9	36.2	74.7	67.1	98.4	97.8	97.5	100.4

Ca-- Calcium was analyzed; PO_4-- Phosphate was analyzed.

Rate of Dissolution of Powdered Tooth Enamel

in Hydrochloric Acid Solutions

Containing 0.5M NaCl

Time Seconds	0.001N		0.0025N		0.005N		0.0075N		0.01N	
	Amts. of Hydroxyapatite Dissolved in 200 ml. Solution, Gm.x10^3									
	PO_4	Ca	PO_4	Ca	PO_4	Ca	PO_4	Ca	PO_4	Ca
100	5.7	5.7	12.3	12.4	25.6	19.6	30.8	33.0	41.8	38.8
300	11.0	10.3	24.3	21.8	47.0	42.0	66.7	56.0	72.0	67.2
500	13.2	12.4	30.2	27.2	60.6	53.3	72.6	68.8	87.2	80.1
700	14.0	13.0	32.8	31.5	63.5	59.6	80.9	77.3	90.6	82.9
900	14.4	13.8	33.9	29.9	66.2	62.3	85.2	96.8	92.9	88.4
1100	14.5	13.8	34.7	28.8	68.0	63.7	85.9	85.1	94.8	88.8
3600	15.1	13.9	35.3	32.0	72.3	68.4	92.6	93.0	95.1	89.5
14 Hrs.	15.7	14.0	35.7	--	73.0	68.4	92.9	--	95.1	89.4

Ca-- Calcium was analyzed; PO_4-- Phosphate was analyzed.

Effect of Common Ions on Rate of Dissolution
of Synthetic Hydroxyapatite Sample A
in a 0.05M Acetate Buffer
pH 4.5

Time Seconds	Common Ions: Calcium					
	0.003M		0.01M		0.05M	
	0.5M NaCl	No NaCl	0.5M NaCl	No NaCl	0.5M NaCl	No NaCl
	Amts. of Hydroxyapatite Dissolved in 200 ml. Buffer, Gm.x10^3					
	by Phosphate Analysis					
100	15.8	10.7	14.1	8.2	8.2	5.6
300	33.0	23.8	28.7	18.1	16.8	12.0
500	44.5	33.3	38.8	25.5	22.4	16.2
700	53.0	40.6	46.5	31.5	27.3	19.5
900	59.1	46.0	51.0	36.8	30.5	22.8
1100	64.8	49.5	55.5	41.0	34.8	25.5
	Common Ions: Phosphate					
	by Calcium Analysis					
100	17.2	9.2	14.5	7.5	11.0	6.8
300	37.5	22.1	28.0	18.2	18.0	16.0
500	47.0	30.4	36.8	27.5	22.9	21.8
700	54.2	37.8	43.7	33.4	25.8	22.5
900	59.2	45.5	43.8	37.3	27.8	23.0
1100	61.5	52.0	43.8	41.7	32.3	23.5

Effect of Common Ions on Rate of Dissolution
of Synthetic Hydroxyapatite Sample A
in 0.05M Lactate Buffer
pH 4.5

Time Seconds	Common Ions: Calcium		
	0.003 M	0.01 M	0.05 M
	0.5M NaCl		
	Amts. of Hydroxyapatite Dissolved in 200 ml. Buffer, Gm.x10^{-3}		
	PO_4	PO_4	PO_4
100	7.0	6.0	2.9
300	14.7	11.4	5.3
500	20.5	15.4	7.2
700	25.1	19.0	8.6
900	28.4	21.5	10.0
1100	30.9	23.0	10.6
	Common Ions: Phosphate		
	Ca	Ca	Ca
100	7.1	6.4	--
300	16.7	13.6	--
500	23.4	16.8	--
700	28.9	20.4	--
900	31.5	20.8	--
1100	34.8	22.4	--

Ca-- Calcium was analyzed; PO_4 -- Phosphate was analyzed.

Effect of Common Ions on Rate of Dissolution
of Synthetic Hydroxyapatite Sample P
in 0.05M Acetate Buffer
pH 4.5

Time Seconds	Common Ions: Calcium		
	0.003 M	0.01 M	0.05 M
	No NaCl		
	Amts. of Hydroxyapatite Dissolved in 200 ml. Buffer, Gm.x10^3		
	PO_4	PO_4	PO_4
100	11.6	8.2	4.4
300	22.7	16.5	8.5
500	29.7	21.4	10.0
700	34.6	25.6	12.4
900	39.4	28.5	13.9
1100	42.7	31.0	15.7
	Common Ions: Phosphate		
	Ca	Ca	Ca
100	7.1	7.1	5.9
300	20.0	16.9	11.1
500	31.4	23.5	11.9
700	35.0	24.3	14.0
900	43.0	25.2	15.3
1100	43.0	25.7	15.3

Ca-- Calcium was analyzed; PO_4-- Phosphate was analyzed.

Effect of Common Ions on Rate of Dissolution
of Synthetic Hydroxyapatite Sample P
in 0.05M Lactate Buffer
pH 4.5

Time Seconds	Common Ions: Calcium					
	0.003 M		0.01 M		0.05 M	
	0.5M NaCl	No NaCl	0.5M NaCl	No NaCl	0.5M NaCl	NO NaCl
	Amts. of Hydroxyapatite Dissolved in 200 ml. Buffer, Gmx10^3					
	by Phosphate Analysis					
100	10.5	9.5	5.9	6.7	1.6	2.8
300	18.8	18.1	10.7	12.6	3.1	5.6
500	24.1	23.7	13.6	16.5	4.1	7.6
700	28.0	27.7	16.0	19.8	5.0	9.3
900	30.8	31.2	17.6	22.7	6.2	10.5
1100	33.9	34.3	18.7	24.9	6.7	11.8
	Common Ions: Phosphate					
	by Calcium Analysis					
100	8.8	8.3	7.1	6.3	6.9	5.2
300	16.8	17.4	13.6	13.2	11.9	12.4
500	23.3	24.3	18.6	17.1	15.8	14.7
700	24.7	32.0	--	19.7	15.8	17.8
900	26.3	33.3	--	20.1	18.4	17.8
1100	27.9	36.1	--	20.1	18.4	17.8

Effect of Common Ions on Rate of Dissolution
of Synthetic Hydroxyapatite Sample R
in 0.05M Acetate Buffer
pH 4.5

Time Seconds	Common Ions: Calcium							
	0.0 M		0.003M		0.01M		0.05M	
	0.5M NaCl	No NaCl	0.5M NaCl	No NaCl	0.5M NaCl	No NaCl	0.5M NaCl	No NaCl
	Amts. of Hydroxyapatite Dissolved in 200 ml. Buffer, Gm.x10^3							
	by Calcium Analysis							
100	13.2	11.0	9.0	--	5.4	--	4.8	--
300	30.7	23.7	18.6	--	14.5	--	10.2	--
500	42.1	31.6	25.3	--	18.1	--	13.6	--
700	51.5	39.0	30.7	--	23.8	--	16.4	--
900	54.6	44.1	37.0	--	31.3	--	18.8	--
1100	58.3	48.2	41.4	--	37.0	--	20.4	--
	Common Ions: Phosphate							
100	--	--	10.5	10.0	7.5	6.5	5.8	4.8
300	--	--	22.5	21.0	19.2	15.5	12.2	11.5
500	--	--	32.4	29.2	25.6	23.5	17.0	15.8
700	--	--	37.4	36.3	31.7	29.6	21.2	20.0
900	--	--	45.0	41.5	36.0	34.8	24.5	22.5
1100	--	--	48.6	45.4	40.5	40.2	26.7	24.5

Effect of Common Ions on Rate of Dissolution
of Powdered Tooth Enamel
in a 0.05M Acetate Buffer
pH 4.5

Time Seconds	Common Ions: Calcium					
	0.003M		0.01M		0.05M	
	0.5M NaCl	No NaCl	0.5M NaCl	No NaCl	0.5M NaCl	No NaCl
	Amts. of Hydroxyapatite Dissolved in 200 ml. Buffer, Gm.x10^3					
	by Phosphate Analysis					
100	5.8	2.7	--	--	--	--
300	12.7	6.5	--	--	--	--
500	19.1	9.8	10.8	5.0	3.0	2.3
700	24.3	13.0	--	--	--	--
900	28.6	16.2	--	--	--	--
1000	--	--	18.6	9.4	4.5	3.4
1100	32.9	18.4	--	--	--	--
1500	--	--	25.8	12.5	6.3	4.0
2000	--	--	31.3	15.3	7.6	4.4
2500	--	--	35.4	17.7	8.7	5.2
3000	--	--	39.0	19.9	9.7	6.1
	Common Ions: Phosphate					
	by Calcium Analysis					
100	5.1	1.8	--	--	--	--
300	13.9	3.9	--	--	--	--
500	20.7	8.5	14.4	7.6	11.2	7.6
700	26.5	12.2	--	--	--	--
900	30.1	15.0	--	--	--	--
1000	--	--	23.1	15.0	20.1	11.5
1100	34.2	17.7	--	--	--	--
1500	--	--	28.4	18.8	21.7	14.1
2000	--	--	34.8	21.1	21.7	14.9
2500	--	--	40.2	23.9	21.7	17.2
3000	--	--	41.5	25.3	21.7	17.9

Effect of Common Ions on Rate of Dissolution
of Powdered Tooth Enamel
in 0.05M Lactate Buffer
pH 4.5

Time Seconds	Common Ions: Calcium					
	0.003 M		0.01 M		0.05 M	
	0.5M NaCl	No NaCl	0.5M NaCl	No NaCl	0.5M NaCl	No NaCl
	Amts. of Hydroxyapatite Dissolved in 200 ml. Buffer, Gm.x10^3					
	by Phosphate Analysis					
500	8.2	8.2	4.2	4.4	1.1	1.7
1000	13.4	14.7	7.0	7.3	1.7	2.5
1500	17.6	19.7	9.1	9.8	1.9	3.1
2000	21.2	23.5	10.9	11.8	2.1	3.5
2500	22.9	26.4	12.8	13.6	2.5	4.1
3000	24.5	28.4	13.6	15.1	2.7	4.6
	Common Ions: Phosphate					
	by Calcium Analysis					
500	5.9	12.7	6.2	9.6	4.4	8.3
1000	12.0	18.1	9.7	13.7	6.5	13.3
1500	15.7	22.7	10.0	17.2	8.6	15.4
2000	18.4	25.9	10.4	19.8	9.7	15.4
2500	20.6	28.7	10.4	21.3	11.9	16.7
3000	22.1	31.2	10.4	21.3	11.9	18.1

APPENDIX II

Dissociation Constants of Acetic and Lactic Acids with and without the presence of 0.5M NaCl at low and high concentrations of the acids

Acid Concn. Moles/Liter	Acetic Acid Exp'l K_A* Moles/Liter		Lactic Acid Exp'l K_A* Moles/Liter	
	0.5M NaCl	No NaCl	0.5M NaCl	No NaCl
0.5	2.5×10^{-5}	2.0×10^{-5}	2.5×10^{-4}	1.8×10^{-4}
0.025	2.8×10^{-5}	1.8×10^{-5}	2.2×10^{-4}	1.3×10^{-4}

* These were determined experimentally by titrating 20 ml. of the acid solution against sodium hydroxide of known strength and measuring the pH change manually after each incremental addition of NaOH using the Beckman Model G pH-meter. The pH at half neutralization was taken as pK_A.

APPENDIX III

The Values of h' Employed to obtain Fits of Theoretical Gh Values to the Experimental Data (Figures 47-53)

	$h' \times 10^{-4}$					
	K_{HAP}					
	1×10^{-108}	1×10^{-113}	1×10^{-116}	1×10^{-120}		
	Case I					
Acetate Buffers						
Sample A	0.58	--	1.34	--		
Sample P	1.46	--	3.34	--		
Enamel	--	0.20	--	0.44		
Lactate Buffers						
Sample A	0.88	--	1.52	--		
Sample P	1.47	--	2.53	--		
Enamel	--	0.30	--	0.57		
Hydrochloric Acid Solutions	Case I	Case III			Case I	Case III
Sample A	7.00	0.70			7.50	0.75
Sample P	12.6	1.26			13.4	1.34
Sample C	8.20	0.82			8.80	0.88
Enamel	6.10	0.61			6.50	0.65

Case I is the Theory with all Diffusion Coefficient values = 1×10^{-5} cm.^{2}/sec. Case III is the Theory with all Diffusion Coefficient Values same as in case I except for the value of Diffusion Coefficient for Hydrogen ions, which is 1×10^{-4} cm.^{2}/sec. Case III h' values in hydrochloric acid compares well with the case I

h' values in weak acids. Case I h' values in hydrochloric acid are ten times greater than those of case III in the same acid. This suggests that the diffusion coefficient of hydrogen ions might be 1×10^{-4} cm.^{2}/sec. However, it must be noted that the value of diffusion coefficient for hydrogen ions is important only in the case of strong acids as shown in the theoretical study.

LIST OF REFERENCES

1. Miller, W. D., J. Brit. Dent. Assn., 5, 104 (1884).
2. Fosdick, L. S., and Wessinger, G. D., J. Am. Dent. Assn., 27, 203 (1940).
3. Summerson, W. H., and Neuwirth, I., J. Dent. Res., 20, 157 (1941).
4. Bunting, R. W., and Palmerlee, F., Proc. Soc. Exp. Biol. N.Y., 22, 296 (1925).
5. Enright, J. J., Friesell, H. E., and Trescher, M. O., J. Dent. Res., 12, 759 (1932).
6. Hardwick, J. L., Brit. Dent. J., 89, 1 (1950).
7. Wachtell, L. W., J. Dent. Res., 43, 237 (1964).
8. Volker, J. F., Ibid., 19, 35 (1940).
9. Manly, R. S., and Harrington, D. P., Ibid., 38, 910 (1959).
10. Fischer, R. B., Muhler, J. C., and Wust, C. J., Ibid., 33, 50 (1954).
11. McCann, H. G., and Bullock, F. A., Ibid., 34, 59 (1955).
12. Leach, S. A., Brit. Dent. J., 106, 122 (1959).
13. Malaowalla, A., and Myers, H. M., J. Dent. Res., 41, 413 (1962).
14. Spiers, R. L., Spinelli, M., and Brudevold, F., Ibid., 42, 811 (1963).
15. Stralfors, A., Tr. Roy. Schools Stockholm and Umei, Series 2:1, 52 (1958).
16. Gray, J. A., J. Dent. Res., 41, 633 (1962).
17. Noyes, A. A., and Whitney, W. R., Z. Physik. Chem., 23, 689 (1897).
18. Glasstone, S., Laidler, K. J., and Eyring, H., "The Theory of Rate Processes", pp. 522-525, McGraw-Hill Book Co., Inc., New York, 1941.

19. Higuchi, W. I., Parrot, E. L., Wurster, D. E., and Higuchi, T., J. Am. Pharm. Assoc. Sci. Ed., 47, 376 (1958).

20. Higuchi, W. I., Gray, J. A., Hefferren, J. J., and Patel, P. R., J. Dent. Res., 44, 330 (1965).

21. Higuchi, W. I., Patel, P. R., and Hefferren, J. J., J. Pharm. Sci., 54, 587 (1965).

22. Brown, W. E., Soil Sci., 90, 51 (1960).

23. Robinson, R. A., and Stokes, R. H., "Electrolyte Solutions", p. 482, Academic Press, Inc., London, 1959.

24. Rootare, H. M., Deitz, V. R., and Carpenter, F. G., J. Colloid Sci., 17, 179 (1962).

25. Levinskas, G. J., and Neuman, W. F., J. Phys. Chem., 59, 164 (1955).

26. Strates, B. S., Neuman, W. F., and Levinskas, G. J., Ibid., 61, 279 (1957).

27. Kielland, J., J. Am. Chem. Soc., 59, 1675 (1937).

28. Becks, H., and Wainwright, W. W., J. Dent. Res., 20, 627 (1941).

29. Brudevold, F., "Chemistry and Prevention of Dental Caries", Chap. 2, p. 69, editor: Sognnaes, R. F., Publisher: Charles C Thomas, Springfield, Ill., 1962.

30. Dawes, C., and Jenkins, G. N., Arch. Oral Biol., 7, 161 (1962).

31. Egan, E. P., Wakefield, Z. T., and Elmore, K. L., J. Am. Chem. Soc., 72, 2418 (1950).

32. Hefferren, J. J., and Higuchi, W. I., J. Dent. Res., 44, 455 (1965).

33. Manly, R. S., and Hodge, H. C., Ibid., 18, 133 (1939).

34. Gee, A., Domingues, L. P., and Deitz, V. R., Anal. Chem., 26, 1487 (1954).

35. Herrero-Lancina, M., and West, T. S., Ibid., 35, 2131 (1963).

36. Roseman, T. J., and Higuchi, W. I., Personal Communication.

37. Van Wazer, J. R., "Phosphorus and Its Compounds. Vol.I. Chemistry", Chap. 9, pp. 479-599. Interscience Publishers, New York, 1958.

38. Posner, A. S., Perloff, A., and Diorio, A. F., Acta Cryst., 11, 308 (1958).

39. Pigman, W., Brasher, J., and Koulourides, T., Nature, 195, 190 (1962).

40. Soni, N. N., and Brudevold, F., J. Dent. Res., 39, 233 (1960).